UNIVERSITÀ DEGLI STUDI DI MILANO

CORSO DI DOTTORATO IN SCIENZE FARMACOLOGICHE, SPERIMENTALI E CLINICHE

Ph.D. COURSE IN PHARMACOLOGICAL, EXPERIMENTAL AND CLINICAL SCIENCES

XXXIII Cycle

DEPARTMENT OF PHARMACOLOGICAL AND BIOMOLECULAR SCIENCES

DEPARTMENT OF HEALTH SCIENCES

β-GLUCOCEREBROSIDASE MEDIATES MICROGLIAL NEUROPROTECTIVE FUNCTIONS: A POSSIBLE LINK BETWEEN PARKINSON'S AND GAUCHER'S DISEASES

BIO/14

Electra Athena Salome Brunialti

Matr. n. R11957

Tutor: Prof. Paolo Ciana

Coordinator: Prof. Alberico Luigi Catapano

A.A. 2019-2020

gli esperimenti

sono come le ciliegie…

SUMMARY

1 ABSTRACT 5
English 6
Italiano 8
2 INTRODUCTION 10
2.1 Parkinson's disease 11
2.2 Gaucher's disease 15
2.3 The relationship between GBA1 and PD 18
2.4 Microglia 21
2.4.1 Introduction to the cell 21
2.4.2 Microglia functions 21
2.4.3 Neuron-microglia communication 25
2.4.4 Analogy between microglia and macrophages 28
2.4.5 Microglia in inflammatory and neurodegenerative diseases 29
2.5 Regulation of cellular redox state: the role of NRF2 34
2.5.1 NRF2 pathway 34
2.5.2 NRF2 regulations into the brain 36
2.5.3 The role of NRF2 in Parkinson's disease 38
2.6 TFEB master regulator of autophagy–lysosomal pathway 41
3 MATERIALS AND METHODS 44
3.1 Reagents 45
3.2 Plasmids 45
3.3 ES manipulation 46
3.4 Screening PCR for TFEB-STOP 46
3.5 Cell culture 46
3.6 Flow cytometry assay 48
3.7 Luciferase enzymatic assay 48
3.8 Glucocerebrosidase assay 48
3.9 Immunohistochemical analysis 48
3.10 Animal treatments 51
3.11 *In vivo* and *ex vivo* imaging 51
3.12 Microglial image processing and quantification 52
3.13 Real-time PCR 52
3.14 Statistical analysis 53
4 AIM 54
5 RESULTS 56

5.1 Reporter systems generation 57
5.1.1 Generation and validation of reporter system to monitor oxidative stress response 57
5.1.2 Generation and validation of transcription factor EB reporter system 60
5.1.3 Generation of ARE-*luc2* and TFEB-*luc2* reporter mice 62
5.2 Nrf2 regulation during early stages of dopaminergic degeneration induced by MPP+ 66
5.2.1 NFR2 activation precedes cell death in MPP+ treated SK-N-BE cell line 66
5.2.2 *In vivo* imaging of Nrf-2 activity in the ARE-*luc2* reporter transgenic mouse. 67
5.2.3 Activation of Nrf2 is an early event preceding neuronal cell death induced by MPTP *in vivo* 69
5.3 Reporter systems reveal that the pharmacological inhibition of microglial GCase, the Gaucher's disease gene product, hinders the Nrf2-mediated neuroprotective response in neurons 71
5.3.1 GCase inhibition impairs Nrf2 response *in vivo.* 71
5.3.2 GCase inhibition hinders the microglial-mediated induction of NRF2 signal in neurons 74
5.3.3 Microglial GCase is essential for the efficient activation of the NRF2 pathway in neurons ... 77
5.4 GCase inhibition hampers neuroprotective functions of microglia 79
5.5 Inhibition of microglial GCase increases the expression of genes associated with neurodegeneration 80
5.6 Image-based morpho-functional analysis of living microglia reveals that GCase inhibition induces signatures of morphological changes in specific subpopulations 82
5.6.1 Image-based microglia analysis reveals the existence of functional clusters 82
5.6.2 GCase inhibition induces signature changes in microglia subpopulations 86
5.7 Microglia require functional actin-dependent structures to induce NRF2 in neuronal dopaminergic cells 88
5.8 Microglial energetic toning might be a pharmaceutical approach to decrease the risk of neurodegeneration 90
5.9 Peripheral macrophages to study cerebral microglial dysfunctions 93
6 DISCUSSION 94
7 ACKNOWLEDGMENT 102
8 BIBLIOGRAPHY 104
***Ph.D. ACTIVITIES* 117**

1 ABSTRACT

English

The Parkinson's disease (PD) evolves over an extended period of time with the onset occurring long before clinical signs begin to manifest. Characterization of the molecular events underlying the PD onset is instrumental for the development of diagnostic markers and preventive treatments but progress in this field is hindered by technical limitations. Risk factors are the obvious target of prevention; mutations in the GBA1 gene, encoding for the lysosomal β-glucocerebrosidase (GCase) enzyme, have been associated with the highest risk of PD, while homozygous individuals invariably develop Gaucher's disease (GD), a pathology characterized by several deficits including neuronal damages. GBA1 mutations impair GCase activity and generate a lysosomal disorder in macrophages considered the hallmark of GD, while in the brain most of the effects of GBA1 mutations have been so far attributed to the GCase deficit in neuronal cells.

During my Ph.D. project, I have generated innovative reporter tools and applied different optical imaging approaches to study the activation of brain-protective response in models representative of prodromal phases of PD *in vitro* and *in vivo*. The study was focused on nuclear factor erythroid 2-related factor (NRF2), regulating antioxidant/detoxifying response, and the transcription factor EB (TFEB), the master regulator of autophagy and lysosomal pathways, as key signals underlying the early stage of neurodegeneration. In dopaminergic SK-N-BE neuroblastoma cells and in the *substantia nigra pars compacta* area of the mouse brain, we detected that Nrf2 activation precedes dopaminergic neurodegeneration driven by neurotoxin as demonstrated by cellular, *in vivo* and *ex vivo* optical imaging, a finding confirmed by co-localization experiments carried out by immunohistochemistry. Since activation of this transcription factor anticipates dopaminergic neurodegeneration, I focused the study on the cross-talk between a potential PD triggering signal, namely inhibition of the GCase enzyme, and the Nrf2 signaling pathway. Remarkably, I discovered a novel mechanism of microglia-to-neuron communication mediated by cell-to-cell contact, supported by functional actin structures and by an efficient energetic metabolism. Surprisingly, the experiments performed in microglia/neuron co-cultures and in the brain of living mice provided compelling evidence that inhibition of microglial GCase interferes with the ability of these cells to stimulate the NRF2-mediated response in neurons resulting in increased neuronal susceptibility to a xenobiotic. Assays performed in co-culture suggest that counteracting such dysfunction by metabolic compensation could represent a potential therapeutic approach to decrease the risk of neurodegeneration.

In conclusion, my thesis demonstrated that the developed reporter systems can be used to study the dynamic modulation of molecular pathways in the living brain; this technology has been developed in particular for the dynamic measurement of oxidative stress and lysosomal/autophagy pathways. Application of these systems allowed to demonstrate that GCase inhibition impairs microglia/neuron communication, thus increasing the susceptibility of neurons to detrimental insults. Taken together, the data identified a novel mechanism underlying the increased risk of neurodegeneration observed in carriers of GBA1 mutations and suggest novel therapeutic strategies for prevention.

Italiano

La degenerazione dopaminergica che caratterizza il morbo di Parkinson antecede la manifestazione dei segni clinici. Identificare gli eventi molecolari responsabili dell'insorgenza della malattia di Parkinson rappresenta un traguardo fondamentale sia per poter sviluppare marcatori diagnostici che trattamenti preventivi; tuttavia, lo studio della patogenesi è limitato dalla carenza di modelli appropriati e dalla difficoltà di studiare la malattia umana che evolve lungo un arco temporale di decenni. Le indicazioni che provengono dall'analisi dei fattori di rischio, sono in questo contesto fondamentali per comprendere l'eziopatogenesi. Tra di esse, particolarmente rilevanti sono le mutazioni nel gene GBA1, che codifica per l'enzima lisosomiale β-glucocerebrosidasi (GCasi), essendo considerate il maggiore fattore di rischio per lo sviluppo della malattia di Parkinson; questa proteina risulta essere fondamentale anche per la malattia di Gaucher, in quanto individui portatori di mutazioni in omozigosi sviluppano tale patologia che, in un sottogruppo di pazienti, è caratterizzata anche dalla presenza di neurodegenerazione. Le mutazioni in tale gene sono quindi considerate al crocevia di due malattie; nel caso della malattia di Gaucher l'alterazione dell'attività della GCasi induce nei macrofagi un disturbo lisosomiale considerato il segno distintivo della malattia; nel morbo di Parkinson, invece, si pensa che il difetto enzimatico produca i suoi effetti negativi soprattutto sulla componente neuronale.

Allo scopo di studiare gli eventi molecolari caratterizzanti l'incipit della malattia di Parkinson, durante il corso di Dottorato, ho generato sistemi *reporter* innovativi che permettono di misurare la modulazione di segnali neuroprotettivi in colture cellulari e *in vivo*, nel cervello di modelli animali, rappresentativi delle fasi prodromiche della malattia di Parkinson, attraverso approcci basati sull'*imaging* ottico. In particolare, lo studio si è concentrato sul fattore di trascrizione nucleare eritroide-2 (NRF2), che regola la risposta citoprotettiva allo stress ossidativo e agli xenobiotici, e sul fattore di trascrizione EB (TFEB), il principale regolatore delle vie autofagiche e lisosomiali, poiché è noto che la loro deregolazione può comportare danno cellulare. Attraverso l'imaging ottico, esperimenti di immunocitochimica ed immunoistochimica ho dimostrato che nella linea di neuroblastoma dopaminergico SK-N-BE e nell'area celebrale murina corrispondente alla *substantia nigra par compacta* l'attivazione di Nrf2, ma non quella di Tfeb, precede la neurodegenerazione dopaminergica indotta dalla neurotossina MPP+. Lo studio è stato quindi focalizzato sulla dinamica di attivazione del fattore Nrf2 durante le fasi iniziali del processo neurodegenerativo indotto dall'inibizione dell'enzima GCasi, un evento che, come citato sopra, rappresenta il principale fattore

di rischio di contrarre la malattia di Parkinson. Gli esperimenti condotti su linee immortalizzate, su cellule primarie e modelli murini hanno permesso di identificare un nuovo meccanismo di comunicazione tra la microglia ed il neurone, basato sul contatto diretto tra le due tipologie cellulari che avviene attraverso strutture actina-dipendenti presenti nella microglia e che richiede un metabolismo energetico cellulare funzionale. Sorprendentemente, l'inibizione farmacologica della GCasi microgliale è sufficiente per interferire con la capacità della microglia di stimolare una comunicazione neuroprotettiva attraverso l'induzione del segnale NRF2. Lo studio ha infine fornito evidenze che tale disfunzione indotta dall'inibizione della GCasi potrebbe essere ripristinata attraverso un effetto compensatorio sul metabolismo energetico, suggerendo una nuova strategia terapeutica preventiva per la malattia di Parkinson.

In conclusione, la mia tesi ha dimostrato che i sistemi *reporter* sviluppati possono essere strumenti utili per lo studio della dinamica di segnali neuroprotettivi; questa tecnologia è stata sviluppata in particolare per quantificare la risposta allo stress ossidativo e delle vie autofagico/lisosomiali. In particolare, l'applicazione di tali sistemi ha permesso di dimostrare che l'inibizione della GCasi altera la comunicazione citoprotettiva microglia/neurone, aumentando la suscettibilità dei neuroni agli insulti neurotossici. In tal modo abbiamo identificato un nuovo meccanismo che potrebbe spiegare l'aumentato rischio di neurodegenerazione osservato nei portatori di mutazioni GBA1 fornendo un nuovo potenziale bersaglio per possibili strategie terapeutiche preventive.

2 INTRODUCTION

2.1 Parkinson's disease

Parkinson's disease (PD) is the second most common neurological disorder and affects more than 1% of individuals over the age of 60 (De Lau and Breteler, 2006; Pankratz et al., 2009). Symptoms of the disease are induced by the degeneration of dopaminergic neurons located in *the substantia nigra pars compacta* (SNpc) that innervate the corpus striatum (Olanow et al., 2009). The consequent depletion of dopamine in the nigrostriatal pathway, which is deputed to movement control, is at the base of the characteristic PD motor symptoms comprising muscle rigidity, bradykinesia, resting tremor and postural instability (Parkinson, 1817; Tagliaferro and Burke, 2016). PD patients are also affected by different non-motor symptoms, which are not directly related to the dopamine loss, such as constipation, hyposmia, rapid eye movement (REM)-sleep behaviour disorder, depression and cognitive alteration that normally worsen during PD progression, and at later stages frequently dementia (Jankovic, 2008; Obeso et al., 2010; Schapira et al., 2017).

The histopathological characteristic of PD is the presence, within dopaminergic neurons, of cytoplasmic inclusions constituted of proteinaceous aggregates, called Lewy bodies, mainly composed of α-synuclein (α-syn) (Lewy and Fritz, 1912; Braak et al., 1998). Similar abnormally aggregates, that form inclusion in the cell body or axons of neuron or oligodendrocytes, were also found in other brain areas in neurogenerative disorder that are catalogued as synucleinopathies (McCann et al., 2014). It is possible to diagnose the disease by identifying the characteristic motor symptoms but the univocal identification is performed *post mortem* ascertaining the presence of Lewy bodies in SNpc (Oppenheimer, 1992; Caslake et al., 2008). Noteworthy, studies estimate that when the clinical diagnosis of PD is confirmed around 40 to 60% of neurons in the SNpc are already lost and synaptic function is reduced by up to 80% (Fearnley and Lees, 1991; de la Fuente-Fernández et al., 2011); this suggests that PD is diagnosed only in late stages therefore, it becomes essential to identify alternatives method of diagnosis that might allow recognizing the early, mostly asymptomatic, phases in which the dopaminergic death will be negligible (Postuma and Berg, 2016).

PD is currently considered a multifactorial disease, due to the interaction between multiple risk factors, both genetic and environmental, which vary from patient to patient and to date, it has been impossible to identify a single cause. In about 10% of patients, the disease is family-transmitted and is triggered by mutations in specific genes but, in the majority of cases, PD does not have a direct

genetic inheritance and is defined as idiopathic (Lill, 2016). The mutations that inducing genetic PD (e.g. SNCA, LRRK2, PINK1, DJ-1, PRKN, UCH-L1) involve genes that perform a plethora of functions, confirming the complexity of the pathogenic mechanisms (Kalia et al., 2015).

The SNCA gene encoding for α-syn was the first to be identified and multiplication and mutations of SNCA drive autosomal dominant PD (Polymeropoulos et al., 1997; Koros et al., 2017). This evidence, in addition to the fact that α-syn aggregates are present in SNpc, attributes to this protein a key role in the pathogenesis of PD (Villar-Piqué et al., 2016; Koros et al., 2017). The theory proposes that soluble monomeric α-syn progressively transforms from soluble to insoluble fibrillary complexes and finally Lewy bodies (Fig. 1) (Cremades et al., 2017). Some structures acquired by α-syn in this process are noxious for neurons that degenerate and die (Eschbach and Danzer, 2014). Neurons constitutively synthesized α-syn, a protein that seems to be involved in the vesicle synaptic traffic and it is actively exchanged between brain cells, a process that can spread the α-syn neuronal pathology from one cell to another (McCann et al., 2014). A quite number of mechanisms, such autophagy failure, mitochondria dysfunction, endoplasmic reticulum (ER) stress and calcium dysregulation have been proposed to be responsible for the α-syn induced neurodegeneration (Benskey et al., 2016; Wong and Krainc, 2017). Although, the extent to which α-syn is involved in all cases of PD is not clear and some researchers propose that the Lewy body represents a form of damage limitation for the brain (Makin, 2016).

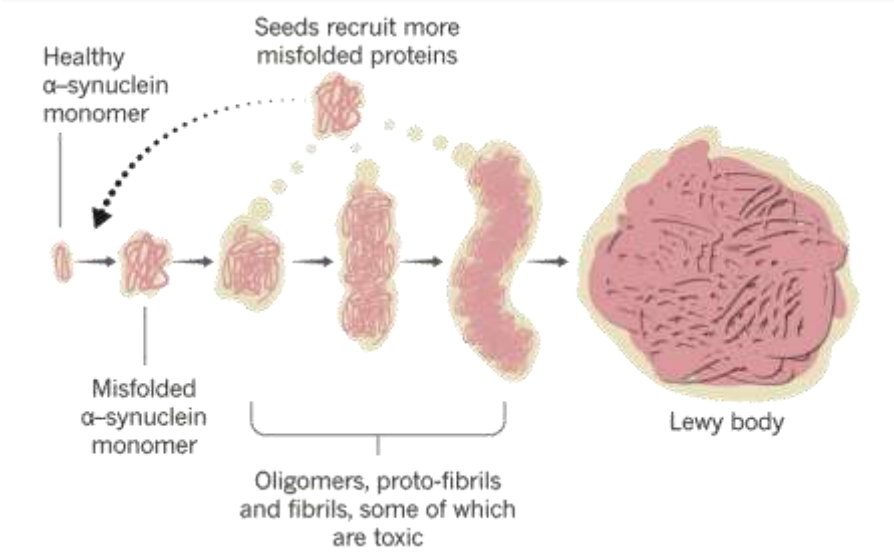

Figure 1: The prion principle of α-syn. Single molecules of α-synuclein can misfold and induce other monomers to do likewise, this process could generate oligomer, proto-fibrils and fibrils some of these forms are toxic for the cells. The precise role of α-syn in synucleinopathies is still unclear and certain researchers think that the aggregation into Lewy bodies might limits their toxicity. Image from (Makin, 2016).

Mutations in the LRRK2 gene, encoding for a kinase involved in synaptic morphogenesis, vesicular traffic, autophagy, protein synthesis and immune response, are the most frequent cause of autosomal dominant PD (Corti et al., 2011; Martin et al., 2014). Mutations that cause a reduction in the degradation capacity of the oligomers by the cells also contribute to the pathogenesis, these comprise the parkin (PRKN) and ubiquitin carboxyterminal-hydrolase (UCH-L1) genes (Dickson et al., 2009; Ragland et al., 2009). Parkin is abundantly expressed in the SNpc and plays a critical role in the ubiquitination of structurally altered proteins, instead UCH-L1 codes for an enzyme that removes ubiquitin from ubiquitinated proteins before their entry into the proteasome for degradations.

DJ-1, a redox-sensitive chaperone acting as a sensor for oxidative stress, and PINK1, a mitochondrial serine/threonine-protein kinase, suggest also a direct role of oxidative stress and mitochondrial pathways (Cookson, 2012) in PD pathogenesis. Mutations in PINK1, PRKN and in DJ-1 are defined as autosomal recessive.

It is also recognized that there are risk factors increasing the probability of developing the disease. These include environmental factors and lifestyle, such as exposure to pesticides (Paraquat), prolonged use of β-blockers, previous brain damage, living in rural areas, exposure to metals and an excessively iron-rich diet (Noyce et al., 2012). Some neurotoxins such as MPTP (1-methyl-4-phenyl-1,2,3,6-tetrahydropyridine) (Langston et al., 1983) and 6-hydroxydopamine (6-OHDA) (Ungerstedt et al., 1974) trigger selective degeneration of dopaminergic neurons in SNpc and cause Parkinsonism; these molecules are often used to generate animal models of PD (Blandini and Armentero, 2012). Furthermore, mutations in the GBA1 gene are recognized as the main risk factor for the disease (Migdalska-Richards and Schapira, 2016) (further detail in chapter 2.3).

Regarding the treatment, there are no cures able to block or revert the disease progression, which worsens during the time until patient death. Current therapies are based on the use of drugs able of increasing dopamine levels or stimulating dopaminergic receptors, in order to relieve motor symptoms and improve the patient's quality of life. In the long term, however, these therapies cause fluctuations in motor and non-motor symptoms and psychosis, while, in the later stages of the disease, motor symptoms no longer respond effectively to treatment (Savitt et al., 2006; Connolly and Lang, 2014).

Currently, one of the main objectives in pharmacological research is to develop drugs able of acting in the initial stages of the pathology, a phase in which the neuronal death will be less relevant, with the idea that it will be possible to slow down its progression (Coune et al., 2012; Lindvall, 2013; Postuma and Berg, 2016). These drugs would greatly reduce the socio-economic impact but, for effective discovery, is essential to shedding light on the early events triggering the dopaminergic neurodegenerations (Postuma and Berg, 2016).

2.2 Gaucher's disease

Gaucher's disease (GD) is the most common lysosomal storage disorder with an incidence between 1/40'000 and 1/60'000 births (Grabowski, 2008; Stirnemann et al., 2012), is an autosomal recessive pathology caused mainly by mutations of the GBA1 gene, which encodes the lysosomal enzyme β-glucocerebrosidase (GCase) (Hruska et al., 2008) and more rarely by the lack of saposin C, a GCase activator (Vaccaro et al., 2010).

β-glucocerebrosidase is a ubiquitous lysosomal enzyme that hydrolyses glucosylceramides into ceramides and glucose. Homozygous mutations in the GBA1 gene are responsible for the accumulation of lipid substrates within the lysosome and the consequent impairment of the structure and functionality of this organelle (Stirnemann et al., 2017). Mutations mainly affect phagocytic cells such as macrophages that acquire an abnormal morphology: they appear enlarged, with an eccentric nucleus and with cytoplasmic inclusions. These dysfunctional cells, known as Gaucher cells (Fig. 2), are the hallmark of the pathology and accumulate in different tissues (Grabowski and Beutler, 2001; Stirnemann et al., 2012).

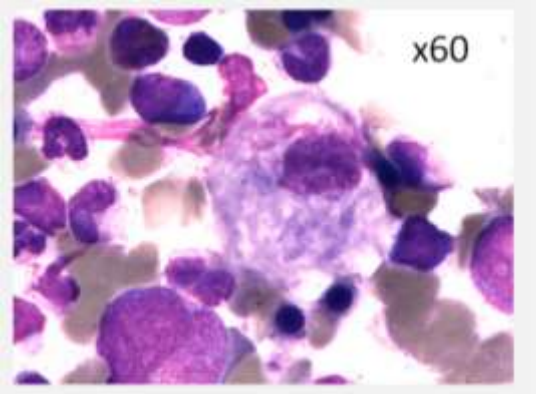

Figure 2. Gaucher cell. Optical microscope image of a macrophage with intracytoplasmic lipid accumulation and with a decentralized nucleus. Image from (Stirnemann et al., 2017).

More than 300 mutations in the GBA1 gene have been identified so far (Stirnemann et al., 2017). The most frequent mutations are N370S, which leads to partial inactivity and is usually associated with a non-neuropathic form of GD (type 1), and L444P, which involves a drastic reduction in the enzyme activity and is associated with a high risk of developing neurological impairment (type 2 and 3) (Hruska et al., 2008); although the loss of GCase activity is relevant for the pathology, the residual enzymatic activity and symptoms frequently do not correlate. GD rarely occurs as a result of

mutations in the PSAP gene coding for saposin C, a small lysosomal glycoprotein that functions as a cofactor for the degradation of sphingolipids within the lysosomes (Vaccaro et al., 2010).

GD is a heterogeneous pathology defined as a multiorgan disorder, the symptoms can arise at any age, from early childhood to adulthood, and they can range from asymptomatic forms to perinatal lethality. The main symptoms are hepatosplenomegaly, anemia, thrombocytopenia, bone disorders, and in a smaller number of cases, interstitial lung disease, pulmonary hypertension and neurodegeneration (Grabowski and Beutler, 2001). Gaucher cells accumulate in the spleen, hepatic sinusoids, bone marrow and more rarely in the lungs, worsening the symptoms (Stirnemann et al., 2017). According to the degree of neurological involvement, the disease is classified into three distinct clinical types (Erikson et al., 1997; Grabowski, 2008):

• type 1 - non-neuropathic: it is the most widespread form and represents about 94% of cases, the onset is mainly in adulthood and is characterized by very extensive symptoms with variable severity. Patients normally display visceral, blood and skeletal symptoms, in rare circumstance were also reported asymptomatic cases, or interstitial disease and pulmonary hypertension;

• type 2 - acute neuropathic: it is characterized by a rapid onset, progressive neurological deterioration and visceral symptoms. It can start in the prenatal phase, at birth or within the first year of life, has a serious prognosis with a life expectancy of fewer than 2 years;

• type 3 - sub-acute or chronic neuropathic: it is characterized by heterogeneous clinical manifestations such as more or less severe visceral symptoms and neuronal involvement. It has a later onset than type 2 and those affected can survive up to the third or fourth decade.

The diagnosis of GD is normally established through the test of a deficient GCase activity in total leukocytes, mononuclear cells, or cultured fibroblasts. GD patients retain a residual enzyme activity equal to 5-25% compared to healthy individuals whereas heterozygous healthy carriers show a reduction of 50% (Linari and Castaman, 2015; Migdalska-Richards and Schapira, 2016). Histological analysis of sample derived from bone marrow biopsies, liver or splenic tissues could be analysed to detect the presence of Gaucher's cells to confirm the diagnosis (Alaei et al., 2019).

The aim of current therapies for GD is to reduce the accumulation of glucocerebroside substrates and to prevent progressive disease and complications. There are two main therapeutic approaches,

the enzymatic replacement therapy (ERT) and substrate reduction therapy (SRT). The ERT aims to counteract the reduced catabolic activity by parenteral administration of heterologous GCase. The enzyme through the exposure of correct glycosidic residues interacts with macrophage mannose receptors, it is internalized by macrophages and restores cellular metabolism (Grabowski, 2008; Nagral, 2014). There are three recombinant enzymes approved: imiglucerase, velaglucerase and taliglucerase that have to be administered as an intravenous infusion normally over 2 hours every 15 days. This type of therapy is used to treat visceral symptoms as recombinant GCase are unable to cross the blood brain barrier (BBB) (Grabowski, 2008; Nagral, 2014). SRT aims at reduction of the synthesis of the substrates of the GCase thus allowing the residual endogenous enzyme to operate in order to avoid the accumulation of lipid substrates. The most used drugs are miglustat and eliglustat (Nagral, 2014), that are both selective inhibitor of glucosylceramide synthase and are administered orally exclusively in adult patients. Inhibitors are employed for a milder disease where treatment with ERT is not possible and the first effective results need approximately 1-2 years (Grabowski, 2008; Nagral, 2014).

Since nowadays the treatments for GD are not able to revert or block neurological symptoms the research is focused on molecules able to reduce the CNS pathology. In line with this, ambroxol, a BBB permeable GCase chaperone, is currently in clinical trials (Charkhand et al., 2019; Kumar et al., 2019). This molecule binding at high pH the abnormal GCase in the endoplasmic reticulum, favours its correct conformation, and once transported into the lysosome, the low pH allows the detachment from the GCase that can perform its function (Maegawa et al., 2009).

To improve quality of life and increase life expectancy, the discovery of new pharmacological treatments would be aimed at identifying molecules able to counteract neurological manifestation and that will not require complex administration procedures.

2.3 The relationship between GBA1 and PD

More than 20 years ago was discovered that numerous patients with Gaucher's type 1 had a high probability of developing PD (Neudorfer et al., 1996). It was subsequently confirmed, by multiple studies, that GBA1 mutations, both homozygous and heterozygous, confer a 20- to 30-fold increased risk for the development of PD (Maor et al., 2013; Li et al., 2014; Migdalska-Richards and Schapira, 2016) with those variants associated with the most severe neuropathic form of GD, displaying the highest risk. These studies identified GBA1 mutations as the major risk factors for PD; it was estimated that at least 5–10% of PD patients have a mutation in the GBA1 gene (Goker-Alpan et al., 2004), although not all GBA1 heterozygous/homozygous individuals will develop PD (Lesage and Brice, 2009; Lesage et al., 2011).

PD patients carrying GBA1 mutations (PD-GBA1) have a slightly younger age of onset, major incidence of neuropsychiatric features, and have a greater risk for worst cognitive impairment (Tan et al., 2007; Sidransky et al., 2009; Brockmann, 2020), but at the clinical level, they cannot be distinguished from idiopathic PD. PD-GBA1 pathology is identical to idiopathic PD, with an asymmetric pattern of SNpc dopamine cell loss, Lewy bodies, and neurites containing α-syn. Also, the response to dopaminergic therapy appears to be the same as that seen in idiopathic PD, including the development of motor complications (Ziegler et al., 2007; Schapira, 2015).

The mechanism by which GBA1 mutations increase the risk of PD is still unidentified. However, given the similitude between PD-GBA1 and idiopathic PD patients, it has been hypothesized that GBA1 mutations may play a role in α-syn accumulation, mitochondrial and autophagic dysfunction, oxidative imbalance, ER stress and inflammation (Schapira and Tolosa, 2010; Migdalska-Richards and Schapira, 2016).

Studies trying to assess the mechanistic role of GBA1 regarding PD-GBA1 impairment supports both loss- and gain-of-functions theories for GCase. The loss-of-function theory is sustained by the fact that some PD-GBA1 patients have GBA1 alleles not encoding a GCase (Aharon-Peretz et al., 2004; Gan-Or et al., 2008; Clark et al., 2009), moreover, inhibition of GCase activity with conduritol-B-epoxide (CBE) in cells and animal models leads to α-syn accumulation (Cleeter et al., 2013; Migdalska-Richards and Schapira, 2016). Furthermore, homozygous knock-out (KO) of the Gba1

gene in mice leads to mitochondrial dysfunction and α-syn accumulations (Enquist et al., 2007; Osellame et al., 2013). The gain-of-functions hypothesis for GBA1 mutations is supported by the fact that most PD-GBA1 patients carry missense mutations resulting in the production of misfolded GCase, that can interact directly with α-syn (Sidransky and Lopez, 2012). At present, both loss- and gain-of-function theories have limitations and contradictory evidence are present in literature (Migdalska-Richards and Schapira, 2016).

Interaction between GCase and α-syn in lysosomes may have functional consequences in neurodegeneration (Yap et al. 2011). Such interactions are supported by immunohistochemical assays on brain tissue samples from PD-GBA1 patients showing that mutant GCase and α-syn co-localize *in vivo* into Lewy bodies (Goker-Alpan et al., 2010). In cell and animal models were demonstrated that i) overexpressing mutant GCase (containing N370S, L444P, D409H, D409V, E235A, or E340A), ii) knocking down the Gba1 or iii) inhibiting GCase activity, resulted in an increased α-syn level (Cullen et al., 2011; Osellame et al., 2013; Fernandes et al., 2016). Conversely, it has also been demonstrated that α-syn accumulation causes a decrease in activity and protein levels of GCase (Gegg et al., 2012). Reduced GCase activity was found in the brain and in the cerebrospinal fluid in PD patients and is associated with an increased level of α-syn (Murphy et al., 2014; Parnetti et al., 2014). Altogether these findings led to the bidirectional feedback loop hypothesis according to which GCase deficiency facilitates the formation and accumulation of α-syn oligomers, which in turn leads to the further decreases in GCase activity, able to promote the formation of additional α-syn oligomers (Migdalska-Richards and Schapira, 2016).

GCase impairment has been shown to affect also lysosomal functionality, which leads to the accumulation of misfolded proteins with a high bent of aggregation due to inhibition of their degradation pathway. Unfolded GCase can be inappropriately translocated to the lysosome remaining trapped, promoting ER stress and triggering negative impacts on cell viability (Cleeter et al., 2013; Osellame et al., 2013).

In PD pathogenesis, mitochondrial impairment plays an important role (Schapira et al., 1989, 1990) and the decline of mitochondrial functionality normally results in the generation of reactive oxygen species (ROS) and free radicals that are able to trigger neuronal death. In line with these findings, in cell and animal models, it was observed that GCase inhibitions and GBA1 mutations lead to : i) generation of dysfunctional and fragmented mitochondria, ii) decline in mitochondrial membrane

potential, iii) reduction in respiratory chain complex activities and oxygen consumption and iv) increase in free radical generation (Cullen et al., 2011; Osellame et al., 2013).

Further support to the close casual relation between GCase and PD pathogenesis is the increased dopaminergic susceptibility to toxic molecules used to experimentally induce parkinsonism, such as MPTP, rotenone and α-syn (Fishbein et al., 2014; Schöndorf et al., 2014; Noelker et al., 2015; Migdalska-Richards et al., 2017; Kim et al., 2018; Yun et al., 2018; Mus et al., 2019) upon pharmacological inhibition of GCase activity in cell and animal models; furthermore, these studies suggest that GCase and neuroprotective pathways could be entangled in a common mechanism.

Finally, the contribution of neuroinflammation in the GCase-mediated neurodegeneration is far to be clarified, although, inflammatory response and microglia activation were detected in different GD mouse models including the dopaminergic-specific GBA1-KO and after the pharmacological inhibition of GCase with CBE (Rocha et al., 2015; Soria et al., 2017; Musgrove et al., 2019). These studies support that the interplay among neurons with other brain cells should be taken into account to unravel the mechanism underlying the PD-GBA1 pathology.

Whatever is the mechanism, still it is unclear why the majority of individuals with GBA1 mutations do not develop PD; current hypothesis is that mutated GCase on its own produces several effects that are collectively not sufficient to induce PD, and other triggering events must occur before PD-GBA1 can develop (Migdalska-Richards and Schapira, 2016).

2.4 Microglia

2.4.1 Introduction to the cell

Microglia represent approximately the10% of the total cells constituting the CNS in adult humans (Lawson et al., 1990; Aguzzi et al., 2013) and while they perform typical tasks of glial and immune cells they were historically defined as the resident macrophages of the brain (Ginhoux et al., 2010). Dissimilar from other CNS cells, which derive from the neuroectoderm (Prinz and Priller, 2014), microglia originate from erythromyeloid precursors in the mesoderm of the yolk sac, during embryonic development, they migrate to the brain parenchyma where they start to proliferate and differentiate into microglial cells (Ginhoux et al., 2010; Kierdorf et al., 2013) able to self-renewing and maintaining a constant number (Tay et al., 2017).

Microglia are plastic cells able to change their function and morphology in response to the signals received. Microglia are constantly sensing the cerebral microenvironment through extremely mobile processes (Davis et al., 1994; Heindl et al., 2018; Cserép et al., 2020) and play an active role in promoting correct neuronal development, in maintaining the physiological state of the brain and in countering the damage caused by endogenous or exogenous agents (Fig. 3) (Nimmerjahn et al., 2005; Kettenmann et al., 2011). In line with their nodal function, microglia cells are able of influencing the pathological course of multiple brain diseases ranging from brain trauma to psychiatric disorder (Prinz and Priller, 2014). As microglia can have different behaviour they were described both as protective or detrimental players (Popovich and Longbrake, 2008; Song and Colonna, 2018), making the study of these cells essential in order to elucidate the etiopathogenesis and develop effective therapeutic strategies.

2.4.2 Microglia functions

Microglia cells in physiological conditions have a “branched morphology” typical of the surveillance state and scan the brain parenchyma using large tubulin-dependent cell processes and filopodia, small actin-dependent filaments (Bernier et al., 2019). In addition to monitoring the cerebral microenvironment, microglia are able to sense signals from the systemic circulation through direct contact with the blood vessels of the BBB (Gomez-Nicola and Perry, 2015) and mediate information

to other brain cells (Perry and Teeling, 2013) (Fig. 3). Microglia constitute the component of the innate immunity of the CNS, in the presence of pathogens and toxic compounds, such as protein aggregates and apoptotic cells, trigger the inflammatory response by releasing cytokines and ROS (Smith et al., 2012). Accordingly, microglia assumes a pro-inflammatory phenotype characterized by an amoeboid shape and a specific pattern of exposed cellular proteins such as the major histocompatibility complex II (MHC II) and the chemokines CCL2 and CCL20. Once the pro-inflammatory stimulus is concluded, microglia shift their phenotype to a reparative one characterized by an increase in the expression of the arginase 1 (ARG1) gene and are able to support the repair of damaged tissues (Cherry et al., 2014; Orihuela et al., 2016). A balance between pro- and anti-inflammatory states is necessary, since if the phlogistic state is protracted over time it can have a toxic effect on neuronal cells and exacerbate the neurodegeneration (Heneka et al., 2014; Lively and Schlichter, 2018).

Microglia maintain a clean environment by engulfing apoptotic cells, debris and protein aggregates. These phagocytic functions increase especially during development or consequently to brain damage or infection (Kettenmann et al., 2011). Microglial migrate to different regions of CNS following the signal released by cells undergoing programmed cell death and interact with the material to be degraded. The compound to be internalized must interact appropriately with microglial receptors to induces the extroflexion of microglia membrane and the formation of the phagosome around the target. The incorporated material is degraded through the autophagic-lysosomal pathway: the internalized phagosome is fused with lysosomes to form the phagolysosome that is subsequently incorporated together with other phagolysosomes into the gastrosome, the final organelle of degradation (Villani et al., 2019). The phagocytosis process is highly regulated: one of the main regulatory mechanisms is mediated by eat me signals such as phosphatidylserine residues which are normally localized in the cytoplasmic side of the membrane and are externalized by apoptotic cells in order to be degraded. Other phagocytosis activators are phospholipids and lipoproteins that interact with TREM2 (triggering receptor expressed on myeloid cells 2); which is a direct phagocytosis mediator inducing a peculiar phenotype in neurodegeneration-associated microglia (Takahashi et al., 2007; Ulland et al., 2017a). Interestingly, hypomorphic TREM2 mutations increase the risk of developing Alzheimer's disease (AD) and PD (Parhizkar et al., 2019); it was demonstrated that the consequence of these mutations is a

dysfunctional autophagic pathway in microglia that can exacerbates the accumulation of protein aggregates such as amyloid fibrils and α-syn (Janda et al., 2018).

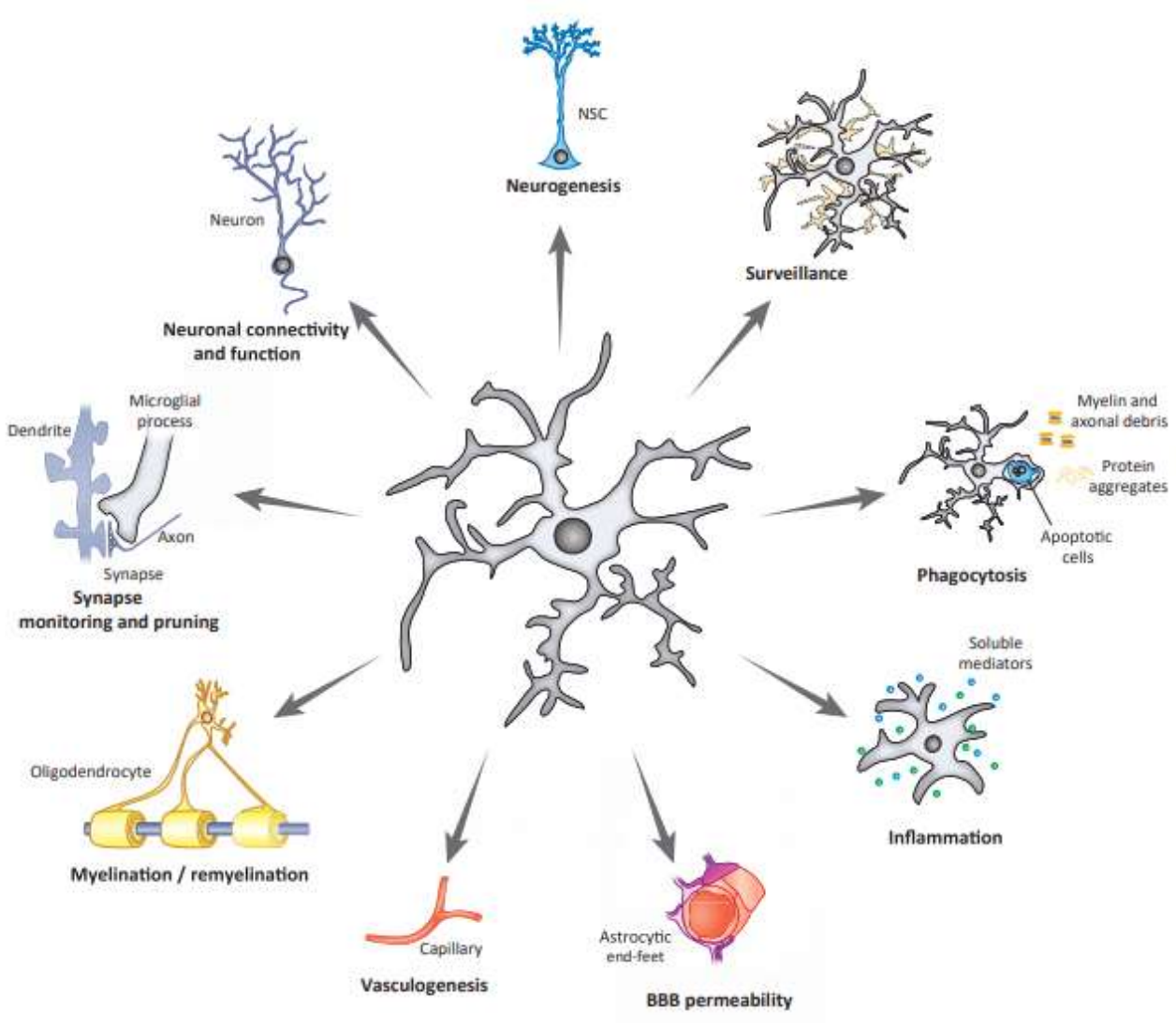

Figure 3. Microglia key functions. Microglia have high motility processes that assist brain surveillance tasks. In pathological conditions, microglia perform classical immune functions, such as release of inflammatory mediators and phagocytosis of cellular debris. Moreover, microglia perform several homeostatic duties e.g synapse monitoring and pruning, and are able of interacting with other brain cells, impacting on their function and development. Image from (Sierra et al., 2019).

In addition to the functions described above, microglia from the embryonic stage and throughout the duration of adult life have a fundamental role in directing and controlling the formation of the CNS; by secreting trophic factors such as insulin-like growth factor (IGF-1), brain-derived neurotrophic factor (BDNF), nerve growth factor (NGF), glial-derived neurotrophic factor (GDNF) and prostaglandins (E2PGE2) (Garden and Möller, 2006; Lenz and Nelson, 2018), microglia are able

to induce neurogenesis and oligodendrogenesis, thus sustaining brain homeostasis (Shigemoto-Mogami et al., 2014).

Microglia contribute to synaptogenesis and synaptic remodelling with a process called pruning playing an essential role during CNS development since ensure the correct establishment of neuronal network connections (Paolicelli et al., 2011; Bilimoria and Stevens, 2015; Filiano et al., 2015; Baxter and Hardingham, 2016). Microglia remove excess and malfunctioning synapses through a C1q and C3 complement factors mediated mechanism (Veerhuis et al., 2011; Schafer et al., 2012) and fractalkine molecules (CX3CR1 and CX3CL1) (Tremblay et al., 2010; Gomez-Nicola and Perry, 2015). There are increasing evidences that microglial cells are responsible for the removal of synapses also in the normal healthy brain contributing to neuronal plasticity (Kettenmann et al., 2013; Šišková and Tremblay, 2013; Hong et al., 2016; Hristovska and Pascual, 2016). Microglia regulate the neuronal activity assessing the engulfment of synaptic structures and removing those that display reduced inputs, establishing neuronal circuits by forming associations between neuronal axons and synaptic targets (Sierra et al., 2019)

Immunometabolism studies have highlighted metabolism as a factor able to control peripheral and CNS immune responses. Microglia can rapidly switch from glycolysis to other metabolic pathways and adapt their energy metabolism to nutrient availability under acute metabolic stress, a mechanism that consents to maintain their essential functions. The microglia metabolic reprogramming from oxidative toward aerobic glycolysis is necessary for proper immune actions and cytokine release. In line with this, microglial metabolic adaptation to disease rises as a critical aspect of the pathogenesis of neurological disorder (Bernier et al., 2020); an example is that elevated risk of developing AD is associated with hypomorphic variants of TREM2. Ulland and collaborators (Ulland et al., 2017b) studying microglia with TREM2 risk variants and Trem2-deficient mice with AD-like pathology detected anomalous autophagic functionality linked to ATP cellular levels, a phenotype that they partially rescue administrating molecules able to supply ATP. Their experiment corroborates that TREM2 supports microglial responses during AD by increasing energetic and biosynthetic metabolism in cells. Thus, confirming that bioenergetic regulation must be taken into account when microglia response was studied.

2.4.3 Neuron-microglia communication

Microglia is able to communicate with other CNS cells, in particular, it is known that the neurons are able to control the activation and motility of the microglia through "off" signals, expressed in physiological conditions in order to keep the microglia in the resting state, and "on" signals expressed when cellular damage occur to trigger microglial activation (Biber et al., 2007); at the same time, microglia are able to modulate neuronal activity (Szepesi et al., 2018). These bidirectional interactions can be carried out both by contact-independent mechanisms (Fig. 4), based on the release of soluble factors such as neurotrophins, neuropeptides, neurotransmitters, chemokines, cytokines (Kerschensteiner et al., 2009) and extracellular vesicles (Szepesi et al., 2018), and *via* a direct contact requiring physical interaction between cells (Marinelli et al., 2019).

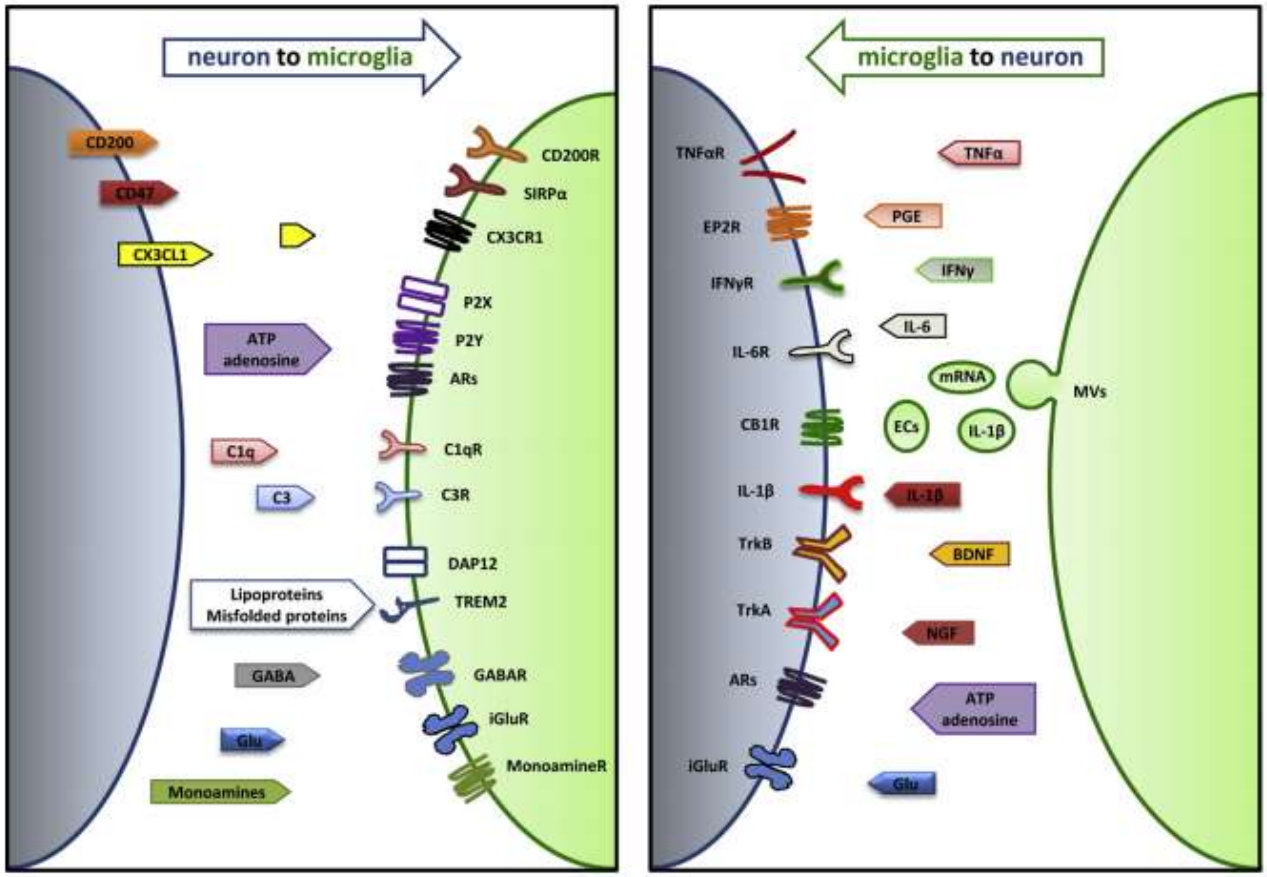

Figure 4. Bidirectional communication between neuron and microglia. It is schematic reported the main molecular signalling involved in the bidirectional neuron-microglia communication concerning the release of soluble factors. Image from (Marinelli et al., 2019).

Contact-independent mechanisms

Neurons release specific molecules able of reducing the pro-inflammatory microglial response, such as transforming growth factor beta (TGF-β), BDNF, NGF and neurotrophin 3 (NT-3) molecules able to preventing excessive microglial pro-inflammation, thus limiting potential tissue damages (Abutbul et al., 2012; Tian et al., 2012; Szepesi et al., 2018). CD22 glycoprotein is also a factor involved in the negative control of inflammation; CD22 is released into the extracellular space following cell damage, and, upon binding to the microglial transmembrane tyrosine phosphatase receptor (CD45) (Stamenkovic et al., 1991), it reduces the production of pro-inflammatory cytokines including IL-β and TNF-α (Mott et al., 2004).

The nucleotides ATP, ADP and UDP are released from the damaged cells and, by interacting with their purinergic receptor P2Y12, attract microglia to the site where the damage occurred, through a process called chemotaxis (Davalos et al., 2005). It is known that the expression of P2Y12 increases in the initial stages of the microglial response, while it decreases following cell activation, confirming its role in initiating phagocytosis (Haynes et al., 2006). TREM2, when activated by "eat me" signals released by apoptotic neurons (Hsieh et al., 2009), stimulating pathways able to reduce the pro-inflammatory response avoiding the exacerbation of the damage derived from chronic inflammation (Takahashi et al., 2007). Neurotransmitters, such us γ-aminobutyric acid, noradrenaline, glutamate, dopamine and glycine, through the interaction with their own membrane receptors, are able to differentially modulate microglia proliferation and activity in relation to microenvironmental conditions influencing the neuroinflammatory response (Zeilhofer, 2008; Szepesi et al., 2018). Microglia control homeostasis in response to changes occurring in the cerebral microenvironment or upon direct stimulation by molecules secreted by neurons; a response mediated by the finely tuned release of cytokines like IL-β, or neurotrophic factors such as BDNF, IGF-1, NGF, GDNF and PGE2 supporting neurogenesis, oligodendrogenesis and synaptic pruning (Garden and Möller, 2006; Pribiag and Stellwagen, 2014; Shigemoto-Mogami et al., 2014; Lenz and Nelson, 2018).

In addition to paracrine communication, microglia and neurons are able to communicate across long distances by releasing and receiving extracellular vesicles (EVs). The microglial cells secrete EVs (0.1-1μm) which contain a large number of molecules e.g. miRNA, enzymes and proteins able of regulating miscellaneous functions (Paolicelli et al., 2019).

Cell-to-cell communication mechanisms

Communications can be also mediated by direct interaction between proteins present on the microglial membrane and on the membrane of CNS cells, which require the cells to be confined to a neighbouring space. In physiological condition, microglia are kept in a resting state by the interaction between the neuronal protein CD200 and its target receptor located on microglial and macrophage cells (Hoek et al., 2000; Wright et al., 2000). Cell communication mediated by CD200 is fundamental for the microglia-mediate neuroprotection, as decreased activation of this pathway has been demonstrated to be essential for the onset and progression of the neuroinflammation associated to neurodegenerative diseases. CX3CL1 is a chemokine that is constitutively expressed in neurons, while its receptor, CX3CR1, is predominantly found on the microglia membrane. CX3CL1–CX3CR1 signalling is a neuronal '"off" signal that keeps microglia in a surveying phenotype (Nishiyori et al., 1998; Biber et al., 2007; Paolicelli et al., 2014; Sultana et al., 2016). In particular, in the presence of cell damages it is released by neurons as a soluble molecule to modulate chemotaxis, while as a membrane receptor activates a series of pathways inducing microglial activation and increasing phagocytosis (Szepesi et al., 2018). The expression of this receptor increases during the genesis of the CNS and promotes the establishment of functional neuronal circuits and synaptic remodelling (Ueno et al., 2013).

The phagocytosis process is mediated by the complement factor receptor C3 (C3R), located on microglia cells, that is activated by the interaction with complement factors, expressed by neurons in pathological conditions (Marinelli et al., 2019). C3 has been involved in synaptic remodelling and in the elimination of those neurons that have not been integrated into functional circuitries, especially during neurogenesis (Colonna et al 2017, Marinelli et al 2019). Alteration in C3 and C3R expression has been demonstrated in neurodegenerative diseases characterized by significant neuronal loss, accumulation of abnormal proteins and synaptic alterations (Veerhuis et al., 2011; Ulland et al., 2017a). A correct phagocytosis control requires inhibitory molecules such as the neuronal integrin CD47, which binds the signal regulator protein α (SIRPα) located both on myeloid cells and on neurons, negatively regulating phagocytosis and microglial secretion of pro-inflammatory cytokines (Sato-Hashimoto et al., 2019).

Recent evidence supports the existence of somatic microglia–neuron junctions characterized by specialized nanoarchitecture optimized for purinergic signalling, and that microglial processes at these junctions could potentially monitor and protect neuronal functions in a process that involves

P2Y12 receptor (Cserép et al., 2020). Overall, an appropriate interaction and communication between brain cells are considered to be instrumental to support the homeostasis of neuronal networks.

2.4.4 Analogy between microglia and macrophages

Microglia share with macrophages some similar functions that will be briefly described herein. Macrophages are immune system cells responsible for diverse tasks in homeostatic and immune responses. They eliminate all potentially harmful factors through phagocytosis and the secretion of pro-inflammatory cytokines with the aim of restoring homeostasis and promoting tissue repair (Viola et al., 2019). Macrophages originate, during embryonic development, from progenitors located in the yolk sac (similarly to what previously described for microglial cells) and in the foetal liver. These erythromyeloid precursors migrate throughout the body, differentiating into specialized cells and generate sub-populations, such as microglia in the CNS (Ginhoux et al., 2010), Kupffer cells in the liver and other resident macrophages present in several tissues. Unlike microglia, during the course of inflammatory phenomena, monocytes derived from hematopoietic stem cells of the bone marrow differentiate and replace the population of resident macrophages (Ginhoux and Guilliams, 2016).

Macrophages are extremely active cells, they respond to changes in the microenvironment, carrying out a series of functions. In the physiological state, macrophages express high levels of the CX3CR1 and execute continuous surveillance of the tissue in which they reside to identify and counteract any alterations to restore homeostasis (Murray and Wynn, 2011); they also communicate bidirectionally with other cells, throughout physical interactions and the release of secreted factors (Gordon and Martinez-Pomares, 2017).

Macrophages engulf apoptotic cells during development and in adult life, eliminate debris and pathogenic microorganisms by the release of enzymes, free radicals and a series of cytokines such as TNF-α, IL-1β and NO (nitric oxide), which attract and orchestrate the response by other immune cells (Murray and Wynn, 2011; Gordon and Martinez-Pomares, 2017). As like microglia, when macrophage cells express high levels of ARG1 participate in the reduction of the intensity and duration of inflammation. In this polarization macrophages promote tissue repair by releasing

growth factors e.g. TGF-β, which stimulate epithelial cells and fibroblasts and participate in the turnover of the extracellular matrix (Murray and Wynn, 2011). Unbalanced activation of macrophages and protracted inflammation lead to the onset of numerous pathologies (Sica et al., 2015).

2.4.5 Microglia in inflammatory and neurodegenerative diseases

In multiple sclerosis microglia and macrophages are considered as the damaging elements (Bogie et al., 2014; Giunti et al., 2014). In the mouse model of autoimmune encephalomyelitis (EAE), the depletion of microglia induces a delay in the onset, reduces the severity of clinical symptoms and decreases inflammation, indicating that microglial can be detrimental. Activated microglial cells correlate with clinical disability in human brains and microglial clusters form before the onset of clinical symptoms. These evidence indicate that microglial cells are involved in the early development of this disease and their activation precede demyelination and lesion formation; at the same time, microglia might be involved in the disease progression since axonal degeneration has been shown to trigger microglial activation. Conversely, stimulation of microglia phagocytosis was demonstrated to increase the removal of apoptotic cells and myelin debris resulting in a marked amelioration on the clinical outcome.

Microglia play a differential role in early and later stages of ischemia (Gelosa et al., 2014; Lee et al., 2014; Benakis et al., 2015; Fumagalli et al., 2015; Savitz and Cox Jr, 2016). Stroke is associated with neuronal depletion, activation of microglia, and infiltration of blood-borne immune cells. After the lesion, microglial are the first cells to be activated to clear cell debris by phagocytosis and to contribute to the resolution of inflammation; however, in later stages, in association with infiltrated macrophages, they can prolong inflammation and worsen the outcome.

In the aged brain, it is often found a peculiar microglia subtype, named “primed” microglia, that is more responsive to proinflammatory *stimuli*. Compared to naïve microglia, primed microglia prolong the proinflammatory responses and are less sensitive to anti-inflammatory *stimuli; w*ith their unbalanced response, they promote neuronal loss and enhance the progression of neurodegenerative diseases (Norden and Godbout, 2013; Perry and Holmes, 2014). Primed microglia present a peculiar morphology with enlarged soma and shorter branches and can be detected in a variety of neuropathological conditions. It is believed that these peculiar microglia

originate from persistent neuroinflammation and/or exposure to misfolded proteins and/or neuronal debris occurring during aging or neurodegenerative diseases.

Microglia express specific pattern recognition receptors (PRRs) able to detect damage-associated molecular patterns (DAMPs) comprising misfolded proteins, aggregates, and cellular debris that can be released by damaged cells and are found under neurodegenerative conditions (Santoni et al., 2015). Aggregated Aβ, α-syn, mutant huntingtin, the superoxide dismutase 1 act as DAMPs and activate PRRs with a consequent sustained release of neuroinflammatory factors, which causes cell death, promotes pathology, and contributes to disease progression.

There is a frank link between brain immune alterations and AD pathogenesis (Gold and El Khoury, 2015; Heppner et al., 2015; Malik et al., 2015; ElAli and Rivest, 2016). Genome-wide association (Zhang et al., 2013a; Heneka et al., 2014) studies have revealed that some single nucleotide polymorphisms (SNPs) that are risk factors for AD encode proteins that are related to signalling pathways leading to phagocytosis and microglial cytokine production (e.g. TREM2, CD33, CR1, ABCA7, SHIP1, APOE). A transcriptome study on *post mortem* brain tissues from AD patients identified immune- and microglia-specific modules strongly associated with late-onset AD pathology, which contained the TREM2-associated protein as the main regulator (Zhang et al., 2013a).

Reactive microglia secreting proinflammatory cytokines, chemokines, ROS, and acute phase proteins were detected in the microenvironment surrounding Aβ plaques (Heneka et al., 2013; Wolf et al., 2017), but the Aβ plaques-associated microglia displayed a less motile phenotype compared to wt, suggesting a decreased functionality of microglial cells. Recent studies showed that microglia is able to phagocytise Aβ and that this process involves TREM2 receptor activation, metabolic reprogramming (Ulland et al., 2017b) and the presence of secreted Aβ-degrading enzymes; however, microglia clearance capacity decreases with the age and with the overload of Aβ plaque in a possible vicious loop (Krabbe et al., 2013; Ulland et al., 2017a). Thereby, the decreased phagocytic activity in AD pathology may have the final consequence to promote protein aggregations.

Several studies addressed the microglia involvement in amyotrophic lateral sclerosis (ALS) (Boillée and Cleveland, 2008; Henkel et al., 2009; Brites and Vaz, 2014) collectively proposing that at the early stage microglia exert protective effects increasing the expression and release of BDNF, but at

a later stage it was shown to enhance motor neuron death due to secretion of neurotoxic factors. In this case, microglia may ultimately accelerate disease progression. Moreover, since missense variants of TREM2, granulin, and profilin 1 are acknowledged as risk factors for ALS, seems to be reasonable that phagocytic activity and inefficient degradation of phagocytized material could play a role in the disease onset and progression.

A plethora of studies suggested a key role of microglia in PD pathogenesis. The progressive accumulation of α-syn parallels inflammatory changes occurring in the brain and in the periphery (Kannarkat et al., 2013); the chronic inflammatory process associated with the overproduction of pro-inflammatory cytokines and oxidative stress has been shown to contribute to neuronal degeneration. The immune response in PD does not involve only microglial cells, peripheral monocytes (Funk et al., 2013; Grozdanov et al., 2014), lymphocytes (Bas et al., 2001; Gruden et al., 2011; Schafer et al., 2012), as well as the release of immune soluble mediators, have been reported by several studies. Interestingly, a genome-wide association analysis identified polymorphisms related to increased risk of PD among genes primarily expressed by microglia and macrophages (Nalls et al., 2014). Microgliosis, a term comprising any deviation from what is considered physiological microglia status (including cell number, morphology or protein expression) (Joers et al., 2017), has been detected in animal models of PD and in the brain of PD patients both *post mortem* and in living subjects by *in vivo* PET imaging analysis (Gerhard et al., 2006; Stokholm et al., 2017). A tight association between microgliosis and presence of α-syn aggregates has been described, irrespectively from the presence or absence of neuronal cell death (Hunot et al., 1996; Knott et al., 2000; Imamura et al., 2003; Croisier et al., 2005), suggesting that microglia activation may precede neuronal death. A differential expression pattern of molecules involved in the inflammatory process including MHCII+, iNOS, COX, CD68, TNF-α and a chronic pro-inflammatory milieu due to increased cytokines such as IL-1β, IL-2, IL-6, EGF, and TGF-α and TGF-β, has been reported by comparing the brain of PD patients with matching normal controls (McGeer et al., 1988; Boka et al., 1994; Hunot et al., 1996; Banati et al., 1998; Croisier et al., 2005; Orr et al., 2005). Immunohistochemistry analysis of the brain of PD patients clearly identified activated microglia in close contact with neurons presenting α-syn pathological accumulation (Croisier et al., 2005). Indeed, deposits of α-syn is a strong chemo attractive stimulus towards microglia for the physiological attempt of clearing the extracellular waste (Lee, 2008), in order to avoid the spreading of the pathology to neighbouring neurons. However, the status of microglia activation heavily

influences the ability to remove the extracellular waste (Lee, 2008; Park et al., 2008); intriguingly, it was demonstrated that certain molecular species of α-syn were able to interfere with the phagocytic microglial activity. On top of this complexity, microglia/macrophages ability to engulf α-syn was also show to decrease with age (Bliederhaeuser et al., 2016).

In this picture, it is not surprising that defective autophagy could have an important role, a conclusion supported by the fact that deficiency in the DJ-1 gene, responsible for 1% of the PD hereditary cases, impairs autophagy and reduces α-syn phagocytosis by microglia (Nash et al., 2017). The direct relationship between α-syn and neuroinflammation is also sustained by other studies showing that α-syn can act as DAMP and trigger the inflammatory response mediated by NF-κB (Ferreira and Romero-Ramos, 2018). They reported that NF-κB activation can lead to the secretion of high levels of oxygen species (ROS) and inflammatory cytokines such as IL-1β, IFN-γ and TNF-α (Klegeris et al., 2008; Su et al., 2008; Lee et al., 2009; Roodveldt et al., 2010; Couch et al., 2011) causing widespread inflammation and generating an increased level of oxidative stress (Kim and Joh, 2006).

From the molecular point of view, inflammatory and oxidative stress pathways are deeply entangled in PD. In particular, there are evidences showing that the NF-kB and NRF2 pathways are differentially triggered by diverse forms of α-syn presented by the neurons, which in turn induce different microglial behaviours: in fact, when α-syn is complexed to dopamine, instead of inducing NF-κB pathway, activate Nrf2, a transcription factor essential to tuning the balance between pro- and anti-inflammatory microglial activation (Rojo et al., 2010). This alternative response leads to the upregulation of antioxidant genes and reduces the expression of genes involved in the generation of ROS (Béraud et al., 2013). Lack of NRF2 results in the failure of the microglia response that exacerbates α-syn toxicity due to increased production of IL-6, IL-1β, iNOS, reduced phagocytosis and α-syn accumulation (Lastres-Becker et al., 2012). Accordingly, overexpression of Nrf2 in the brain has been shown to be neuroprotective in models of synucleinopathy (Gan et al., 2012).

Several studies observed the role of α-syn from another corner: other cell lineages in patients express α-syn including monocytes, lymphocytes and other immune cells (Shin et al., 2000). Further investigation highlighted that the B cells (Xiao et al., 2014b) and T cells functions were impaired knocking down the α-syn gene (Shameli et al., 2016); moreover, lack of α-syn in microglia resulted in an overheled response to LPS and reduced phagocytic ability (Austin et al., 2006) likely due to a

defective α-syn-dependent intracellular signalling in microglia (Austin et al., 2011). On the contrary, the overexpression of α-syn in immune cells impaired their phagocytic activity (Rojanathammanee et al., 2011); this observation was confirmed in the immortalized BV-2 microglia cell clones overexpressing α-syn, in macrophages derived from iPSC with triplication of SNCA gene or overloading α-syn in culture media (Haenseler et al., 2017). Accordingly, lymphocytes derived from PD patients and peripheral monocytes/macrophages from α-syn transgenic mouse line showed impaired vesicle transport, defective phagocytosis and defective cytokines release (Gardai et al., 2013). Therefore, both α-syn loss- and gain-of-function can have significant consequences in the capacity of microglia to phagocyte and handle the protein and maintaining a healthy CNS environment.

Resuming, microglia response during neurodegenerative diseases can produce opposite consequences: any change in neurons occurring during the pathogenetic course (e.g. neurotransmitter release, ATP production, synaptic loss) is sensed by microglia whose selective reaction can either increase or contrast cell death (Sanchez-Guajardo et al., 2010; Moehle and West, 2015). Moreover, microglial dysfunctions affecting their essential functionality produce alterations in brain physiology. In this context, it is tempting to speculate that therapeutic strategies able to pharmacologically modulate microglia functionality to shift the equilibrium towards the beneficial effects will be used to tackle neurodegenerative diseases. However, since microglia play an ambivalent role during brain pathogenesis it appears essential to identify robust markers associated with the selective pathogenesis stage and to profile the patient's immune system in order to select the pertinent immunomodulatory agent (Ferreira and Romero-Ramos, 2018).

2.5 Regulation of cellular redox state: the role of NRF2

2.5.1 NRF2 pathway

The body is continuously exposed to ROS and reactive nitrogen species (RNS) derived from endogenous metabolic processes such as cellular respiration or exposure to external agents. ROS constitute molecules able to activating physiological processes for instance cell division, immune responses, phagocytosis, inflammation and the detoxifying response (Finkel, 2011) but when they are not counterbalanced by antioxidant defense systems induce the oxidation of cellular macromolecules and increase the probability of the onset of various types of pathologies (Bossy-Wetzel et al., 2004; Kaidery et al., 2013; Hayes and Dinkova-Kostova, 2014).

The nuclear factor erythroid 2-related factor 2 (NFE2L2, also known as NRF2), a member of the CNC (cap 'n' collar) transcription factor subfamily bZip (basic region leucine zipper), is a transcription factor expressed in all tissues and constitutes one of the main regulators of the adaptive response to oxidative stress, induced by oxidizing and electrophilic species (Gan and Johnson, 2014). Under physiological conditions, NRF2 has a half-life of about 20 minutes and is mainly localized in the cytoplasm linked to Kelch-like ECH-associated protein 1 (KEAP1) which drives NRF2 to the ubiquitination (Kensler et al., 2007). After oxidative stress, the electrophilic molecules interact with the reactive cysteines of KEAP1, altering their conformation. Following the change in structure, KEAP1 is no longer able to bind NRF2 which can migrate to the nucleus where, following dimerization with small MAF proteins, binds to the specific DNA sequences called Antioxidant Response Elements (ARE) and drives the transcription of specific genes to initiate the detoxifying response. Furthermore, NRF2 activity can also be finely regulated by epigenetic factors, miRNA, post-translational modifications, transcriptional modulators and KEAP1 competitors (Hayes and McMahon, 2009; Hayes and Dinkova-Kostova, 2014).

NRF2 controls the basal expression and induction of about 250 genes that code for enzymes involved in various cellular pathways (Fig. 5): i) metabolism of phase 2 xenobiotic, ii) antioxidant response, iii) inflammation, iv) removal and repair of damaged cell proteins or organelles and v) control of mitochondrial homeostasis (Nguyen et al., 2003; Hayes and Dinkova-Kostova, 2014).

NRF2 regulates the expression of drug-metabolizing enzymes and key components in endogenous antioxidant systems (Fig. 5) such as NAD(P)H, quinone dehydrogenase (NQO1), heme oxygenase 1 (HMOX1) and glutathione-S-transferase (GSTA1). These proteins contribute to intracellular glutathione homeostasis, catalysis of oxidized protein thiols, reduction reactions coupled with cofactors and detoxification from toxic molecules.

The promoter of the murine Nrf2 gene contains two ARE-like sequences, which enable Nrf2 to autoregulate its own expression when exposed to electrophilic inducing agent (Kwak et al., 2002)

GENERAL BIOCHEMICAL FUNCTION	SYMBOL OF SOME GENES POSITIVELY REGULATED BY NRF2
Detoxication: Phase I drug oxidation, reduction and hydrolysis	NQO1, ADH7, CBR1 ,CYP1B1,
Detoxication: Phase II drug conjugation	GSTA1, GSTM1, MGST1
Detoxication: Phase III drug transport	ABCB6, ABCC1, ABCC2
Antioxidant: GSH-based system	GCLC, GCLM, GGT1, GPX2
Antioxidant: TXN-based system	PRDX1, PRDX6, XNRD1
Carbohydrate metabolism and NADPH regeneration	G6PD, HDK1, TALDO1, UGDH
Lipid metabolism: fatty acid oxidation	ACOT7, ACOT8, AWAT1,
Lipid metabolism: lipases	LIPH, PLA2G7, PNPLA2
Heme and iron metabolism	HMOX1, BLVRA, BLVRB
Transcription factors and associated proteins	NFE2L2, AHR, MAFG
Ubiquitin ligase substrate adaptor	KEAP1

Figure 5. General biochemical functions regulated by NRF2. In table are reported some genes regulated by NRF2 in mice and humans (Hayes and Dinkova-Kostova, 2014)

NRF2 regulates proteasome and therefore the removal of damaged and misfolded proteins that might otherwise lead to the formation of inclusion bodies (Kapeta et al., 2010). NRF2 can activate autophagy, which is the process necessary for protein turnover and for the elimination of damaged organelles such as mitochondria. Whether autophagy is reduced the level of autophagosome cargo protein p62 and ROS released by damaged mitochondria increases. Both ROS and p62 are able to

induce a release of NRF2 from KEAP1, and the transcription factor in turn is able to enhance the expression of p62, thus triggering a positive feedback loop (Komatsu and Ichimura, 2010); this NRF2 effect could be relevant for PD since pharmacological activation of NRF2 was reported to induce α-syn clearance in neurons (Skibinski et al., 2017). NRF2 plays a key role in the anti-inflammatory process by inhibiting the NF-κB pathway and the secretion of pro-inflammatory cytokines (Ma et al., 2006; Li et al., 2008). When the NRF2 pathway is altered, cells are much more sensitive to oxidative stress, protein aggregation and pro-inflammatory activation, factors that are able to the lead the onset of diseases including cancer and neurodegeneration (Gan and Johnson, 2014).

2.5.2 NRF2 regulations into the brain

The preservation of redox homeostasis is essential for maintaining normal brain function which is perturbed by high levels of ROS and RNS. Both neurons and glial cells possess intrinsic mechanisms that allow them to establish protective responses to harmful *stimuli* (Baxter and Hardingham, 2016). NRF2, in physiological state, is widely expressed in the CNS especially in astrocytes and microglia and to a reduced extent in neurons, in spite of this, the e cap'n'collar factor concentration may differ in function of acute damage and during neurodegenerative diseases progression (Cuadrado et al., 2014; Baxter and Hardingham, 2016).

Neurons have a reduced intrinsic defense capacity towards oxidizing agents, they express low levels of catalase and glutathione and they have reduced basal activity of the NRF2 pathway (Bell et al., 2015). Neuronal cells are metabolically very active, requiring high levels of ATP to maintain membrane potential and perform all their functions. To respond to the high energy demand, neurons obtain ATP through oxidative phosphorylation, a process associated with a high production of ROS (Fernandez-Fernandez et al., 2012). Since neurons are characterized by high metabolic activity and poor intrinsic defence mechanisms against oxidative stress, several theories were proposed to explain how neurons can survive. The most accredited is that astrocytes are the cells types responsible for their protection able to supply to neurons reducing molecules and providing a buffered environment. *In vitro* studies showed that astroglia produce and stores high quantity of glutathione, which is released into the culture medium in response to oxidative stress. Glutathione is degraded in the extracellular environment and the cysteine products are captured by neurons for the synthesis of glutathione necessary to counteract free radicals (Shih et al., 2003; Gupta et al.,

2012). *In vivo* studies in transgenic mice, show that Nrf2 overexpression in astrocyte is sufficient to confer neuroprotection in some models of neurodegenerative diseases, but the mechanism still unknown (Chen et al., 2009; Gan et al., 2012; Baxter and Hardingham, 2016).

NRF2 in microglial cells regulates the induction of the anti-Inflammatory phenotype by carrying out a cytoprotective action, reducing phagocytic capacity and the secretion of pro-inflammatory cytokines. However, the role of NRF2 in the regulation of chronic inflammation that characterizes neurodegenerative diseases is still poorly understood (Innamorato et al., 2008; Rojo et al., 2010, 2014). Active microglia induces the expression of antioxidant genes in astrocytes, which in turn could modulate microglia responses (Klegeris et al., 2007; McGeer and McGeer, 2007). For example, HMOX1, a NRF2 target gene, involved in the modulation of the inflammatory response, is highly expressed in microglia (Stahnke et al., 2007), in the presence of harmful *stimuli* microglia are activated and release ROS and pro-inflammatory cytokines (Rojo et al., 2010). These molecules generate a redox imbalance, both in the surrounding tissue and in microglia, which contributes to the spreading of the inflammatory response through the activation of NF-κB (Innamorato et al., 2008). At the same time, intracellular increase in ROS levels induces the activation of NRF2 which rises the expression of cytoprotective target genes such as HMOX1, restoring redox homeostasis by inhibiting NADPH oxidase and the NF-κB pathway, leading to microglia shift towards anti-inflammatory phenotype (Innamorato et al., 2008).

Notwithstanding several studies have enriched the picture regarding the regulation of NRF2 in the brain, little is still known about the role of this transcription factor in the crosstalk among brain cells and its role in neuroprotection against the elevated oxidative phosphorylation due to the level of oxygen consumption characterizing this organ (Clarke, 1999).

2.5.3 The role of NRF2 in Parkinson's disease

Neurodegenerative diseases are characterized by high levels of oxidative stress (Kensler et al., 2007) due to widespread inflammation, accumulation of aberrant protein, such as β-amyloid in AD and α-syn in PD, and mitochondrial alterations (Johnson et al., 2002; Ma and He, 2012). *Post mortem* histological analyses carried out on brain tissues of patients affected by neurodegenerative diseases show the presence of high levels of ROS and numerous markers of oxidative damage (lipids, nucleic acids and oxidized proteins) were found (Kensler et al., 2007). To date, it is not clear whether NRF2 regulation in neurodegenerative diseases such as PD and AD represents a compensation mechanism in the final stages of neurodegeneration, but there is evidence that its activation fluctuates during the pathology (Gan and Johnson, 2014).

Several evidence suggest the involvement of the NRF2 pathway in the pathogenesis of PD. *Post-mortem* examination (Ramsey et al., 2007) highlighted that NRF2 expression is altered in both neurons and astrocytes in the brain of PD patients compared with age-matched controls. In the patients, nuclear NRF2 was increased in neurons but not in glia cells of SN. Increased NRF2 in nigral area could be interpreted as a response to oxidative *stimuli* implemented by the surviving neurons, but since dopaminergic neurodegenerations continued during the time, were also suggested that a proper glial NRF2 activation was required for appropriate neuroprotection; further studies remain necessary to understand why the NRF2 nuclear translocation in neurons is not sufficient to prevent oxidative stress.

Altered glutathione levels were found in the blood of PD patients, probably reflecting a response to oxidative damage (Spencer et al., 1995; Bogdanov et al., 2008). Genetic analysis found protective NRF2 haplotypes for PD (von Otter et al., 2010, 2014; Todorovic et al., 2015) confirming that NRF2 may contribute to the pathogenesis of PD. Despite functional study should be performed to unpick these results, authors hypothesized that these haplotypes may promote a more efficient response to oxidative stress and thereby a higher capacity to withstand PD risk factors.

Regarding the study on animal and cellular models of PD, they commonly converge to the same result: Nrf2 pathway is dysregulated and a Nrf2 activation has a protective role from PD insults. Treatment of mice with MPTP, a molecule responsible for the onset of iatrogenic PD by increasing oxidative stress and inflammation leading to a degeneration of dopaminergic neurons, induces a different expression of Nrf2 target genes in the brain, that decrease in the striatum but increase in SNpc (Ye et al., 2016). In animal models of PD it has been observed that the synthesis of glutathione

induced by Nrf2 is greater in the early PD stages, while it is reduced in the final stages paralleling to an increased Nrf2 expression: this augmented expression has been attributed to the establishment of a compensatory response to reduced levels of glutathione and NRF2 target genes (Gan and Johnson, 2014).

Neuronal Nrf2 activation in cell culture protects neurons from the oxidative insult induced by parkinsonian neurotoxins such as paraquat, 6-OHDA, MPP+, and rotenone (Cao et al., 2005; Hara et al., 2006a; Jakel et al., 2007; Wruck et al., 2007; Hwang and Jeong, 2008; Niso-Santano et al., 2010). Shih and colleagues provided supports to the idea that Nrf2 activation in astroglia produces a robust antioxidant response, predominantly via the glutathione synthesis, sufficient to enhance neuronal viability from toxic insults (Shih et al., 2003). The gene expression analysis of Nrf2 activation induced by tert-butylhydroquinone (tBHQ), highlighted that changes in the neuronal gene expression program were dependent on the Nrf2 activity in astrocytes; these results suggested that Nrf2-dependent genetic alterations could modify neuron-glia interactions conferring neuroprotection from oxidative insults initiated by H_2O_2 or glutamate neurotoxic stimulations (Kraft et al., 2004).

Astrocyte modulation of the Nrf2 pathway plays a pivotal role also *in vivo*; Nrf2 knockout mice exhibit increased brain vulnerability to 6-OHDA neurotoxin, a susceptibility that can be rescued by transplantation of astrocytes overexpressing Nrf2 (Jakel et al., 2007). Nrf2 expression restricted to astrocytes is sufficient to protect against MPTP in transgenic mice, and Nrf2 genetic deficiency increases MPTP sensitivity (Chen et al., 2009). MPTP chronic administration in Nrf2-KO mice induces exacerbated microgliosis, augmented dopaminergic nigrostriatal degeneration and proinflammatory cytokine production (Colton, 2009; Innamorato et al., 2010).

The brain network of cell-to-cell communication in response to neurodegeneration may include also astrocytes that can secrete factors capable of modulating microglial activation; in this network, a relevant node might be represented by microglial Nrf2: it has been shown that treatment of microglia with conditioned media derived from astrocyte cultures induces Nrf2 expression and activation leading to increased microglial HMOX1 activity (Min et al., 2006). These results demonstrate a pivotal role of Nrf2 in the modulation of microglial dynamics and suggest the existence of tripartite crosstalk between neuron and glial cells in reply to neurotoxic stimulations.

From the pharmacological point of view, there are several compounds able to potently induce Nrf2 upregulation (Lau et al., 2008) including sulforaphane (Kensler et al., 2007), curcumin (Balogun et

al., 2003) resveratrol (Chen et al., 2005), t-BHQ (Li et al., 2002), dimethyl fumarate (Jing et al., 2015) and further novel synthetic compounds. Noteworthy, the chemical upregulation of NRF2 with these compounds was demonstrated neuroprotective against a plethora of Parkinsonian agents (e.g. MPTP, 6-OHDA, α-Syn, LRRK2) (Zhang et al., 2013b; Kaidery et al., 2019).

Resuming, several evidence are supporting a key role for NRF2 in PD: i) the activity of NRF2 decreases with aging (Sykiotis and Bohmann, 2010) one of the main PD risk factors (Hindle, 2010); ii) dysregulation of the NRF2 was detected in both PD patients and experimental models; iii) NRF2 haplotypes are able to decrease PD risk; iv) activation of antioxidant and detoxification response, both genetic and chemically-induced, is sufficient to protect dopaminergic neurons against parkinsonian molecule both *in vitro* and *in vivo* (Barone et al., 2011); v) on the other side NRF2 deficiency aggravates the outcome in PD models; vi) NRF2 is implicated in mitochondrial biogenesis and autophagy pathways heavily involved in the PD pathogenesis; finally, vi) NRF2 is entangled in the maintenance of proteostasis, and it has been reported that it is able to increase the degradation of α-syn (Lastres-Becker et al., 2012).

Nevertheless, nowadays there are no therapeutic molecules on market acting on the NRF2 pathway capable of reducing the neurodegeneration of PD. Most of the bench and preclinical studies demonstrated beneficial effects when NRF2 activation is elicited before the induction of neurodegeneration. It is tempting to speculate that a deeper understanding of the molecular events responsible for the early steps of neurodegeneration may allow identifying suitable markers and specific therapeutic window, where the protective effects of NRF2 stimulation are clinically beneficial.

2.6 TFEB master regulator of autophagy–lysosomal pathway

Autophagy–lysosomal pathway (ALP) refers to a catabolic degradative mechanism that involves the delivery of cytoplasmic cargo to the lysosome and its degradations. Autophagy is induced by specific *stimuli* such as nutrient starvation, infection, oxidative and environmental stress and converge on the lysosomal pathway, wherein the transcription factor EB (TFEB) plays a key role as the master regulator (Sardiello et al., 2009; Settembre et al., 2011).

ALP is particularly important in non-dividing cells such as neurons and is essential to maintaining their homeostasis, while reduced degradation of molecules could results in their accumulation and adverse pathological outcomes. In line with this, autophagy-deficient mice exhibit neuronal accumulation of proteins and neurodegeneration, suggesting a direct role of ALP in neurodegenerative disorder characterized by proteinaceous accumulations such as PD, AD and Huntington's disease (Hara et al., 2006b; Komatsu et al., 2006). At the same time, the clearance of these aggregates is typically coupled with symptoms improvement (Yamamoto and Simonsen, 2011) indicating that enhancing the activity of the ALP could be a relevant therapeutic strategy against these neurodegenerative diseases. To this aim, TFEB being a key player in the ALP regulation, can be certainly considered as an attractive target for therapies aiming at modulation ALP.

TFEB is a helix-loop-helix leucine zipper transcription factor that is mainly maintained in the inactive form by mTOR1 direct phosphorylation. Upon definite signalling i.e. starvation or lysosomal dysfunction, TFEB is dephosphorylated and translocate into the nucleus, where it binds DNA at a specific palindromic 10-base consensus sequence also known as CLEAR (Coordinated Lysosomal Expression and Regulation) and promotes the transcription of target genes (Palmieri et al., 2011). This responsive element (the consensus sequence reported in Fig. 6) is usually located in the proximity of transcription start sites of the lysosomal genes involved in ALP, lysosomal biogenesis, lysosomal exocytosis (Medina et al., 2011), endocytosis and membrane repair (Sardiello et al., 2009; Palmieri et al., 2011) but also mitochondrial biogenesis, fatty acid oxidation and oxidative phosphorylation (Mansueto et al., 2017).

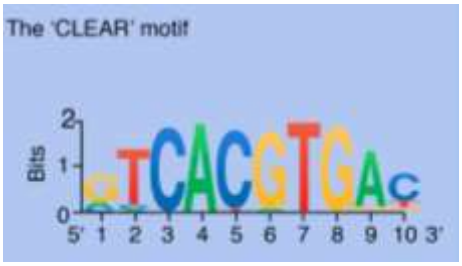

Figure 6. Logo representation of the consensus for TFEB binding sites. The height of nucleotide symbols position is proportional to the conservation of nucleotides in the indicated position (Palmieri et al., 2011).

Alterations in lysosomal function and/or in the autophagic pathway cause lysosomal storage diseases (Platt et al 2018); given that macrophages and microglia are responsible for the elimination of harmful factors through the phagocytic process, it has been shown that there is a link between the phagocytic functionality carried out by these cells and the onset of lysosomal disorders (Ballabio & Gieselmann 2009, Bosche & Kielian 2015) e.g. GD (Stirnemann et al 2017).

TFEB does not coordinate the basal transcription program of its target genes but enhances their transcription levels in response to environmental *stimuli*. The TFEB promoter itself contains multiple CLEAR elements creating a positive autoregulatory loop, where the transcription factor binds to its own promoter and induces its own transcription (Settembre et al., 2013). Interestingly, TFEB overexpression modulates, not only lysosomal, but also lipid droplets and damaged mitochondria autophagy (Fig. 7) (Settembre et al., 2013; Nezich et al., 2015).

Altered TFEB-mediated lysosomal biogenesis has been found in GBA1 mutant neurons (Awad et al., 2015) and boosting TFEB activities was shown to i) protect dopaminergic neurons from cell death, ii) to enhance autophagic clearance of α-syn (Kilpatrick et al., 2015) and iii) to promote the synthesis of functional mitochondria (Ivankovic et al., 2016). In addition, several studies have reported that genetic or pharmacological activation of TFEB improves lysosomal function and promotes protein clearance and neuroprotection in mouse models of diseases characterized by protein misfolding and oxidative stress (Tsunemi et al., 2012; Decressac et al., 2013; Kilpatrick et al., 2015). TFEB activation has been widely demonstrated to ameliorate pathology in neurological diseases (Decressac et al., 2013; Polito et al., 2014; Xiao et al., 2014a; Mazzulli et al., 2016), as well as in models of spinal and bulbar muscular atrophy and in lysosomal storage disorders (LSDs)(Medina et al., 2011; Song et al., 2013; Spampanato et al., 2013; Cortes et al., 2014).

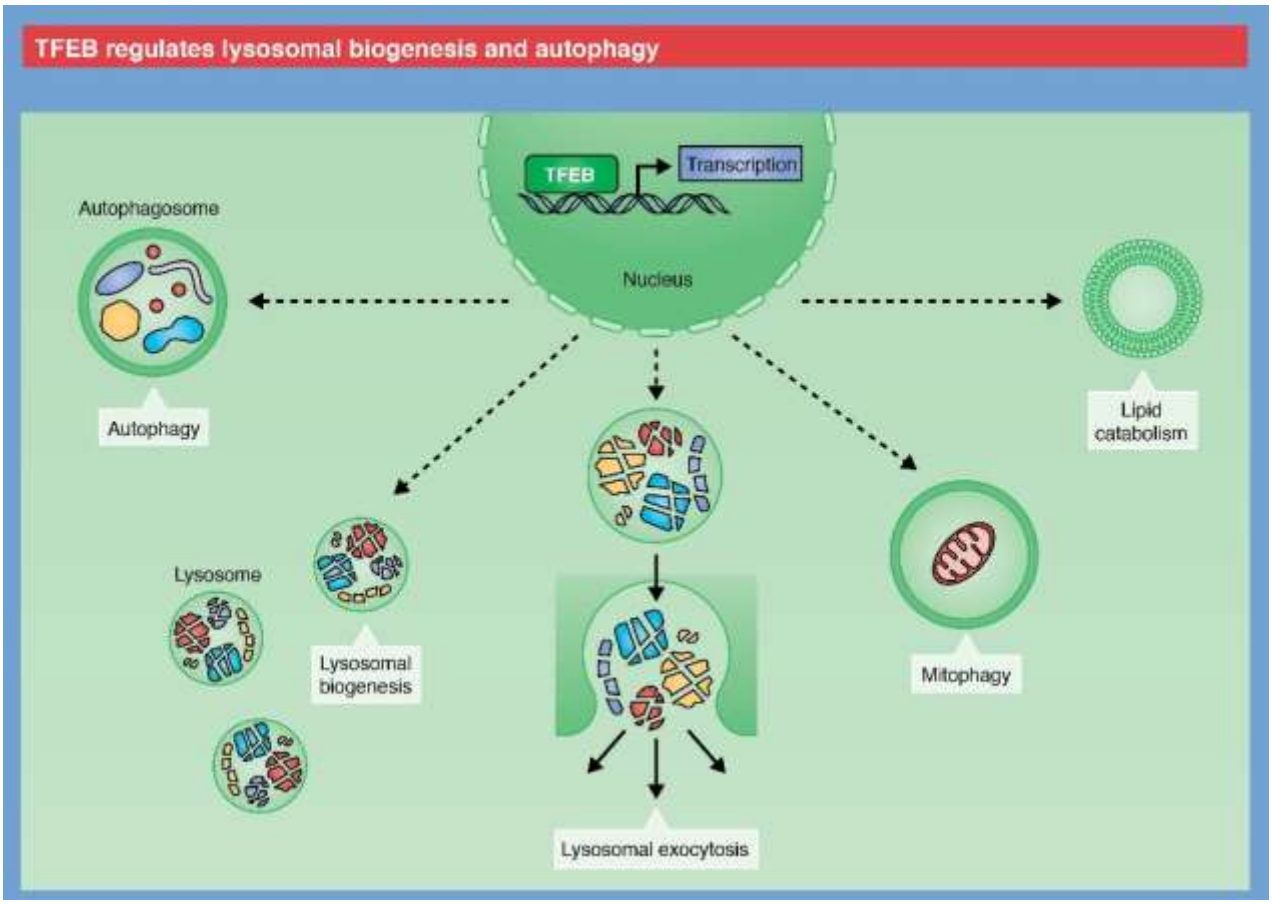

Figure 7. TFEB functions. TFEB regulates lysosomal biogenesis and exocytosis, autophagy, mitophagy and lipis catabolism. Image from (Napolitano and Ballabio, 2016).

3 MATERIALS AND METHODS

3.1 Reagents

All components were purchased from Sigma Aldrich if not differently indicated: tert-Butylhydroquinone (tBHQ, Cat. 112941,), conduritol-B-epoxide (CBE, Cat. 234599), cytochalasin D (Cat. C8273), nocodazole (Cat. M1404), PLX3397 (Cat. S7818-50, DBA), diethylmaleate (Cat. D97703), sulforaphane (Cat. 5441), cystamine (cat. C121509), quercetin (Cat. 337951), curcumin (Cat. C1386), lipopolysaccharides from *Escherichia coli* O111:B4 (LPS, Cat. L4130), insulin (Cat. I0516), ethidium bromide (EtBr, Cat. E1510), β-Mercaptoethanol (βME), DL-Dithiothreitol (DTT, Cat. D5545) and acetylsalicylic acid (ASA, Cat. A5376), 1-methyl-4-phenylpyridinium iodide (MPP+, Cat. D048), 1-methyl-4-phenyl-1,2,3,6-tetrahydropyridine hydrochloride (MPTP Cat. M0896, Sigma Aldrich), chloroquine diphosphate salt (Cat. C6628), trehalose (Cat. 890808P), ambroxol hydrochloride (Cat. A9797-5G).

3.2 Plasmids

The plasmid ARE-*luc2*-ires-TdTomato was generated starting from the vector ARE-loxP-STOP-loxP-*luc2*-ires-TdTomato (Rizzi et al., 2017), the floxed STOP sequence was removed using Cre recombinant enzyme (Cat. M0298S, NEB, Euroclone). The N3-*luc2*-ires-tdTomato was obtained by cloning the 103 bp DNA fragment constituted by the trimerized 51 bp sequence from the promoter region of the rat Nqo1 (NAD(P)H:quinone oxidoreductase 1) into the *XhoI* and *XmaI* restriction sites of the ARE-loxP-STOP-loxP-*luc2*-ires-tdTomato, to substitute the ARE promoter with the synthetic (synthesis done by Eurofins Genomics) DNA fragment. The G8-*luc2*-ires-tdTomato was obtained by cloning the sequence GTGACAAAGCA repeated 8 times into the XhoI/XmaI restriction sites of the ARE-loxP-STOP-loxP-*luc2*-ires-TdTomato, to substitute the ARE promoter with the synthetic (synthesis was done by Eurofins Genomics) 88 bp DNA fragment. The plasmid CLEAR_Optimized-*luc2*-T2A-tdTomato was generated starting from the vector ARE-loxP-STOP-loxP-*luc2*-ires-tdTomato and substituting i) the ires with the T2A sequence using *SnaBI* and *XhoI* restriction sites, and ii) the ARE promoter with the CLAR_Optimized promoter synthetized by Eurofins Genomics, using *SacI* and *BssHII* sites. To generate the reporter mice the reporter vector ARE-*luc2*-ires-TdTomato and CLEAR_Optimized-*luc2*-T2A-tdTomato were cloned into a targeting vector containing MAR and homologous region for chromosome 1 (Rizzi et al., 2017), and a loxP-STOP-puro-loxP inserted downstream the two promoters. The plasmids CLEAR Canonical (Cat. 66800) and TFEB Promoter (Cat. 66801) were purchased from addgene, the plasmid pTFEB expressing constitutively the transcription factor EB protein was gently provided by Ballabio's lab.

3.3 ES manipulation

The targeting vector ARE/CLEAR_Optimized was linearized with *NotI* and transferred into sv6.4 embryonic stem cells by electroporation: 35 g/DNA each using 15 million cells (Core Facility for Conditional Mutagenesis, DIBIT San Raffaele). Positive clones were selected with puromycin (1 g/l). More than four hundred resistant clones for each transgene were screened for homologous recombination by PCR. Positive clones were injected into C57BL/6NCrL blastocysts which are transferred to pseudo-pregnant CD1 females. The chimeric male mice (with 80– 90% of chimerism) were mated to wild-type C57BL female mice to produce F1 transgenic mice, TFEB-STOP, and ARE-STOP, that were crossed with B6.C-Tg(CMV-cre)1Cgn/J to obtain TFEB-*luc2* and ARE-*luc2* reporter mice.

3.4 Screening PCR for TFEB-STOP

The PCR screening was performed on 25 ng of genomic DNA purified from ES, using the standard procedure for Phusion™ High-Fidelity DNA Polymerase (Cat. F530S, Thermoifisher) or Q5® High-Fidelity DNA Polymerase (Cat. NEB #M0515, NEB) in GC buffer. The following primers were used:

PCR1: 5’-GGAGGCCTCATGTGAATTAAGTGC-3', 5’-TGCAGTGCTCATTATGTCAGTTCTGTC-3’;
PCR2: 5’-GGTACAATTGTATTACGGATCACGCGT-3’, 5’-CATCTCTCAGCCCCACCTGTATG-3’;
PCR3: 5’-AGGTATCTCATGTAACAACAGCTATC-3', 5’-ACCACGATCCGATGGTTTGTATTC-3’;
PCR4: 5’-ACTCCACACAGGCATAGAGTGTCTGC-3', 5’-ACGGCCATGTTGTTGTCCTCG-3’;
PCR5: 5’-GAGCAAGGGCGAGGAGGTCAT-3', 5’-AGCCTTCCTTTTCCTGGGTTGC-3’;
PCR6: 5’-GGTACAATTGTATTACGGATCACGCGT-3', 5’-CATCTCTCAGCCCCACCTGTATG-3’.

3.5 Cell culture

All cell lines were purchased from the American Type Culture Collection ATCC (Manassas, VA, USA). Primary neurons were derived from neural tissue following standard operational procedure from p0-1 mice brain using the Neural Tissue Dissociation Kit-Postnatal neurons (Cat. 130-094-802, Miltenyi Biotec). After removing the meninges, brain cortexes from six mice were pooled as a single experimental group and subjected to an enzymatic and mechanical dissociation at 37°C, the cellular suspension were filtered with a 70 µm strainer and seeded on poly-L-ornithine-coated plates. Half of the medium volume was replaced every 2 or 3 days. Microglia were isolated from whole brains of adult (age 3-6 months) male mice with a previously described protocol (Villa et al., 2018). Brains

from two mice were pooled and subjected to an enzymatic and mechanical dissociation, after myelin removal, cells were processed for microglia magnetic sorting with a magnetic column to purify CD11b+ cells, namely microglia. For the generation of human blood-derived macrophages we followed a previously described procedure (Toniolo et al., 2015), human peripheral blood mononuclear cells were isolated from buffy coats after Histopaque® density gradient centrifugation. Before the use, peripheral blood mononuclear cells were grown for 1 week in DMEM media (Cat. 32430-027, Gibco) supplemented with 10% di FBS (Fetal Bovine Serum Ultra-Low Endotoxin, ECS0186L, Euroclone), 1% streptomycin–penicillin (Cat. 15240-062, Gibco), 1 % GlutaMAX™ (Cat. 35050-061, Gibco), 50 ng/ml of M-CSF (Cat. 11343113, Immunotools), and media were exchanged every 2 days. Primary murine macrophages were extracted as described in (Mornata et al., 2020). Three mice of 3-6 months were euthanized and subject to a peritoneal lavage with PBS to extract macrophages subsequently purified using CD11b +magnetic beads (Cat. 130-049-601, Miltenyi Biotec), following the operative manual. SK-ARE-*luc2* cells were obtained from Prof. Elisabetta Vegeto, University of Milan (Mornata et al., 2020). For the preparation of co-cultures, cells were seeded in a 24-well plate at the concentration of 150'000 cell/well for primary neurons, or 70'000 cell/well for SK-N-BE or SK-ARE-*luc2*. Neurons were cultured for 10 days (primary cells) or 1 day (cell lines), then primary microglia, BV-2, MCF-7, RAW 264.7 or primary macrophages were seeded over the neuron layer: If not differently specified, the number of seeded cells were 37'500 cells/well for primary microglia and primary macrophages, or 3'500 cells/well for BV-2, RAW 264.7 and MCF-7. For the transwell experiment, 0.4 µm pore polyester membrane inserts (Cat. 3460, Corning) were used.

Neuronal and neuronal-microglial co-cultures were grown in Neurobasal A medium (Cat. 10888-022, LifeTechnologies) containing 1% streptomycin–penicillin, 1 % GlutaMAX™, 2% B-27™ Supplement (Cat. 17504-044; Gibco), 10 mM HEPES (Cat. H0887, Merk), in a humidified 5% CO_2-95% air atmosphere at 37 °C. Other co-cultures were grown in RPMI 1640 Media (Cat. 61870044, Gibco) containing fetal bovine serum to a final concentration of 10%, 1% streptomycin–penicillin and 1 % GlutaMAX™.

For the transfection, MCF-7 or SK-N-BE cells were seeded in a 24-well plate (50'000 cells/well, 30'000 respectively) and cultured overnight prior to transfection. Transfections were carried out using Lipofectamine LTX & PLUS reagent (Cat. 15338, Thermo Fisher), following the manufacturer's instructions using a DNA: Lipofectamine: Plus reagent ratio of 2,5:6,5:1,5.

3.6 Flow cytometry assay

Flow cytometry experiments were performed on at least 200'000 cells for each sample by using Novocyte 3000 (Agilent Technologies, Inc) equipped with 488 nm lasers. Cells were incubated 2 minutes at 4°C with 0.1 mg/ml propidium iodide (Cat. P4170, Sigma Aldrich). Fluorescence pulses were detected using 585/40 nm collection filter. Results were analyzed using NovoExpress software (Agilent Technologies, Inc).

3.7 Luciferase enzymatic assay

Cells were lysed with Luciferase Cell Culture Lysis Reagent (cat. E1531, Promega) and protein concentration determined with a Bradford assay (Bradford, 1976); the biochemical assay of luciferase activity was carried out in a luciferase assay buffer (470 µM luciferin, 20 mM Tricine, 0.1 mM EDTA, 1.07 mM $(MgCO_3)_4{\cdot}Mg(OH)_2 \times 5H_2O$; 2.67 mM $MgSO_4 \times 7H_2O$ in H_2O, pH 7.8, with 33.3 mM DTT and 530 µM ATP) by measuring luminescence emission with a luminometer (Veritas, Turner Biosystems) and the relative luminescence units (RLU) determined during 10 seconds measurements (Rizzi et al., 2018).

3.8 Glucocerebrosidase assay

Glucocerebrosidase assay was performed as described in Mus and collaborators (Mus et al., 2019). Briefly, cells were lysed with RIPA buffer and protein concentration determined with BCA (Cat. 23227, Pierce). The biochemical assay of GCase activity was carried out in a buffer containing 4-methylumbelliferyl-β-d-glucopyranoside substrate (Cat. M3633, Sigma); after 1 hour at 37°C the reaction was stopped with 0.25 M glycine buffer pH 10.4 and the fluorescence emission of the 4-methylumbelliferyl (4-MU) generated by the reaction was read with a fluorimeter (EnSpire Plate Reader, PerkinElmer) selecting an excitation wavelength of 365 nm and an emission wavelength of 445nm. The enzyme activity was expressed as µmol 4-MU generated in 1 hour per µg of protein and normalized on vehicle-treated cells.

3.9 Immunohistochemical analysis

Co-cultures of SK-N-BE and BV-2 cells were fixed in 4% paraformaldehyde fixative for 15 minutes and washed with PBS. The fixed cells incubated at room temperature for 1 hour in blocking solution containing 0.1% p/v BSA (Cat. A9418, Merk), 10% v/v goat serum (Cat. ECS0200D, Euroclone), 0.1%

v/v Triton-X100 (Sigma, T-9284). Next, the cells were incubated at 4°C with 10% blocking solution in PBS with a rat anti-CD11b antibody (diluted 1:500; Cat. MCA7114, Serotec) and a rabbit anti-NRF2 antibody (diluted 1:500; Cat. C-20, Santa Cruz biotechnology). After a 24 hours incubation fixed cells were rinsed in PBS and incubated 1hour at RT 10% blocking solution in PBS with a mixture of Alexa Fluor 488 conjugated goat anti-rat IgG antibody (diluted 1:300, Cat. A-11006, Molecular Probes Inc.) and Alexa Fluor 555 conjugated goat anti-rabbit IgG antibody (diluted 1:300; Cat. A-21429, Molecular Probes Inc.). Finally, fixed cells were rinsed in PBS and covered with 1:1000 DAPI solution in PBS (Invitrogen, Cat. D1306). The fluorescence image acquisition was performed using an Axiovert 200M microscope with dedicated software (AxioVision Rel 4.9, Zeiss), taking 20 random fields for any condition. The images were elaborated with ImageJ Fiji software, in brief: the ROI of cellular nuclei automatically generated by the software using the field of DAPI was utilized to quantify the average gray value of the NRF2 field. The value related to the nuclei of CD11b+ positive cells were manually excluded from the analysis.

ARE-*luc2* mice were sacrificed and transcardially perfused with cold saline solution followed by 4% paraformaldehyde in PBS. Brains were immediately removed, post-fixed in the 4% paraformaldehyde fixative for 24 h and then transferred in solutions of sucrose at increasing concentrations (up to 30%) during the following 72 h. Samples were then frozen and stored at−80 °C for successive analyses. Serial coronal sections of or 40 µm were cut throughout the brain using a freezing sliding microtome (Leika SM 2000R, Nussloch) and stored at −20 °C in a solution containing 30% ethyleneglycol (Cat. 324558, Sigma Aldrich), 20% glycerol (G5516, Sigma Aldrich, St. Louis, MO, USA) and 0.05 M sodium phosphate (Cat. 342483, Sigma Aldrich) buffer until use. The slide-mounted sections were rinsed in PBS (Cat. P4417, Sigma Aldrich) and incubated in PBS containing 10% NGS (Cat. S2007, Sigma Aldrich) and 0.3% Triton X-100 (TX.-100, Cat. T8787, Sigma Aldrich) at room temperature for 1 h. For Fig. 17E sections were incubated overnight at 4 °C with a rabbit anti-TH antibody (1:2000; Cat. AB152, Chemicon InternationaL), then rinsed in TBS (Cat. T5030, Sigma Aldrich) and incubated for 1 h at room temperature, with a goat biotinylated anti-rabbit IgG antibody (1:1000; Cat. BA-1000). Finally, sections were processed with the avidin-biotin technique using a commercial kit (Cat. PK-6100, Vectastain ABC Elite kit), and reaction products were developed using nickel-intensified 3,3’-diaminobenzidine tetrahydrochloride (Cat. SK4100, DAB Substrate Kit for Peroxidase). After rinsing with TBS, sections were dehydrated in ascending alcohol concentrations, cleared in xylene (Cat. 492303, Carlo Erba), and coverslipped. TH positive cells were counted in the SNc of both hemispheres on comparable sections for each experimental

group. Cell count was performed on every fourth section for a total of six sections per animal and was divided by the area (mm^2) of SNc. For Fig. 18A the sections were rinsed in PBS and incubated 1 h in PBS containing 10% NGS and 0.3% TX-100 at room temperature. Sections were then incubated at 4 °C in PBS/1% NGS/0.3% TX-100 containing a mixture of a rabbit polyclonal anti-Nrf2 (Cat. C-20; diluted 1:300; Santa Cruz Biotechnology Inc.) and a mouse anti-TH antibody (Cat. MAB 318, diluted 1:300; Chemicon International Inc.). After a 24 h incubation sections were rinsed in PBS and incubated 1 h at RT in PBS/1% NGS containing a mixture of Alexa Fluor 488 conjugated goat anti-rabbit IgG antibody (diluted 1:300, Cat. A-11034, Molecular Probes Inc) and Alexa Fluor 594 conjugated goat anti-mouse IgG antibody (diluted 1:300; Cat. A-11032, Molecular Probes Inc). For Fig. 18B the sections were incubated at 4 °C in PBS/1% NGS/0.3% TX-100 containing a mixture of a rabbit polyclonal anti-Nrf2 (Cat. C-20; diluted 1:300; Santa Cruz Biotechnology Inc.). After a 24 h incubation sections were rinsed in PBS and incubated 1 h at RT in PBS/1% NGS containing a mixture of Alexa Fluor 488 conjugated goat anti-rabbit IgG antibody (diluted 1:300, Cat. A-11034, Molecular Probes Inc.). For Fig. 18C the sections were rinsed in PBS and blocked for 1 h at room temperature with M.O.M.™ mouse Ig blocking reagent (M.O.M. kit, Vector Laboratories) diluted in PBS according to the manufacturer's protocol. Sections were then incubated at 4 °C in M.O.M.™ Diluent containing a mixture of a rabbit polyclonal anti-Nrf2 (diluted 1:300) and a mouse anti-GFAP antibody (clone G-A-5; diluted 1:1000; Sigma Aldrich) or a mouse anti-CD11b antibody (diluted 1:300; Biorad). After a 24 h incubation sections were rinsed in PBS and incubated 1 h at RT in M.O.M.™ Diluent containing a mixture of Alexa Fluor 488 conjugated goat anti-rabbit IgG antibody (diluted 1:300, A-11034, Molecular Probes Inc.) and Alexa Fluor 594 conjugated goat anti-mouse IgG antibody (diluted 1:300; A-11032, Molecular Probes Inc.). For Fig 20F. For Fig Finally, all sections were rinsed in PBS and covered with Prolong with DAPI (P36931, Molecular Probes Inc.). Immunohistochemistry image analysis was performed using an AxioSkop 2 microscope connected to a computerized image analysis system (AxioCam MRev3) equipped with a dedicated software (AxioVision Rel 4.8) (Zeiss, Oberkochen, Germany).

Wt mice treated with CBE and tBHQ were sacrificed and transcardially perfused with cold saline solution followed by 4% paraformaldehyde in PBS. Brains were immediately removed, post-fixed in the 4% paraformaldehyde fixative for 24 h and then transferred in solutions of 30% sucrose at increasing concentrations (up to 30%) during the following 72 h. Serial coronal sections of 35 µm were cut throughout the brain using a freezing sliding microtome (Leika SM 2000R, Nussloch, Germany) and stored at −20 °C in a solution containing 30% ethyleneglycol (324558, Sigma Aldrich,

St. Louis, MO 63103, USA), 20% glycerol (G5516, Sigma Aldrich, St. Louis, MO, USA) and 0.05 M sodium phosphate (342483, Sigma Aldrich, St. Louis, MO, USA) buffer until use. The slide-mounted sections were rinsed in Tris-HCl and incubated TBS 5% NHS and 0.3% Triton X-100 at room temperature for 1 h. sections were incubated for 2 nights at 4 °C with a mouse anti-TH antibody (1:300; MAB318) and rabbit anti-Nrf2 antibody (abcam 31163), then rinsed in TBS (T5030, Sigma Aldrich, MO, USA) and incubated for 2 h at 4 C, with Dylight 649 horse anti-mouse (DI-2649 1:300) and Dylight 594 horse anti-rabbit (DI-1094 1:300). After rinsing with TBS, sections were incubated for 3 minutes with DAPI (1:10.000) and coverslipped. Immunohistochemistry images were collected on Zeiss microscopes (LSM800) with a ×40 Plan-Apochromat objective and processed with Fiji software (ImageJ, NIH, version 2.0.0).

3.10 Animal treatments

All animal experimentation was carried out in accordance with the ARRIVE and European Guidelines for Animal Care. All animal experiments were approved by the Italian Ministry of Research, and University's animal welfare committee or approved by the State Agency for Nature, Environment, and Consumer Protection in North Rhine Westphalia, Germany. The animals were fed ad libitum and housed in individually ventilated plastic cages within a temperature range of 22–25 °C, the relative humidity of 50% ± 10% and under an automatic cycle of 12 hours light/dark (lights on at 07:00 AM). Pharmacological treatments: mice were i) received a daily i.p. injection of MPTP (20 mg/kg) or vehicle (PBS) once a day for 4 days (Costa et al., 2013),ii) one i.p 12.5 mg/kg of ASN (Sodium (meta) arsenite, Cat. S7400 Sigma Aldrich) or vehicle (PBS) iii) i.p. injected with 100 mg/kg/die for 3 days of CBE or vehicle (PBS), iv) i.p. injected with tBHQ 75 mg/kg dissolved in PBS + 1% DMSO + 20% PEG300, v) 100 µg PLX3397 or vehicle solution (5% DMSO + 45% PEG300 + ddH2O) were given as nose drops (3µl/drop in each nostril corresponding to 6 µl/administration), alternating between the left and right nostrils for two times, at intervals of 2 min; subsequent doses were given each 12 h, for 1 week. For the transnasal administration mice were placed in supine position, and a heated pad was inserted under the dorsal neck to induce a hyperextension of the head back (Villa et al., 2018).

3.11 *In vivo* and *ex vivo* imaging

For the semi-quantitative analysis of photon emission, animals were injected s.c. with 80 mg/kg of luciferin 15 min prior to the imaging session. Mice were anaesthetized using Isofluorane and kept

under anesthesia during the 5 min of the imaging session carried out with a CCD-camera (IVIS Lumina II Quantitative Fluorescent and Bioluminescent Imaging, PerkinElmer). Photon emission in brain areas was measured using the Living Image Software v. 4.2 (Perkin Elmer). Mice were killed by cervical dislocation after the last *in vivo* acquisition, brains were rapidly dissected and sectioned by means of a "brain matrix" (adult mouse, coronal and sagittal, 1mm spacing). Sections were immediately subjected to *ex vivo* imaging session of 5 minutes. Photon emission was quantified with the Living Image Software v. 4.2.

3.12 Microglial image processing and quantification

Image processing was performed using Fiji software (Schindelin et al., 2012). The background was subtracted to the images, that were sequentially despeckled and smoothed, then was applied a threshold allowing that all the gray values greater than a specified constant were replaced by the constant. The threshold was defined by the operator on the basis of the best segmentation performance on pilot images and maintained across the experimental groups. A further step of pixel erosion and smoothing was applied to best fit cell shape. Shapes with a size greater than 130 μm^2 processed to measure static descriptors such as area, circularity, solidity and position, in all the acquisition during the time. For biparametric analysis: the median of the parameters was used as a cutoff to assign each cell to a descriptive category.

3.13 Real-time PCR

Real-time analyses were performed as previously described (Rizzi et al., 2018). The following primers were used:

36B4: 5'-GGCGACCTGGAAGTCCAACT-3', 5'-CCATCAGCACCACAGCCTTC-3';

Nrf2: 5'-CCCAGCAGGACATGGATTTGA-3', 5'-AGCTCATAGTCCTTCTGTCGC-3';

Arg1: 5'-CAGAAGAATGGAAGAGTCAG-3', 5'-CAGATATGCAGGGAGTCACC-3';

Trem2: 5'-GGAACCGTCACCATCACTCT-3', 5'-CTTGATTCCTGGAGGTGCTGT-3';

Il-1β: 5'-TGCCACCTTTTGACAGTGATG-3', 5'-GCTGCGAGATTTGAAGCTGG-3';

Nqo1 5'-GGTAGCGGCTCCATGTACTC-3', 5'-CGCAGGATGCCACTCTGAAT-3';

Tfeb: 5'-CCAGAAGCGAGAGCTCACAGAT-3', 5'-TGTGATTGTCTTTCTTCTGCCGC-5';

Lamp1: 5'- GCCCTGGAATTGCAGTTTGG-3', 5'-TGCTGAATGTGGGCACTAGG-3';

Cx3cr1: 5'-CTGCTCAGGACCTCACCATG-3', 5'-CACCAGACCGAACGTGAAGA-3';

P2ry12: 5'-GAACCAGGACCATGGATGTG-3', 5'-CCAAGCTGTTCGTGATGAGC-3';

C3: 5'-GGAAGATCCGAGCCTTTTAC-3', 5'-CCACACCATCCTCAATCACTAC-3';

Actin: 5'-GGAAATCGTGCGTGACAT-3', 5'-ACGTCACACTTCATGATGGA-3'.

3.14 Statistical analysis

Statistical analyses, unless otherwise indicated in the figure legend, were done using *t*-test, one-way ANOVA or two-way ANOVA for multiple treatment comparisons (Graph Pad 7 software). A *p*-value lower than 0.05 was considered as statistically significant.

4 AIM

PD is the second most common neurological disorder whose prevalence is steadily increasing due to the rising lifespan of the population (De Lau and Breteler, 2006; Pankratz et al., 2009). It is considered a multifactorial disease, caused by the interaction among multiple genetic and environmental risk factors, as a consequence, the majority of PD cases are defined idiopathic and pathogenesis are doubtful (Lill, 2016). The available therapies for PD are able to partially manage the characteristic motor symptoms induced by the depletion of dopamine in the nigrostriatal pathway (Parkinson, 1817; Tagliaferro and Burke, 2016), but no preventive or neuroprotective treatment exists, meaning that progressive neurological deterioration remains unavoidable (Postuma and Berg, 2016). Efforts to develop neuroprotective therapy are focusing on the early stages of disease, which offer the greatest prospect to intervene, but the discovery of effective therapeutic target it is hindered by the limited knowledge of molecular events triggering neurodegeneration, this is partially attributable to the difficulties to gain dynamic access to the molecular events underlying the initial pathogenetic steps in human patients and to the lack of reliable animal model of the early PD stage.

The aim of my Ph.D. project was to develop useful tools to study molecular events in the *spatio*-temporal dimension in co-culture models and in the parenchyma of living mice to clarify the early molecular steps triggering neurodegeneration. We point our attention on two key nodes in protective pathways essential to maintain brain homeostasis deregulated in PD brains (Toulorge et al., 2016), albeit it is not known whether the alterations are the origin or the outcome of dopaminergic neurodegeneration: the transcription factor nuclear factor erythroid 2-related factor (NRF2), regulating antioxidant/detoxifying response, and the transcription factor EB (TFEB), the master regulator of autophagy and lysosomal pathways. In detail, we decided to study their regulation in system representative of phases preceding dopaminergic neurodegeneration, using MPTP and the pharmacological GBA1 impairment, considered a major risk factor for PD (Maor et al., 2013; Li et al., 2014; Migdalska-Richards and Schapira, 2016). Since severe GBA1 deficiency hampers the mononuclear phagocytic functions causing Gaucher's disease (Grabowski and Beutler, 2001), we hypothesized that in the brain GBA1 impairment in microglia, a cell lineage actively contributing to brain homeostasis (Nimmerjahn et al., 2005; Kettenmann et al., 2011), could entail a key role in the neurodegeneration onset and progression. The study is expected to reveal unexplored microglial to neuron communication mechanisms that could be targeted by preventive strategies.

5 RESULTS

5.1 Reporter systems generation

5.1.1 Generation and validation of reporter system to monitor oxidative stress response

To generate a new synthetic Nrf2-inducible promoter we performed a bioinformatics analysis of the promoter regions of 14 Nrf2-target genes (in detail: Hmox1, Gclc, Nqo1, Usp14, GstYa, Atf3, Sod1, Gpx2, Gsr, Prox1, Ftl-1, Fth-1, SrB1, Fmo1) that were aligned to identify common structural features including the distance from the TATA box, the sequence of the antioxidant responsive elements (ARE) and the surrounding nucleotides. The analysis allowed to generate a new synthetic promoter (named ARE) (Fig. 8A) containing a module of four consensus sequences in duplicate, derived from the promoter regions of Hmox1, Nqo1, GstYa and Grs genes. Initial computational analysis with the Alibaba2.1 and Jaspar software was performed to identify putative transcription factor binding site in the new ARE promoter and in two previously published ARE elements (Fig. 8A) employed to monitor oxidative stress in eukaryotic cells (Johnson et al., 2002; Wang et al., 2006): the N3 promoter, a 3xARE from the rat Nqo1 and the G8 promoter, a 8xARE derived from mouse Gsta1.

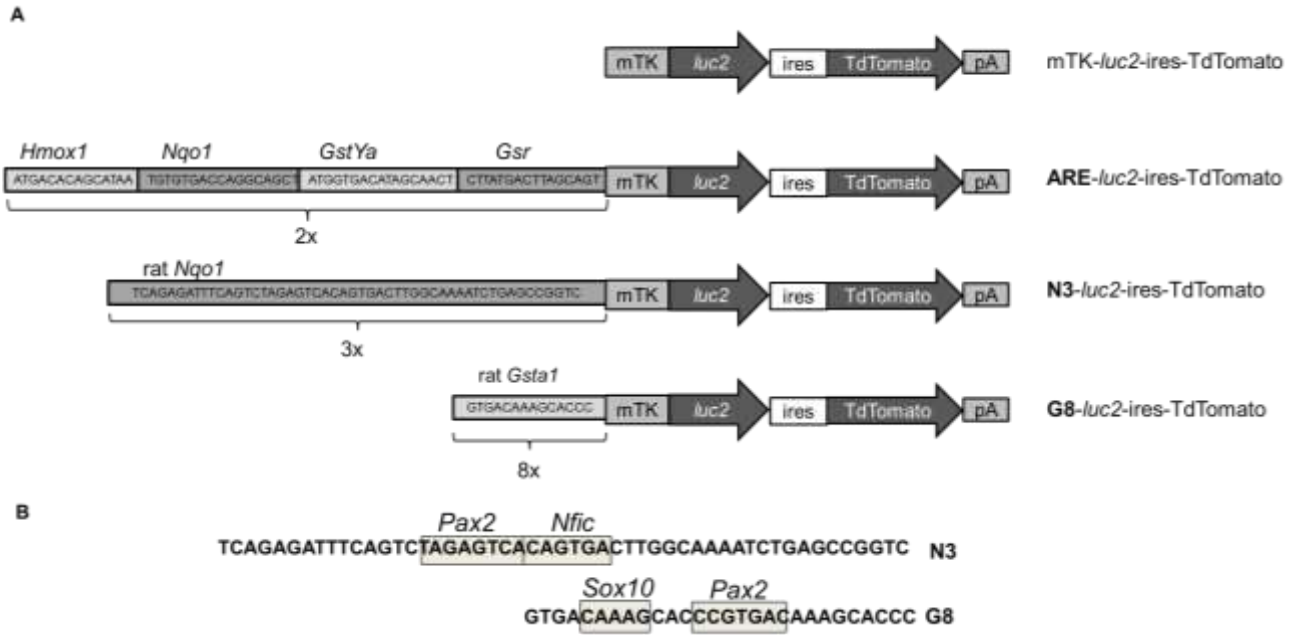

Figure 8. Schematic representation of Nrf2 reporter systems. A) mTK-*luc2*-ires-tdTomato, ARE-*luc2*-ires-tdTomato (ARE), N3-*luc2*-iresTdTomato (N3) and pG8-*luc2*-ires-tdTomato (G8) vectors with indicated the responsive sequence, the gene where it belongs and the number of repetitions; mTK = minimal promoter from HSV thymidine kinase, *luc2* = luciferase gene, ires= internal ribosome entry site, tdTomato = a red fluorescent protein developed in Dr. Roger Tsien's lab, pA = polyadenylation sequence. B) DNA sequence of N3 and G8 promoters with indicated the binding sites for transcription factors different from Nrf2 as defined by AliBaba 2.1 and Jaspar software.

The study revealed binding sites for other transcription factors (Pax2, Sox10 and Nfic) for both the N3 and G8 elements, while no binding sites other than the ARE could be found for the new consensus (Fig. 8B). The promoters were cloned upstream to an optimized expression cassette (mTK-*luc2*-ires-tdTomato) containing a minimal promoter from HSV thymidine kinase (mTK) and a bicistronic system conceived to contain a gene for bioluminescence imaging (BLI) (*luc2* gene, Promega) and a gene encoding a red fluorescent protein ideal for *ex vivo* studies at single-cell level the tdTomato, the two reporters were separated by an internal ribosome entry site (ires) to allow the transcription of both proteins.

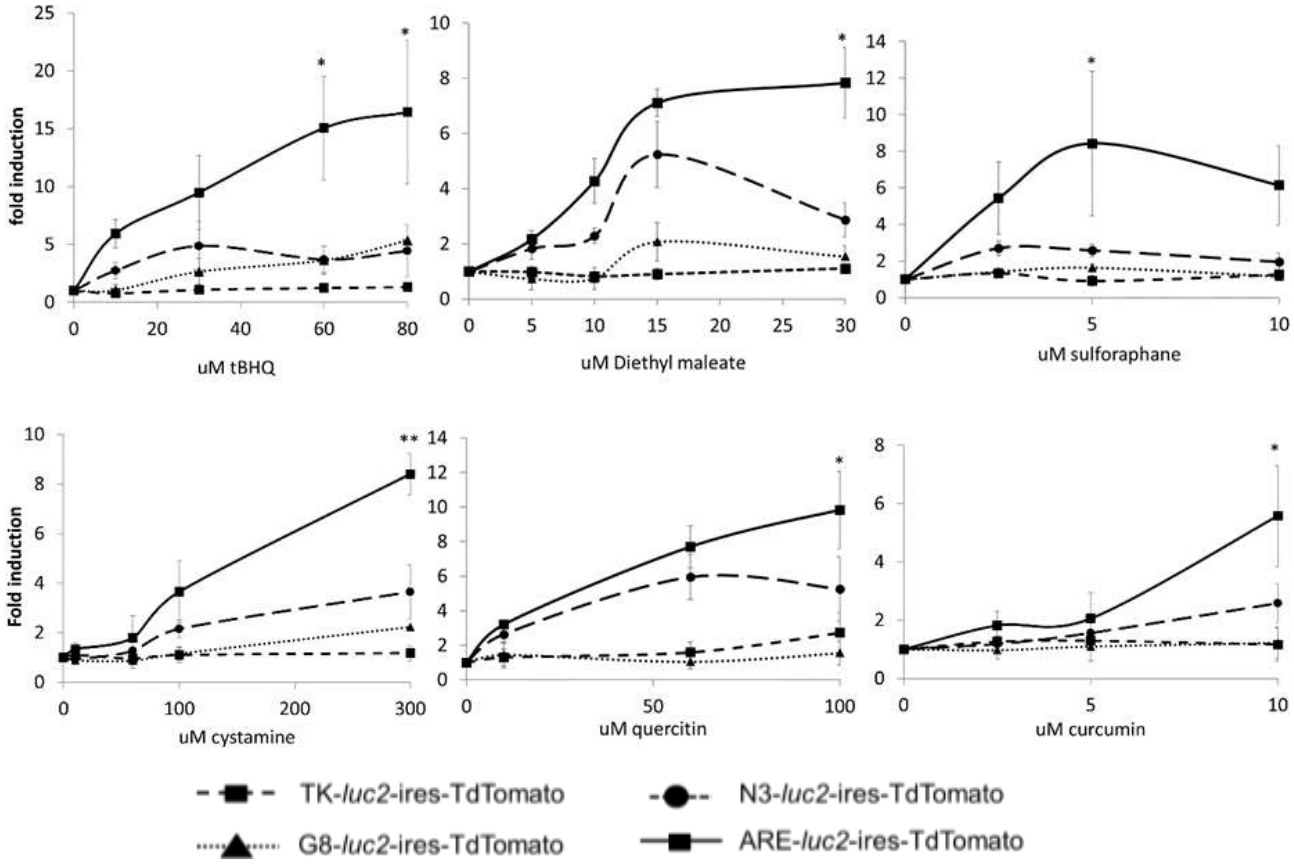

Figure 9. Functional comparison of Nrf2 reporter systems. Luciferase activity was measured in MCF-7 cells transiently transfected with reporter constructs and treated with monofunctional agents (tBHQ, diethylmaleate, sulforaphane and quercetin) and bifunctional agents (cystamine and curcumin) at the indicated doses. Data are mean values ± SEM (n=6) Relative light Unit (RLU) for µg protein normalized with the mean value of the vehicle-treated samples. * p<0.05 *versus (vs)* the corresponding samples transfected with mTK-luc2-ires-tdTomato with vehicle calculated with the Student's t-test.

To verify the extent to which the novel sequence was driving a selective and efficient Nrf2-inducible transcription, we performed transient transfection experiments in MCF-7 line. These assays carried out on both reporter *luc2* (Fig. 9) and tdTomato (Fig. 10A), demonstrated that ARE-*luc2*-ires-

tdTomato drive a more selective and robust response to Nrf2 inductor compared to the other reporter systems (Fig. 9) either using monofunctional agents (Prochaska and Talalay, 1988; Nguyen et al., 2003; Hu et al., 2006), such as tBHQ, diethylmaleate, sulforaphane and quercetin, or bifunctional agents (Calkins et al., 2010; Balstad et al., 2011), like cystamine and curcumin. No increase in the reporter production could be detected when the ARE-*luc2*-ires-tdTomato transfected cells were treated with agents unable to elicit an oxidative stress response (Fig. 10C), confirming the specificity of the reporter system; similar results were obtained in the murine fibroblast NIH 3T3 (not reported). Finally, to establish whether the response of the ARE-*luc2*-ires-tdTomato was paralleling the response of an endogenous target gene, we measured the mRNA of Nrf2, since previous works demonstrated the presence of a mechanism of autologous up-regulation for this gene (Nguyen et al., 2003; Hayes and McMahon, 2009). The concentration-response curve of Luc2 activity and *Nrf2* mRNA showed a similar trend in the same cells transfected with the construct (Fig. 10B, 10D) confirming that the reporter expression is mirroring the endogenous Nrf2 activity. Thus, we concluded that the plasmid ARE-*luc2*-ires-tdTomato can be used as a selective and efficient reporter system for the investigation of the Nrf2 pathway.

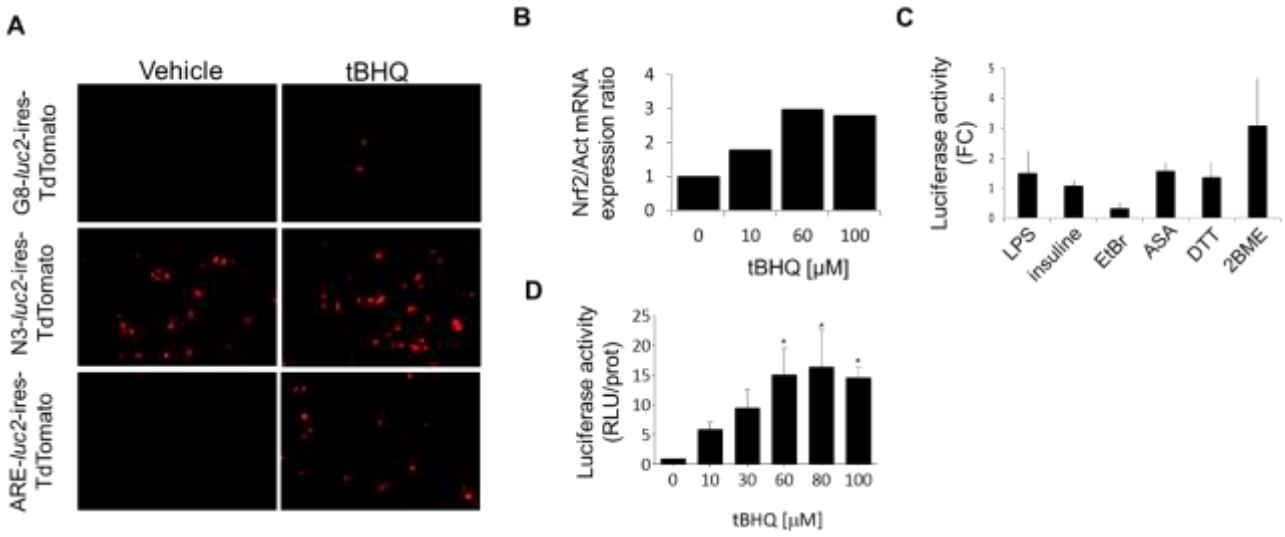

Figure 10. Validation of the ARE-*luc2*-ires-tdTomato vector. A) Representative pictures showing the fluorescence detection of tdTomato reporter protein in transiently transfected MCF-7 cells treated with vehicle (DMSO) or 80 µM of tBHQ for 6 hours. B) Real time PCR analysis of Nrf2 mRNA normalized on the reference gene Actin (n = 3). The analysis was done in MCF-7 cells treated with increasing doses of tBHQ for 24 hours. C) Luciferase activity was measured in MCF-7 cell line transiently transfected with ARE-*luc2*-ires-tdTomato vector and treated with agents that does not elicit an oxidative stress response: 2.5 µg/ml LPS, 0.1 ng/µl insulin, 30 µM ethidium bromide (EtBr), 100 µM acetylsalicylic acid (ASA), 1000 µM dithiothreitol (DTT), 600 µM 2-mercaptoethanol (2BME). Bars are mean values ± SEM (n=6) of RLU/µg proteins normalized with the mean value of the vehicle treated samples. D) Luciferase activity was measured in the extract from transiently transfected MCF-7 cells treated with the indicated doses of tBHQ for 24 hours. Bars represent mean value (RLU/µg of proteins) ± SEM (n = 6); *p < 0.05 *vs* vehicle calculated with the student's t-test.

5.1.2 Generation and validation of transcription factor EB reporter system

To generate a reporter system to monitor the regulation of lysosome biogenesis and autophagy pathway we performed a procedure analogous to the generation of the synthetic Nrf2-inducible promoter. Bioinformatics analysis of the promoter regions of 140 well-characterized TFEB-target genes was performed to identify common structural features such as the distance from the TATA box, the sequence composition of the CLEAR sequences (Sardiello et al., 2009) and the neighbouring nucleotides. The conceived promoter, called CLEAR Optimized, was cloned upstream to the reporter cassette in which the *luc2* gene was separated from the tdTomato by a T2A self-proteolytic peptide able to ensure a stochiometric transcription of both reporters (Fig. 11).

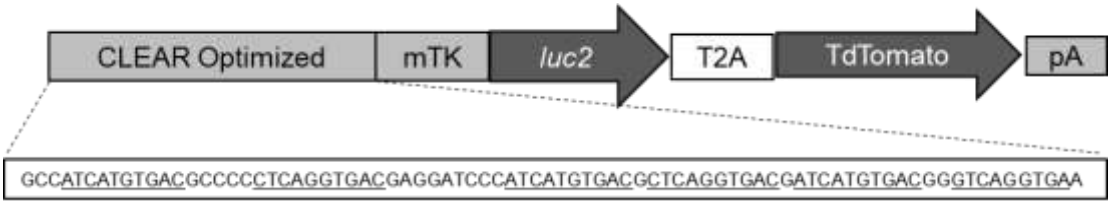

Figure 11. Schematic representation of the TFEB reporter system. The scheme reports upstream the promoter structure, constituted by the CLEAR_Optimized element (the sequence is entirely reported) and the minimal TK promoter (mTK), and downstream the reporter gene cassette, which comprises the firefly luciferase (*luc2*) separated from the *tdTomato* by a sequence encoding for the self-proteolytic peptides T2A and pA.

To verify if the new CLEAR promoter was able to drive an efficient TFEB-dependent transcription of the reporters, the new consensus was tested in transient transfection assays and compared with two previously published reporters used to monitor TFEB modulation in cellular models: a vector containing a minimal promoter constituted by eight CLEAR elements (named CLEAR Canonical) (Cortes et al., 2014) and a construct containing the full TFEB promoter (Tsunemi et al., 2012) (named TFEB promoter). The three constructs were tested in transient transfection assays together with increasing concentration of a vector expressing the transcription factor EB (pTFEB, kindly provided by the Ballabio lab) (Fig. 12A). The results clearly showed that the CLEAR optimized sequence is the best among the responsive element tested since it was able to report the transcription factor activity even when a minimal amount of TFEB expression vector (10 ng) was co-transfected; furthermore, this sequence mediated the highest reporter induction, when compared with other constructs. The fluorescent acquisition of the cells demonstrates that the tdTomato protein is efficiently expressed by the CLEAR_Optimized vector after TFEB overexpression (Fig. 12B).

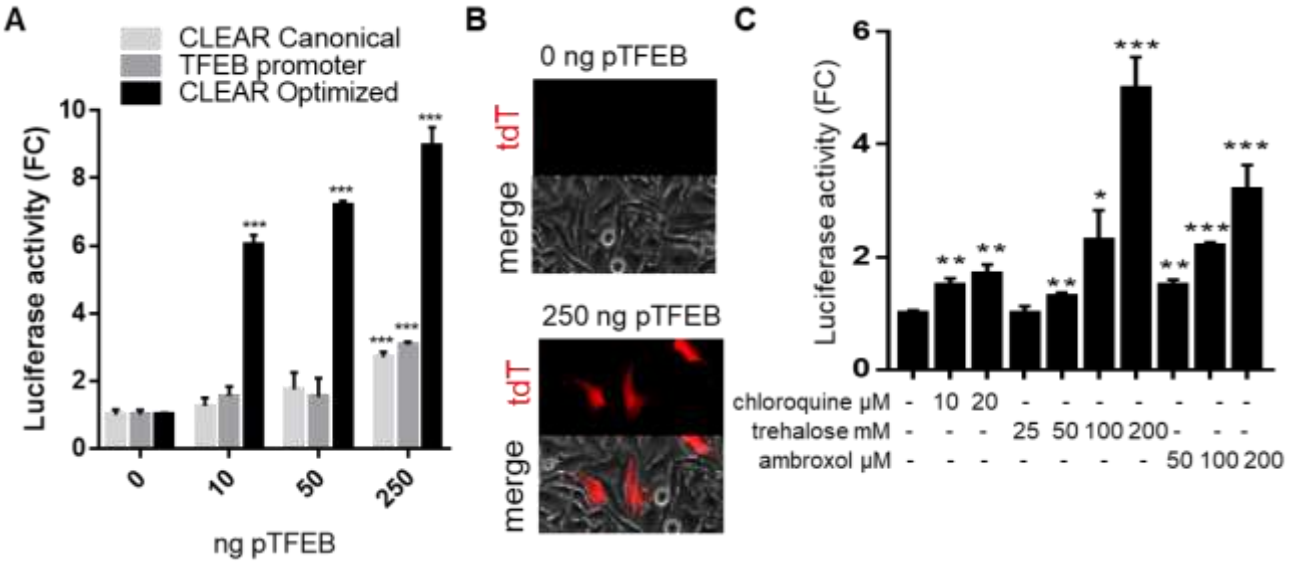

Figure 12. Validation of the TFEB reporter vector. A) Luciferase activity was measured in HeLa cells transiently co-transfected with the reporter vector and a plasmid expressing the TFEB protein (pTFEB). Bars are mean values ± SD, (n=6) in duplicate, the luciferase activity is expressed as fold change (FC) of RLU/µg proteins normalized with the mean value of the construct co-transfected with an empty vector. ***p < 0.001 *vs* empty vector calculated with one-way ANOVA followed by Dunnett's multiple comparisons test. B) representative pictures of the tdTomato (tdT) fluorescence of CLEAR_Optimized-*luc2*-T2A-tdTomato vector and co-transfected with an empty vector (0), or 250 ng pTFEB. C) Luciferase activity was measured in HeLa cell line transiently transfected with CLEAR_Optimized-*luc2*-T2A-tdTomato and treated with agents able to elicit TFEB activation. Bars represent FC of RLU/µg of proteins on vehicle ± SD (n = 6) in duplicate; *p < 0.05, **p< 0.01, ***p< 0.001 *vs* vehicle calculated with one-way ANOVA followed by Dunnett's multiple comparisons test.

To test the ability of the CLEAR_Optimized-*luc2*-T2A-tdTomato construct to report TFEB pharmacological activation, HeLa cells were transiently transfected with the reporter vector and treated for 16 hours with increasing concentrations of molecules able to induce TFEB activation. In detail, to the culture media were added chloroquine (Roczniak-Ferguson et al., 2012), trehalose (Palmieri et al., 2017), and ambroxol, the latter is a candidate drugs for PD known to induce TFEB activation (McNeill et al., 2014). The results of these experiments clearly demonstrated the expected ability of the reporter system to respond to the TFEB activation (Fig. 12C), since a concentration-dependent increase of luciferase-driven bioluminescence was detected. These experiments demonstrated that the new construct CLEAR_Optimized-*luc2*-T2A-tdTomato is an efficient and sensitive reporter system of the TFEB activity.

5.1.3 Generation of ARE-*luc2* and TFEB-*luc2* reporter mice

To study the Nrf2 and the Tfeb pathway *in vivo*, the ARE-*luc2*-ires-tdTomato and the CLEAR_Optimized-*luc2*-T2A-tdTomato vectors were inserted into a permissive locus of the mouse genome (Rizzi et al., 2017) through homologous recombination to produce the ARE-l*uc2* and the TFEB-*luc2* reporter transgenic mice, respectively. In these mice it is possible to measure the Nrf2 or Tfeb activity in the whole body through *in vivo* imaging technologies. In detail, to generate the reporter mice the first step we performed was to assemble the targeting constructs (ARE-targeting and CLEAR-targeting) constitute by the reporter cassette (ARE-*luc2*-ires-tdTomato or CLEAR_Optimized-*luc2*-T2A-tdTomato) containing cre-loxP sequences for the selection of the tissues where the transgene is expressed, flanked by insulator sequences Matrix Attachment Regions (MAR) to decrease the probabilities of position effects (Fig. 13A) (refer European patent No. EP 1298988B1; US patent No. 7 943 81). This sequences were surrounded by 3' and 5' homologous region allowing to integrate the transgene into the chromosome 1 in a locus that we have previously discovered and that is characterized by a constitutively open state (Rizzi et al., 2017), localized 10'208 bp 5'of the *Enah* gene (enable homolog isoform 1) and 94'173 bp 3' of the *Srp9* (signal recognition particle 9kDa protein) (Fig. 13B). For the tissue specific expression of the reporters, it was used the Cre-loxP system and between promoters (CLEAR or ARE) it was integrated a floxed STOP sequence (loxP-STOP-puro-loxP) and the bicistronic cassette (*luc2*-ires/T2A-tdTomato-pA) (Fig. 13A) a strategy that is sufficient to completely block the activity of RNA polymerase II (Rizzi et al., 2017).

The ARE/CLEAR-targeting vectors were linearized and electroporated into sv6.4 embryonic stem cells (ES) and the clones in which the vector was inserted selected with puromycin medium, since the puromycin N-acetyltransferase gene product (puro) was introduced into the construct (Fig. 13A). To further confirm the insertions and integrity of the cassette, we performed on resistant ES cells a sequential screening PCR designed to span the entire construct (example of the PCR scheme for TFEB reported in Fig. 13C); the PCR products obtained were sequenced as further corroboration. More than four hundred resistant clones for each transgene were screened for homologous recombination by PCR. One out of 8 positive clones in the case of ARE and one out of three positive clones in the case of CLEAR, were injected into C57Bl/6 blastocysts and then implanted in the oviducts of *in vitro* culture-held foster mice; the resulting chimeric mice were crossed to C57BL/6 to generate the f1.

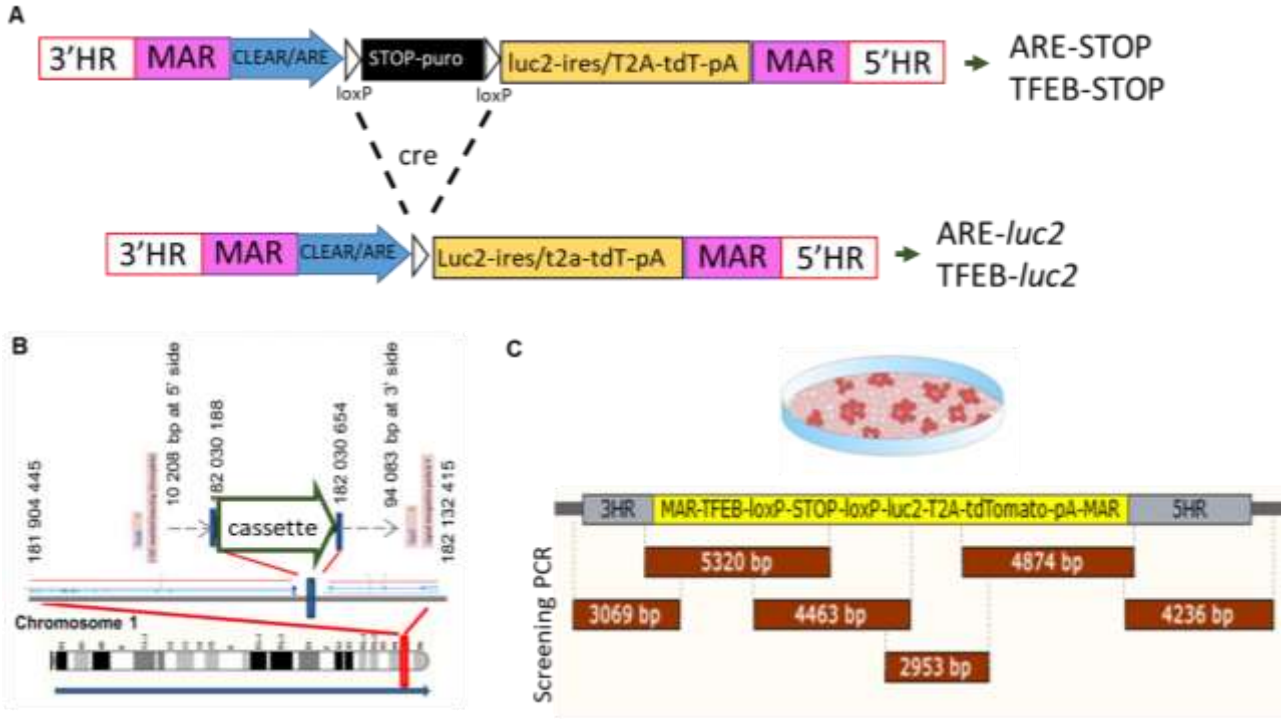

Figure 13. Targeting vector and ES screening. A) Schematic representation of the ARE/CLEAR-targeting vectors utilized to generate the reporter mice prior and after excision of loxP-STOP-puro-loxP sequence by Cre enzyme. The upper construct is inserted into the genome of TFEB-STOP or ARE-STOP mice, the lower construct in TFEB-*luc2* or ARE-*luc2*. B) Graphical representation of the locus in which the ARE/CLEAR-targeting vectors were integrated to generate the reporter mice on chromosome 1. C) Schematic representation of the PCR screening performed on TFEB-ES cells resistant to puromycin. Were performed 5 different PCR to cover all the transgene and confirms the integrity of the construct. In the figure it is reported the expected band size of the PCR products obtained.

The f1 founder mice were selected performing the same PCR scheme utilized for ES screening (Fig. 13C). The mice carrying the full transgene (named TFEB-STOP and ARE-STOP) did not express luciferase as confirmed by the *in vivo* (Fig. 14) and *ex vivo* luciferase assays (not reported). Therefore the f1 was crossed with the B6.C-Tg(CMV-cre)1Cgn/J mouse expressing the Cre recombinase in germ cells (Schwenk et al., 1995), and allowing the excision of STOP cassette to produce ARE-*luc2* and TFEB-*luc2* reporter mice (Fig. 13A). The constitutively open state of the genomic locus (Rizzi et al., 2017) where the transgene was inserted and the MAR insulating activity, supports a correct and ubiquitous activity of the luciferase biosensor (Fig. 14) in both the transgenic line generated, ARE-*luc2* and TFEB-*luc2*.

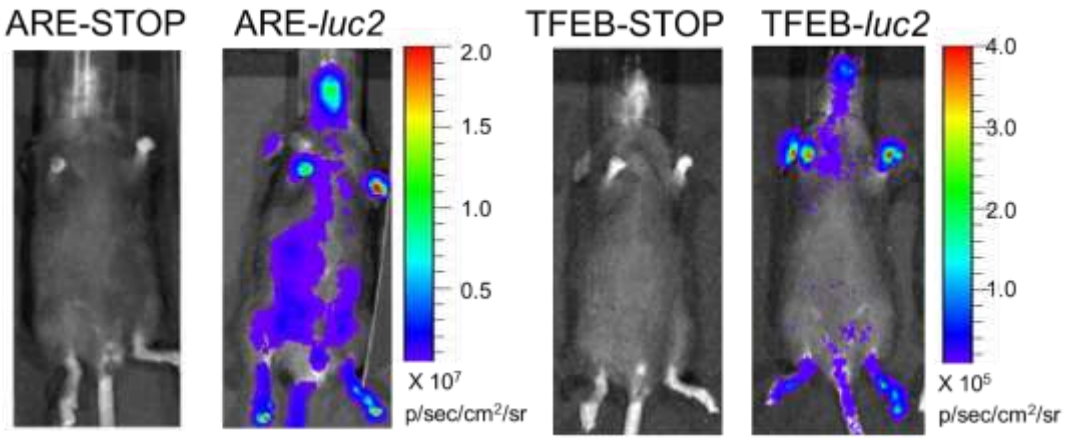

Figure 14. *In vivo* analysis by BLI of luciferase expression. Representative pseudocolor images of ARE-STOP, ARE-*luc2,* TFEB-STOP and TFEB-*luc2* reporter mice showing the *in vivo* imaging pattern of luciferase expression. Images were obtained 15 min after the injection of 80 mg/kg luciferin with 5 min exposition time.

The ARE-*luc2* reporter mouse was validated using Nrf2 inducers such as sodium arsenite (ASN) (Fig. 15) (Szymanska-Chabowska et al., 2002; Pb et al., 2003) and diethyl maleate (not reported). *In vivo* and *ex vivo* imaging analysis showed an increase of the luciferase activity, 6 hours after intraperitoneal injection of 12.5 mg/kg ASN (Fig. 15A-C). To investigate the extent to which Nrf2 mRNA fluctuation reflected the reporter activity, we measured the mRNA expression of *Hmox1* and *Nqo1*, two Nrf2 target genes, in different tissues. ASN treatment differentially affected the expression of these two genes in distinct tissues: a marked increase of *Hmox1* mRNA was detected in the muscle (12- fold), wat (9.5-fold) and lung (8.9-fold), while the *Nqo1* mRNA increase was detected in the lung (7.5-fold) and uterus (5.9-fold) (Fig. 15D). The effects of ASN treatment on luciferase activity in the different tissues was mirroring those observed in the real-time PCR analysis on the mRNA since we measured the highest induction in wat (15.3-fold), uterus (8.5-fold) and lung (7.6-fold) mirroring the activation of the endogenous genes, apart from the induction observed in the muscle of the *Hmox1* mRNA, suggesting that these activation might not be dependent on Nrf2 in this tissue. A detailed immunohistochemical analysis of tdTomato was carried and demonstrated that also the fluorescent reporter was transcribed since was detected red fluorescence only in the brain areas characterized by high luciferase expression (Fig. 15E). Altogether, these data validated the ARE-*luc2* reporter mouse as a valuable tool to study the Nrf2 pathway modulation *in vivo*.

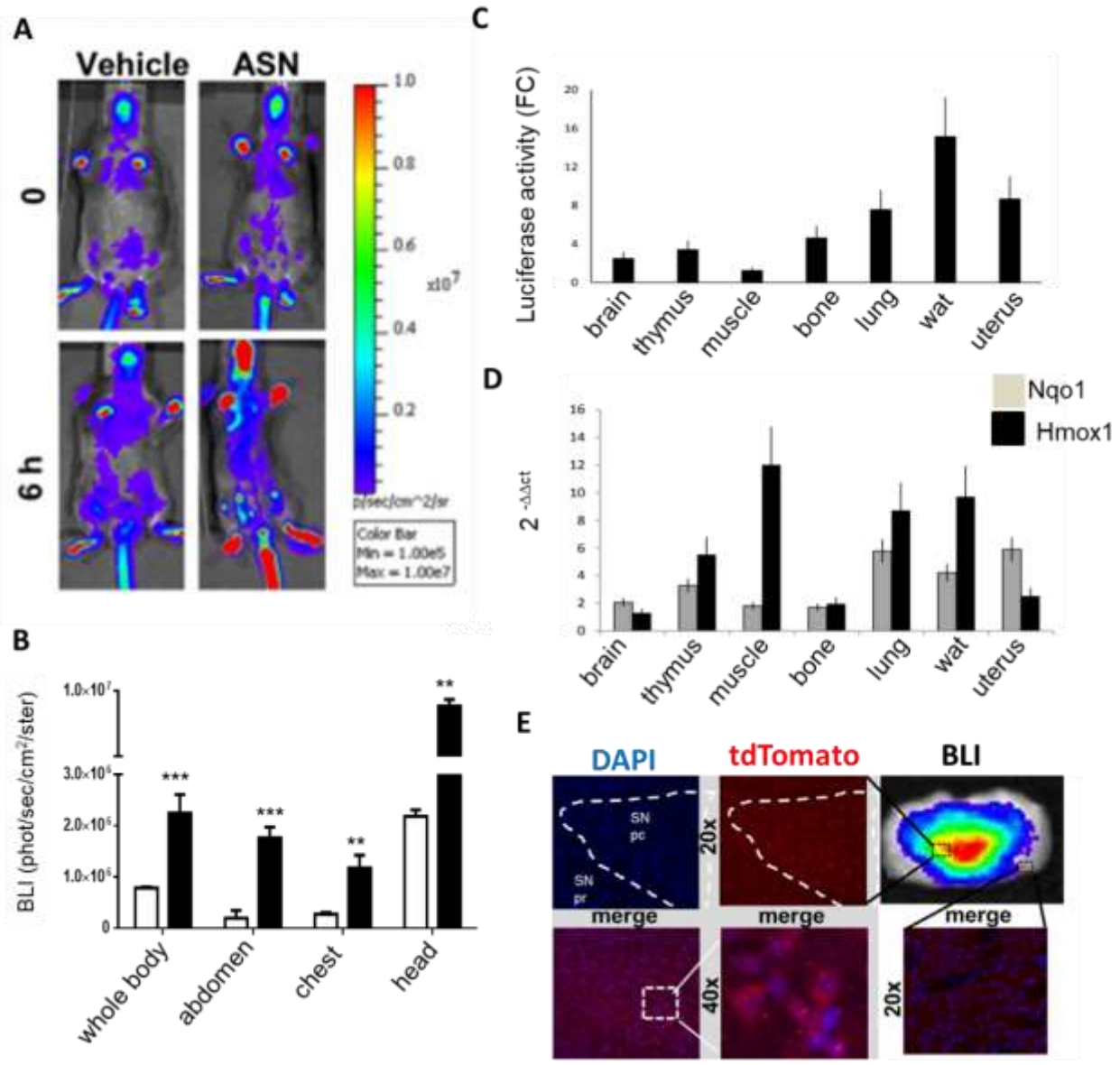

Figure 15. Validation of ARE-*luc2* reporter mouse. A) Pseudocolor images representative of the activation of luciferase expression by the administration of ASN. *In vivo* bioluminescence imaging was done 6 hours after i.p. injection of 12.5 mg/kg ASN. B) BLI measurement in selected body areas after ASN injection. Each bar corresponds to mean ± SEM (n = 4), expressed as photon emission (p/s/cm^2/sr). **p<0.01, ***p<0.001 vs vehicle. C) Luciferase activity measured in 7 organs dissected from ARE-*luc2* mice 6 hours after i.p. injection of ASN (12.5 mg/kg). Each bar corresponds to the fold change in BLI *vs* vehicle treated animals. D) Real time PCR analysis of *Hmox1* and *Nqo1* genes done on 7 organs dissected from ARE-*luc2* mice after 6 hours of i.p. injection of 12.5 mg/kg ASN. Bars represent the levels of indicated mRNAs normalized on the reference gene 36B4, induction are expressed as $2^{-\Delta\Delta Ct}$ respect to vehicle. E) BLI and immunohistochemical analysis of the brain of the mouse reporter for the oxidative stress. Immunohistochemical analysis of brain slices at two magnification (20x and 40x): in blue DAPI staining, in red tdTomato protein and merging of the staining showing the cytoplasmic presence of tdTomato.

5.2 Nrf2 regulation during early stages of dopaminergic degeneration induced by MPP+

5.2.1 NFR2 activation precedes cell death in MPP+ treated SK-N-BE cell line

To study the modulation of TFEB and NRF2 pathways during dopaminergic neuronal death, we have transfected the neuroblastoma cell line SK-N-BE (Biedler et al., 1978) with the CLEAR_optimized-*luc2*-ires-tdTomato vector (described in chapter 3.1.2) or ARE-*luc2*-ires-tdTomato vector (described in chapter 3.1.1), respectively, and we have treated the transfected cells with 1 mM MPP+, the active metabolite of MPTP that induces death selectively in dopaminergic cells (Nicklas et al., 1985; Vyas et al., 1986), or with vehicle (water). The treatment was chosen to induce partial cell death, reported to be equal to 60% after 48 hours (Kim et al., 2010). Quantification of the luciferase activity in the cellular extract showed that the treatment does not modulate TFEB activity since no alteration in luciferase was detected in the cells transfected with CLEAR_optimized-*luc2*-ires-tdTomato (Fig. 16A), on the contrary, increased luciferase expression of about 2 times in ARE-*luc2*-ires-tdTomato transfected cells was observed, meaning that NFR2 activity was augmented as a result of treatment (Fig. 16B).

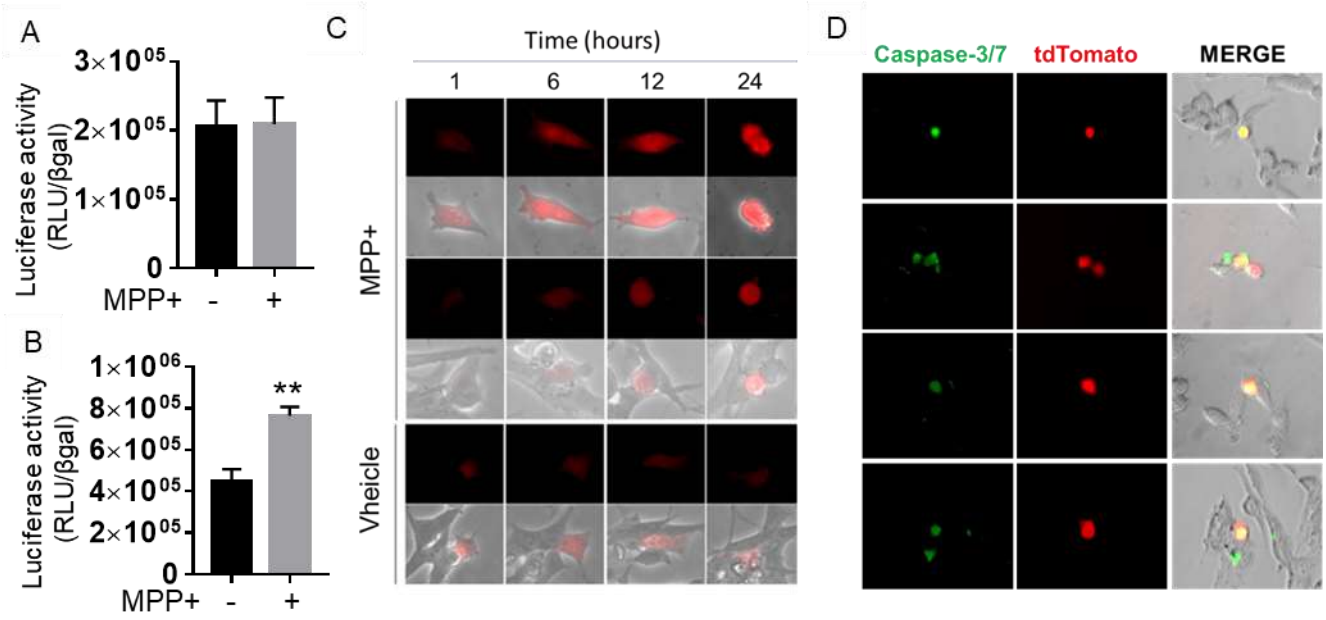

Figure 16. Analysis of NRF2 modulations in MPP+ treated SK-N-BE dopaminergic cells. Luciferase activity measured in cellular extracts of SK-N-BE transiently transfected with the A) CLEAR_optimized-*luc2*-ires-tdTomato or B) ARE-*luc2*-ires-tdTomato vector after 24 hours of treatment with 1 mM MPP+ or vehicle (water). The transfections were standardized by co-transfecting the plasmid CMV-β-gal. Data are expressed as mean values of RLU on β-galactosides activity ± SEM of n = 3 samples measured in duplicate; **p < 0.01 *vs* the corresponding samples treated with the vehicle calculated with the Student's t-test. C) Representative

pictures obtained in a time lapse experiment of the tdTomato fluorescent emission of SK-N-BE cells transiently transfected with the ARE-*luc2*-ires-tdTomato at 1, 6, 12, 24 hours after 1 mM MPP+ treatment, in the upper panel cells responsive to the treatment in the lower panel vehicle treated cells. D) Representative pictures of SK-N-BE cells transiently transfected with the ARE-*luc2*-ires-tdTomato construct and treated with 1 mM MPP+ for 24 hours: in red the tdTomato reporter for NRF2 activity, in green apoptotic cells with activated Caspase-3/7.

To study the fate of the cells in which the NRF2 pathways was activated, we monitored the fluorescence associated with the tdTomato expression by time-lapse microscopy in the dopaminergic cells transfected with the ARE reporter vector. The recorded imaged displayed that tdTomato was induced around 2-6 hours after treatment selectively in cells that after 24 hours manifest typical features of cell death: shrinkage, nuclear fragmentation and blebbing (Fig. 16C). At 24 hours' time point, the cell staining with a probe that emits light after Caspase-3/7 proteolytic cleavage demonstrated that the tdTomato co-localizes with the fluorescent probe (Fig. 16D) confirming that cells increasing NRF2 activity were committed to apoptosis. These data proved that the NRF2 signalling is early activated in cells sensitive to MPP+.

5.2.2 *In vivo* imaging of Nrf-2 activity in the ARE-*luc2* reporter transgenic mouse.

To evaluate *in vivo* the Nrf2 pathway modulation during dopaminergic neurodegeneration, we intraperitoneally (i.p.) injected the ARE-*luc2* reporter mice with a daily dose of 20 mg/kg MPTP for 4 days (Fig. 17A) or vehicle (PBS). We have chosen the subacute treatment in which the degeneration of dopaminergic neurons was observed starting from day 1 after the fourth MPTP administration (Gibrat et al., 2009; Costa et al., 2013), with the aim to investigate the Nrf2 modulation during early events preceding cell death. Mice were subjected to *in vivo* imaging session from day 0 to day 14, to record the bioluminescent emission from the brain area during the different phases of the neurodegenerative process (Fig. 17B, 17C).

The results showed that in the head area the photon emission, which reflects Nrf2 modulation, increased already at 6 hours after the first MPTP administration, with a maximum level of luciferase activity at day 6 which remained high until the end of the experiment at day 14, while in vehicle treated ARE-*luc2* animals the photon emission remain stable during the entire experiment (Fig. 17B). *Ex vivo* imaging of the dissected brains localized the luciferase signal coming from the brain slices containing the SN and not the striatum (Fig. 17D). The immunostaining assays for tyrosine

hydroxylase (TH) (Fig. 17E) showed that the number of positive cells decreased at day 6 with a minimum displayed at day 14, corroborating the notion that the MPTP treatment is able to induce dopaminergic death that continue after the last administration (Fig. 17E). The results of these experiments confirmed that the Nrf2 signalling is early activated in the neurodegeneration, even before the death of dopaminergic neurons.

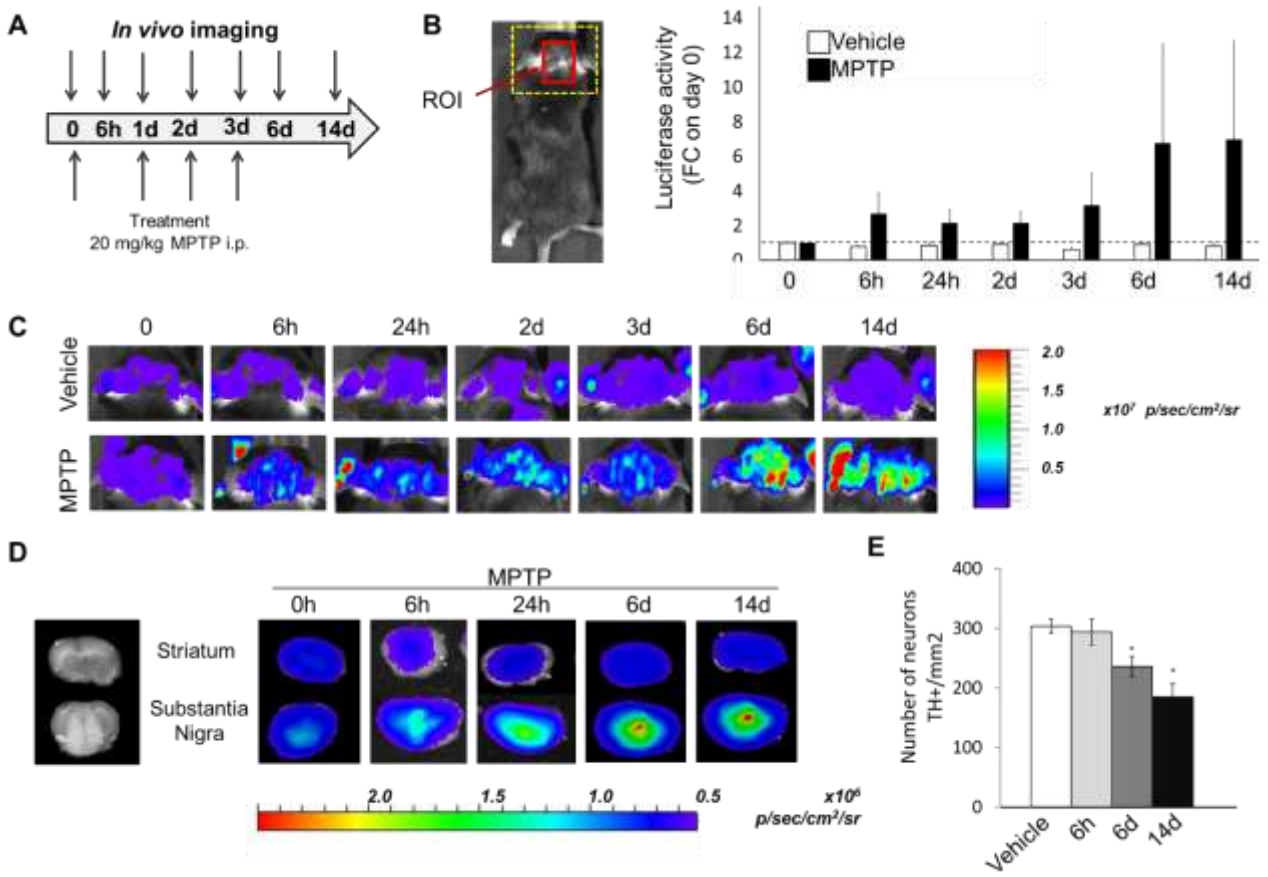

Figure 17. Bioluminescence analysis of Nrf2 activation in MPTP treated ARE-*luc2* mice. A) Schematic representation of the experimental plan: ARE-*luc2* mice were daily treated i.p. with 20 mg/kg MPTP for 4 days; *in vivo* imaging was carried out at the indicated time points. B) Quantification of the bioluminescence light from the dorsal head area (Region Of Interest, ROI: red square). For each animal, photon emissions (p/s/cm^2 /sr) were expressed as FC *vs* time 0, mean ± SEM (n = 12). C) representative pictures showing the *in vivo* imaging of a mouse head (see ROI: yellow square in (B)) from a single representative individual at the indicated time points for each experimental group: vehicle (PBS) or MPTP treated animals. Pseudocolor images of each mouse were obtained 15 min after the i.p. injection of 80 mg/kg of luciferin with 5 min exposition time. D) The grayscale pictures were taken with dimmed light show an example of slices containing striatum (upper panel) and SNc (bottom); pseudocolors images represent the photon emission from the *ex vivo* imaging analysis of luciferase activity from the brain slices of representative MPTP treated animals at the indicated time points. E) Evaluation of the dopaminergic neuronal loss in MPTP treated ARE-*luc2* mice; data are expressed as the number of tyrosine hydroxylase positive (TH+) cells/mm^2 in SNc. Bars represent the mean ± SEM of cells counted in 12 animals/group; *p < 0.05 *vs* samples treated with PBS (vehicle) calculated with the Student's t-test.

5.2.3 Activation of Nrf2 is an early event preceding neuronal cell death induced by MPTP *in vivo*

To characterize which cells are responsible for the early Nrf2 activation observed in the SNpc of ARE-*luc2* reporter mice treated with MPTP, we performed an immunohistochemical analysis of the brain dissected 6 hours after MPTP or vehicle treatment (Fig. 18A). The co-staining experiments with antibodies for tyrosine hydroxylase (TH) and Nrf2 proteins and DAPI for nuclei showed that the treatment with MPTP was producing an increase of the Nrf2 nuclear staining (green) in dopaminergic neurons (TH+ cells, red) compared with vehicle-treated animals (Fig. 18A). Interestingly, the nuclear staining was observed also in some TH-negative cells of the SNpc, and in particular, we found some co-localization with the GFAP marker, indicating that at 6 hours after MPTP treatment, activation of Nrf2 may occur also in astrocytes (Fig. 18C). Finally, as a negative control, we investigated the Nrf2 activation hippocampus CA3 (Fig. 18B) and as expected we did not find any Nrf2 activation. As reported in the SK-N-BE cell line (Fig. 16B, 16C), the early increase of Nrf2 activity preceded the neuronal cell death induced by MPTP that *in vivo* usually began 1 day after the fourth MPTP treatment (Gibrat et al., 2009; Meredith and Rademacher, 2011). Collectively, the results obtained in cells and *in vivo* identified activation of the Nrf2 signaling as an early event during the process driving the dopaminergic neuronal cell death induced by MPTP.

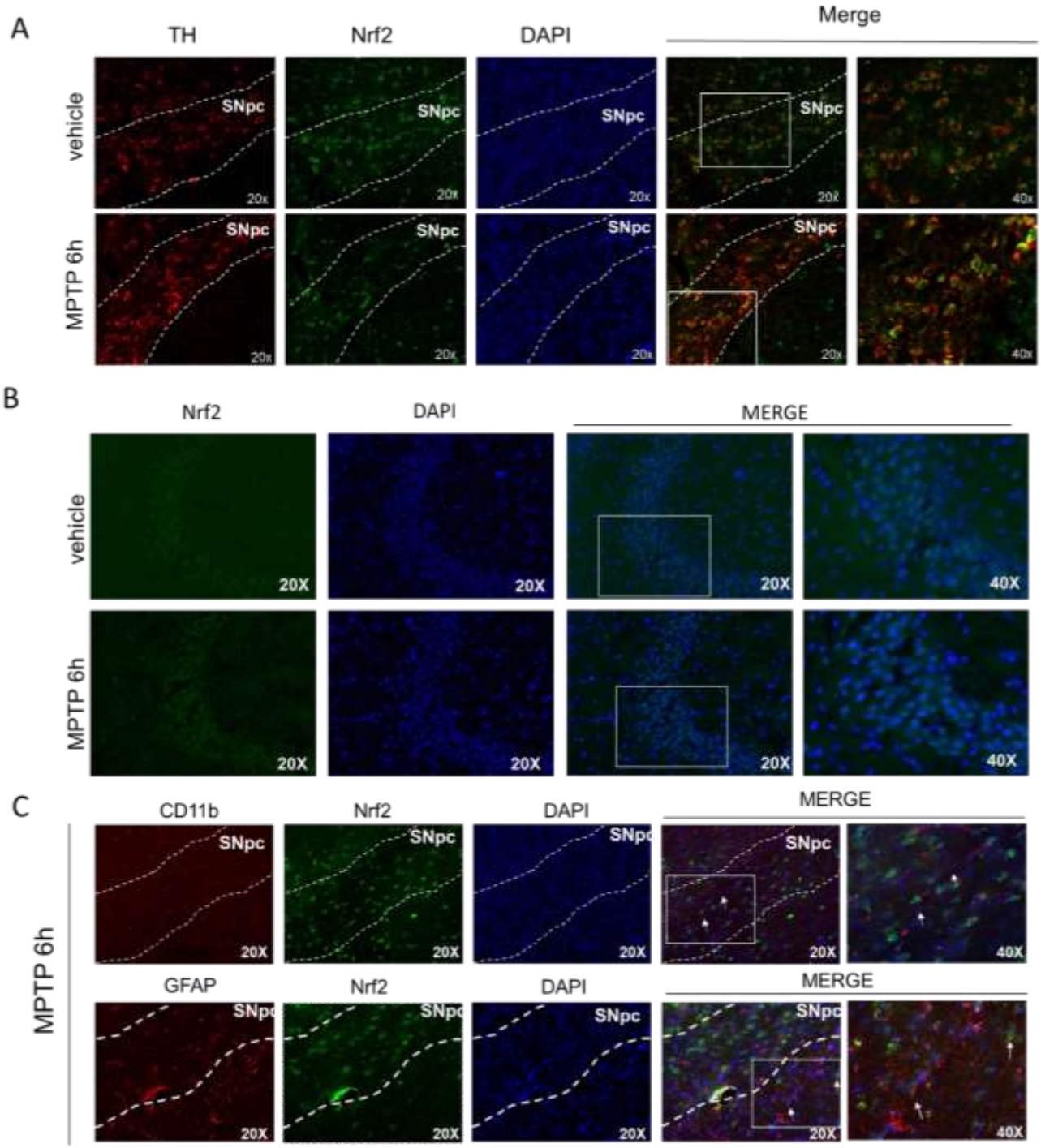

Figure 18. Immunohistochemical analysis of Nrf2 activation in MPTP treated mice. A) Representative images of immunohistochemical analysis of SNpc in the brain slices at two magnifications (20X and 40X): in red tyrosine hydroxylase (TH), in green Nrf2, in blue DAPI: merging of the staining shows nuclear localization of the Nrf2 protein in neurons of the SNpc of mice 6 hours after treatment with MPTP. B) Immunohistochemical analysis of hippocampus (CA3) in the brain slices of mice 6 hours after treatment with MPTP at two magnifications (20X and 40X): in green Nrf2, in blue DAPI. C) Immunohistochemical analysis of SNpc in the brain slices of mice 6 hours after treatment with MPTP at two magnifications (20X and 40X): in red CD11b or GFAP (as indicated), in green Nrf2, in blue DAPI. Merging of the staining shows nuclear localization of the Nrf2 protein and, in some cases, colocalization with GFAP signal. All the sections were 40 µm thick and visualized and digitally photographed using a Zeiss microscope equipped with a MosaiX-AxioVision Rel 4.8 Software.

5.3 Reporter systems reveal that the pharmacological inhibition of microglial GCase, the Gaucher's disease gene product, hinders the Nrf2-mediated neuroprotective response in neurons

5.3.1 GCase inhibition impairs Nrf2 response *in vivo.*

Since our data confirmed that the Nrf2 pathway is activated before the death of the neurons, we investigated the relationship between the Nrf2 activation and the inhibition of GCase, the enzyme encoded by the GBA1 gene which mutation leads to GD and is associated with high risk of developing PD, with the aim to verify if such impairment could interfere with this cytoprotective pathway. Two groups of 16 ARE-*luc2* reporter mice were treated i.p. with a daily dose of 100 mg/kg/die of conduritol-B-epoxide (CBE) or vehicle (PBS) for three days, a dose sufficient to decrease GCase activity down to 50% of baseline levels (Fig. 19B): the same reduction has been observed in fibroblasts obtained from heterozygous patients carrying severe GBA1 mutations (Migdalska-Richards and Schapira, 2016; Sanchez-Martinez et al., 2016). At day 2, half of the mice from both groups were further treated i.p. with two doses (20 and 16 hours before the end of the experiment) of 75 mg/kg tert-butylhydroquinone (tBHQ), a well-known Nrf2 inducing agent crossing the blood-brain barrier (Abiko et al., 2011; Silva-Palacios et al., 2017; Rizzi et al., 2018) (Fig. 19A). Bioluminescent emissions were measured before and after tBHQ administration by *in vivo* imaging sessions (Fig. 19A). Quantitative analyses of photon emissions from the head area of CBE- and vehicle-treated mice revealed a comparable luciferase activity in the two groups of animals (Fig. 19C, 19D), suggesting that CBE administration did not modulate the physiological Nrf2 signaling pathway. As expected, tBHQ treatment induced a significant (three-fold) increase of luciferase activity in vehicle-treated animals, while in mice pre-treated with CBE, the Nrf2 response was impaired (Fig.19C, 19D).

At the end of the experiments, brains were dissected and *ex vivo* imaging was carried out on brain slices from 2 to 3 mm thick (Fig. 20A): quantification of luciferase activity in the whole brain (Fig. 20B) and in different brain sections (Fig. 20C-E, 20G, 20H) confirmed the observations made *in vivo* and localized the major reduction of Nrf2 activity in brain slices I (- 53%), II (- 20%), and IV (- 21%) (Fig. 20C, 20D, 20G) containing the olfactory bulb (OB) and the SNpc, two relevant areas for PD.

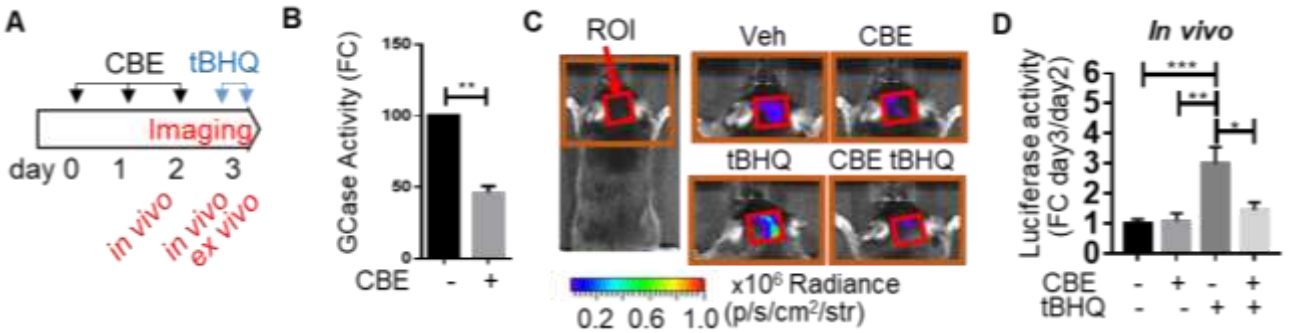

Figure 19. Bioluminescence analysis of Nrf2 activation in CBE treated ARE-*luc2* mice. Scheme of the pharmacological treatments and *in vivo/ex vivo* imaging sessions applied to the ARE-*luc2* reporter mouse model. B) Effect of CBE treatment on residual GCase activity in the brain of mice treated with 100 mg/kg/ for three days. Data are expressed as mean ± SD. **p<0.01 *vs* vehicle by student t-test. C) Representative pictures of the bioluminescence emitted from the region of interest (ROI) highlighted by the red square on the head area: the intensity of photon emission is reproduced with pseudocolor images generated by the software on the basis of the indicated scale bar. D) Quantification of the bioluminescence signal from the dorsal head area (measured in the ROI reported in panel (C) in each animal). Changes in radiant flux (p/s/cm^2/sr) were expressed as FC *vs* day 2. Bars represent mean ± SD, for n=4 animals measured in duplicate. *p<0.05, **p<0.005, ***p<0.001 by one-way ANOVA followed by Tukey's multiple comparison test.

Next, wild-type C57BL/6 mice were divided into 4 experimental groups and treated with vehicle, CBE, tBHQ or CBE plus tBHQ as described above. *Post mortem* analyses were performed on tissue sections of the ventral mesencephalon that contained the SNpc and were immunostained with anti-tyrosine hydroxylase (Th) and anti-Nrf2 antibodies (Fig. 20I). Immunoreactivity for Nrf2 (Red) was detected within the cytosolic compartment of Th-positive nigral dopaminergic neurons (Green) in sections from vehicle- and CBE-treated mice. Quite in contrast, Nrf2 staining became mostly nuclear after tBHQ administration, consistent with nuclear translocation. Nrf2 nuclear immunoreactivity was apparently less robust in the SNpc of animals injected with both CBE and tBHQ if compared to tBHQ alone (Fig. 20I). Semi-quantitative analysis of nuclear NRF2 intensity confirmed these histochemical observations. It showed a 3-fold increase in nuclear NRF2 after treatment with tBHQ alone and a significant reduction (- 30%) of this effect in mice with CBE-induced GCase inhibition (Fig. 20F). Taken together, results provided the first evidence of a relationship between GCase activity and the NRF2 pathway, with enzyme inhibition impairing neuronal antioxidant response in brain regions such as the SNpc. Follow-up studies were then designed to investigate mechanisms underlying this relationship.

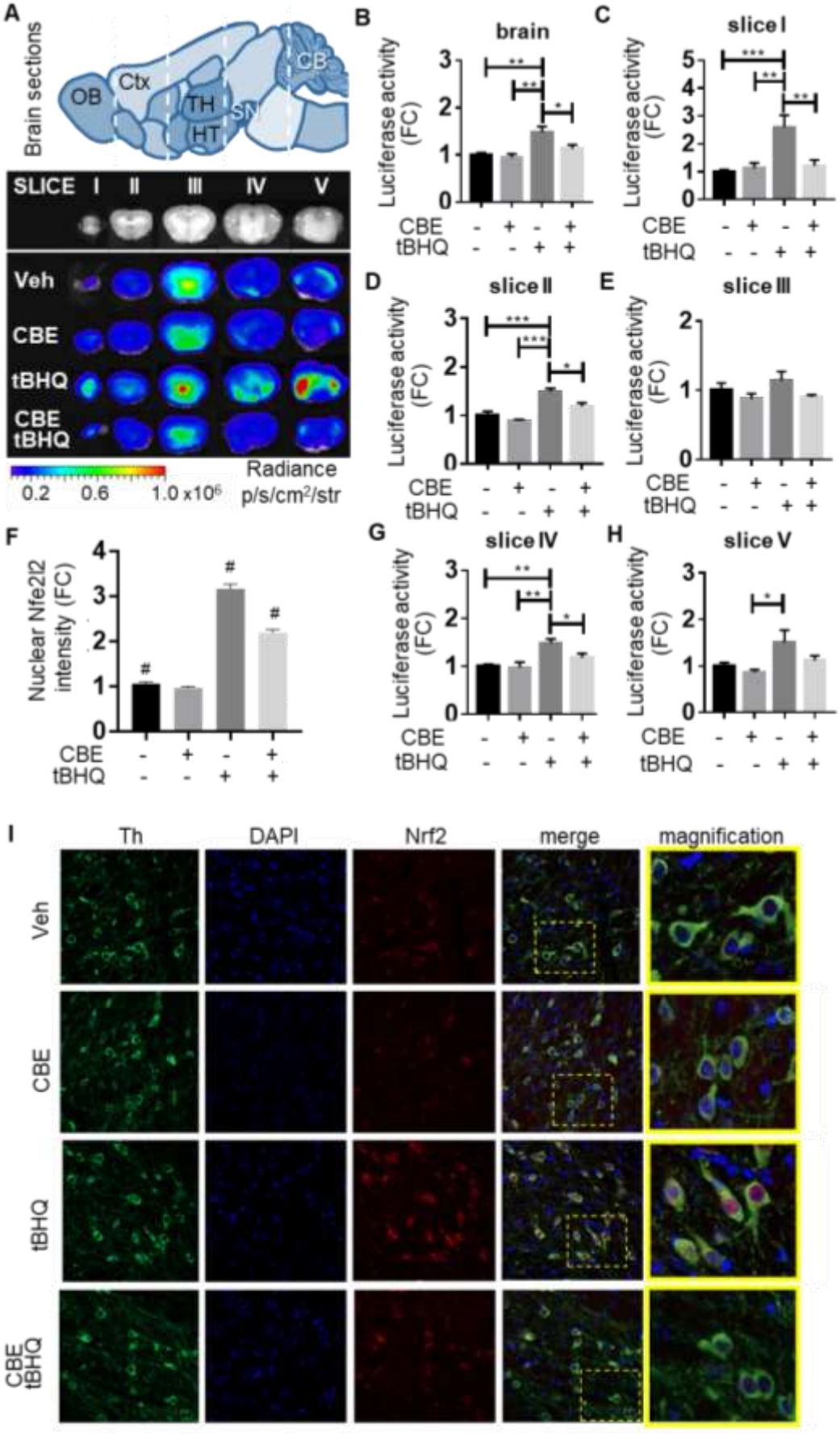

Figure 20. Nrf2 activation in CBE treated brain. A) Representative *ex vivo* BLI analysis on slices of brains dissected from vehicle, CBE, tBHQ, tBHQ+CBE treated animals. The upper panel reports a schematic

representation of brain areas (CB: cerebellum, Ctx: cerebral cortex, Hp: hippocampus, HT: hypothalamus, ob: olfactory bulb, SN: substantia nigra, TH: thalamus) included into the brain slices I, II, III, IV, V. Quantification of the bioluminescence signal from A) in (B-E,G, H) brain slices and C) whole brain. Changes in radiant flux (p/s/cm^2/sr) were expressed as FC *vs* vehicle. Bars represent mean ± SD, for n=4 animals measured in duplicate. *p<0.05, **p<0.01, ***p<0.001 by one-way ANOVA followed by Tukey's multiple comparison test. (I) Representative immunohistochemical images of brain slices from the SNpc area of vehicle, CBE, and CBE+tBHQ treated mice: in green tyrosine hydroxylase (TH), in red Nrf2, in blue nuclear DAPI staining. Sections (35µm thick) were visualized and digitally photographed using a Zeiss microscope (LSM880). (F) Semi-quantitative immunofluorescence analysis of nuclear Nrf2 staining in SN expressed as FC of mean grey nuclear value *vs* vehicle-treated mice. # P<0.001 *vs* each of the other three groups, calculated by one-way ANOVA followed by Tukey's multiple comparison test, ± SEM, n=4.

5.3.2 GCase inhibition hinders the microglial-mediated induction of NRF2 signal in neurons

To characterize the mechanism of GCase inhibition, we investigated the effect of CBE in neuronal cells and in microglia/neuron co-cultures. Initial experiments were carried out in SK-N-BE neuroblastoma cells stably transfected with the bioluminescent reporter of NRF2 activity ARE-*luc2*-ires-tdTomato, named SK-ARE-*luc2* (Mornata et al., 2020). Cells were treated with 200 µM CBE or vehicle (distilled water) for 48 hours in order to ensure the inhibition of GCase activity (Fig. 21A), with negligible effects on the activity of additional glycosidase targets (Kuo et al., 2019); 24 hours before harvest, cultures were also treated with increasing concentrations of tBHQ (5, 15 µM) or vehicle (water). The enzymatic quantification of luciferase in protein extracts demonstrated a concentration-dependent increase of reporter activity in tBHQ treated cells; however, in contrast with the *in vivo* observation (Fig. 20B), the CBE treatment did not affect the NRF2 activation induced by tBHQ (Fig. 21B), suggesting that CBE could not directly interfere with the NRF2 pathway in neuronal cells.

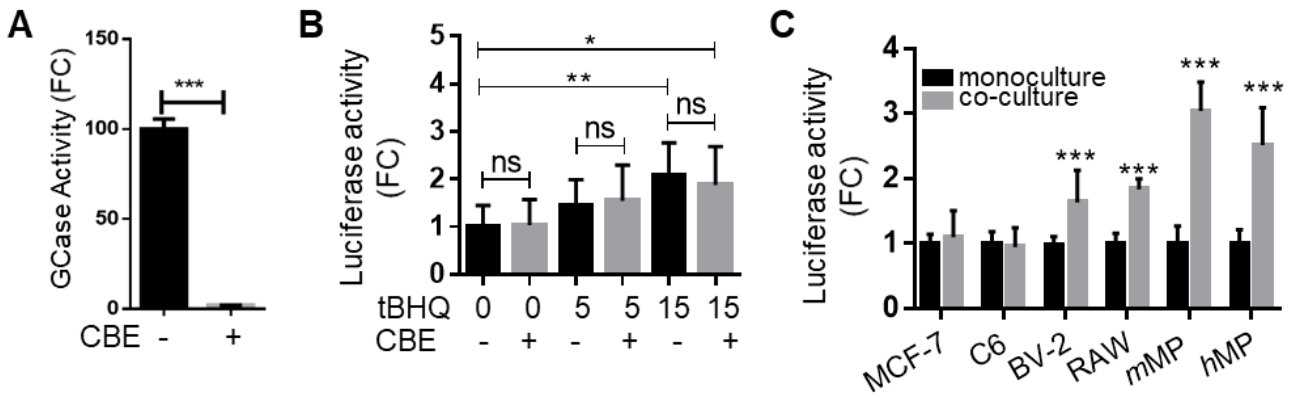

Figure 21. Modulation of the neuronal NRF2 signalling by macrophagic and microglial cells. A) Residual activity of the enzyme GCase in brain cell culture treated with 200 µM CBE for 48 hours. Data are expressed

as mean ± SD. ***p < 0.001 vs vehicle by student t-test. B) The effect of GCase inhibition on neuronal NRF2 activation was tested by treating SK-ARE-*luc2* cells with 200 µM CBE for 48 hours or vehicle (water) and with 5, 15 µM of tBHQ or vehicle (water) for 24 hours to induce Nrf2 activity. Luciferase activity in the graph is expressed as RLU/µg protein extracts normalised *vs* vehicle, bars represent mean values ± SD of n=4 measures in triplicate. *P<0.05, **P<0.01 calculated by one-way ANOVA followed by Dunnet's multiple comparison test *vs* vehicle; ns: not significant by unpaired *t*-test *vs* vehicle. C) NRF2 activity was measured in SK-ARE-*luc2* cultured for 48 hours with different cell lines or primary macrophages, including: MCF-7, C6, BV-2, RAW 246.7 (RAW), murine peritoneal macrophages (*m*MP), human macrophages derived from PBMC (*h*MP). Luciferase activity, expressed as RLU is reported on the graph as FC on monoculture of SK-ARE-*luc2* cells; bars are mean values ± SD for n=3-9 measures in triplicate. ***p<0.001 by 2way ANOVA followed by Sidak's multiple comparisons test.

Previous data showed that other brain cell types could be involved in the regulation of oxidative stress responses in the PD-associated neurodegeneration (Rojo et al., 2010; Rizzi et al., 2018), thus, needed for the correct modulation of the NRF2 pathway in neuronal cells. To this aim, microglial BV-2 and glioma C6 cell lines were co-cultured for 48 hours with SK-ARE-*luc2,* afterward, luciferase enzymatic activity was measured in the protein extract; results of these experiments clearly demonstrated that BV-2 cells, but not C6 cells were able to increase the neuronal NRF2 response, a property also shared by cells from the macrophage/monocyte lineages (RAW 264.7, mouse and human primary macrophages), but not from other lineages (MCF-7) (Fig. 21C). Then we experimentally determined the optimal ratio between BV-2 and SK-ARE-*luc2* to produce the highest NRF2 activation and we identified the interval 1/20-1/10 (BV-2/SK-ARE-*luc2*), which is also representative of the physiological neuron/microglia ratio in the brain (Lawson et al., 1990; Mittelbronn et al., 2001; Bartheld et al., 2016), as the ratio providing the highest level of NRF2 activity (+60%) in SK-ARE-*luc2* cells (Fig. 21C). The effect was not due to peculiar features of transformed cell lines since an increased Nrf2 activity of 250% was also observed in co-cultures of primary mouse microglia and neurons, the latter obtained from the ARE-*luc2* reporter mouse, thus carrying the luciferase reporter system for the Nrf2 pathway (Fig. 22F). Next, we tested whether co-cultures was reproducing the CBE effects observed *in vivo* (Fig. 19): indeed, the treatment with 200 µM CBE, while did not significantly reduce the basal level of NRF2 activity (Fig. 21B, 22E), significantly inhibited the microglia-mediated induction of the neuronal NRF2 pathway in both transformed lines (-10%) (Fig. 22B) and primary cells (-20%) (Fig. 22G). The observed inhibitory effect was greater in primary cultures than in cell lines, indicating that the microglia-induced activation of the neuronal NRF2 pathway is more effective in naïve cells. Finally, these results were confirmed by the semi-quantitative analysis of the fluorescence intensity in immunohistochemistry experiments with an

anti-NRF2 antibody showing an increased nuclear localization of NRF2 in SK-N-BE cells when co-cultured with the microglial cell line, an effect less marked when co-cultures were treated with CBE (Fig. 22C, 22H).

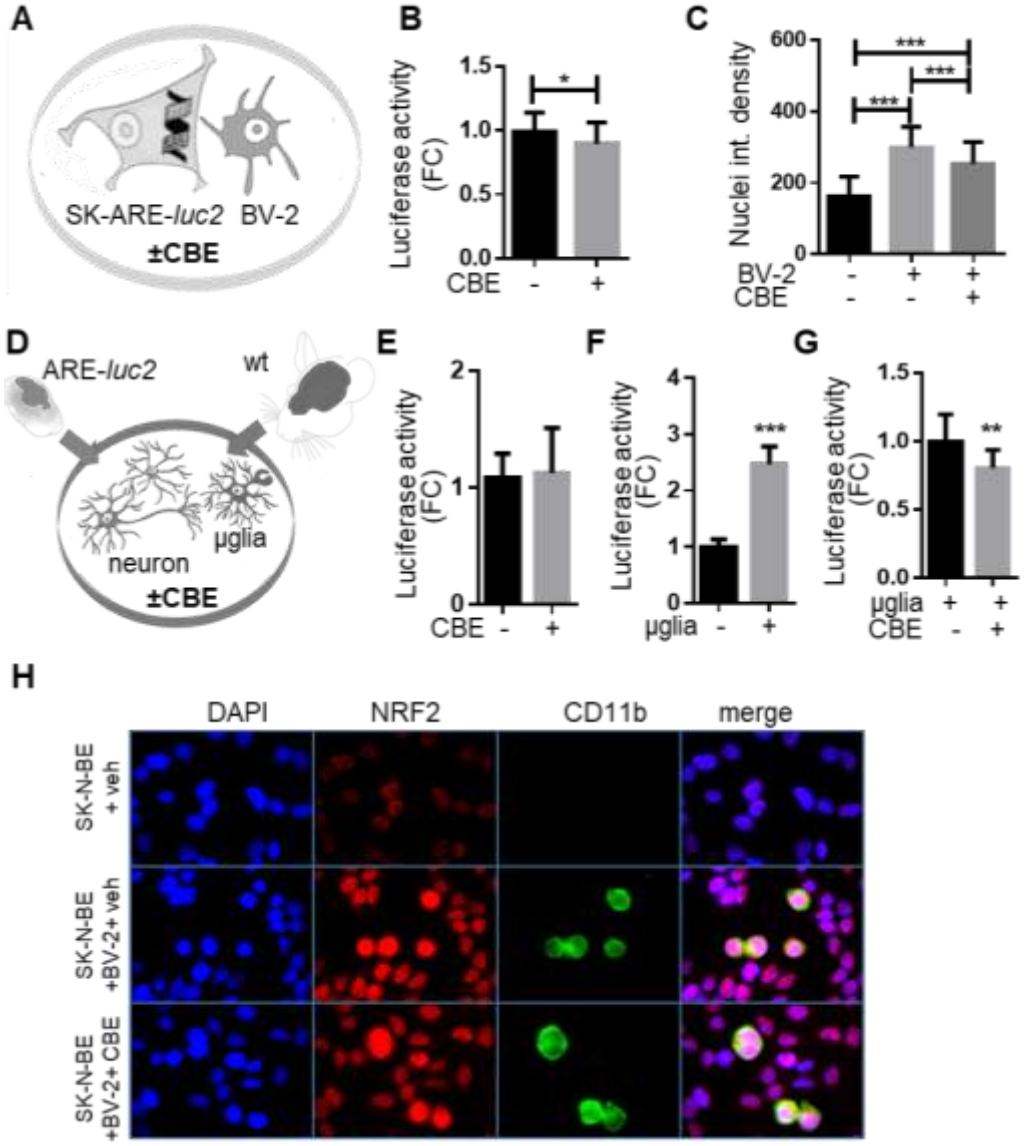

Figure 22. CBE treatment reduce the neuronal NRF2 response induced by microglia. A) Schematic representation of the experiments reported in (B-C) to assess the effect of CBE on neuronal NRF2 activation in co-culture of SK-ARE-*luc2* and BV-2 cell lines. B) Graph report the luciferase activity from SK-ARE-*luc2* cells cultivated with BV-2 cells and treated with 200 µM CBE or vehicle for 48 hours; RLU/µg proteins was normalized *versus* vehicle. Bars represent mean ± SD of n=9 measures in triplicate. *p<0.05 ***p<0.001 calculated by unpaired *t*-test. C) Data derived from the semi-quantitative immunofluorescence analysis of nuclear NRF2 staining (H) on co-cultures of SK-N-BE and BV-2 cell lines treated with 200 µM CBE or vehicle for 48 hours. Data are represented as mean ± SD of the analysis of N= 6000 nuclei measured in 20 fields for each condition. ***p<0.001 calculated by one-way ANOVA followed by Tukey's multiple comparison test. D) Schematic representation of the experiments reported in (E-G) testing the effects of CBE in primary co-cultures of microglial and neuronal cells: the latter cells obtained from ARE-*luc2* reporter mice. Graphs report the luciferase activity from ARE-*luc2* primary neurons treated with 200 µM CBE for 48 hours in monoculture (E), co-cultivated with wild type primary microglia treated with vehicle (F) or with 200 µM CBE for 48 hours

(H). Luciferase activity is expressed as FC *vs* vehicle-treated samples (E), *vs* neuron monoculture (F) and *vs* vehicle-treated co-cultures (G). Data are represented as mean ± SD of n=5 measures in triplicate. **p*<0.05, ****p*<0.001 calculated by unpaired *t*-test. Luciferase activity is expressed as RLU/µg of proteins; in co-cultures data were not normalized since microglia did not express luciferase. H) Representative immunocytochemistry analysis of SK-N-BE and BV-2 cell lines in monoculture and co-culture, treated with 200 µM CBE or vehicle for 48 hours; cells were co-stained with anti-NRF2 (red), anti-CD11b antibodies (green), and with DAPI (blue).

5.3.3 Microglial GCase is essential for the efficient activation of the NRF2 pathway in neurons

To investigate whether the CBE-mediated down-modulation of the neuronal NRF2 activity could be ascribed to the microglial or to the neuronal GCase inhibition, either BV-2 or SK-ARE-*luc2* cells were pre-treated with 200 µM CBE for 48 hours before seeding the co-culture (Fig. 23A). Luciferase activity in protein extracts decreased significantly (-25%) only when BV-2 were pre-treated with CBE (Fig. 23B, 23C), demonstrating that inhibition of microglial GCase was necessary and sufficient to reduce the neuronal NRF2 activity in the co-culture. This conclusion was confirmed in primary cells i.e. microglia obtained from mice previously i.p. injected with 100 mg/kg/die CBE for 3 days or vehicle (PBS) cultivated for 24 hours on primary neuronal cells derived from ARE-*luc2* mice (Fig. 23D, 23F): microglia obtained from CBE treated mice showed halved GCase activity (Fig. 23E) and a reduction of about 20% of the NRF2 activation in primary ARE-*luc2* neurons (Fig. 23F), compared to microglia co-cultures obtained from vehicle-treated mice. The key role played by microglia in the neuronal NRF2 activation was firmly demonstrated through pharmacological depletion experiments using PLX3397, a Colony Stimulating Factor-Receptor 1 (CSF-1R) inhibitor (Elmore et al., 2014). Depletion of microglia (Villa et al., 2018) in the ARE-*luc2* mice was obtained after seven intranasal daily administrations of 100 µg PLX3397, twice a day, and half of the treated mice received also two i.p. doses of 75mg/kg tBHQ, 20 and 16 hours before the end of the experiment to induce the Nrf2 pathway (Fig. 23G). *In vivo* and *ex vivo* imaging quantification of the photon emission from the head area and from the dissected brains of the ARE-*luc2* mice showed that depletion of microglia hindered the induction of the Nrf2 pathway observed upon tBHQ administration (please, compare graphs in Fig. 19D, 20B with Fig. 23H, 23I). Taken together, these data demonstrated that the neuronal Nrf2 response in the brain requires the presence of functional microglia.

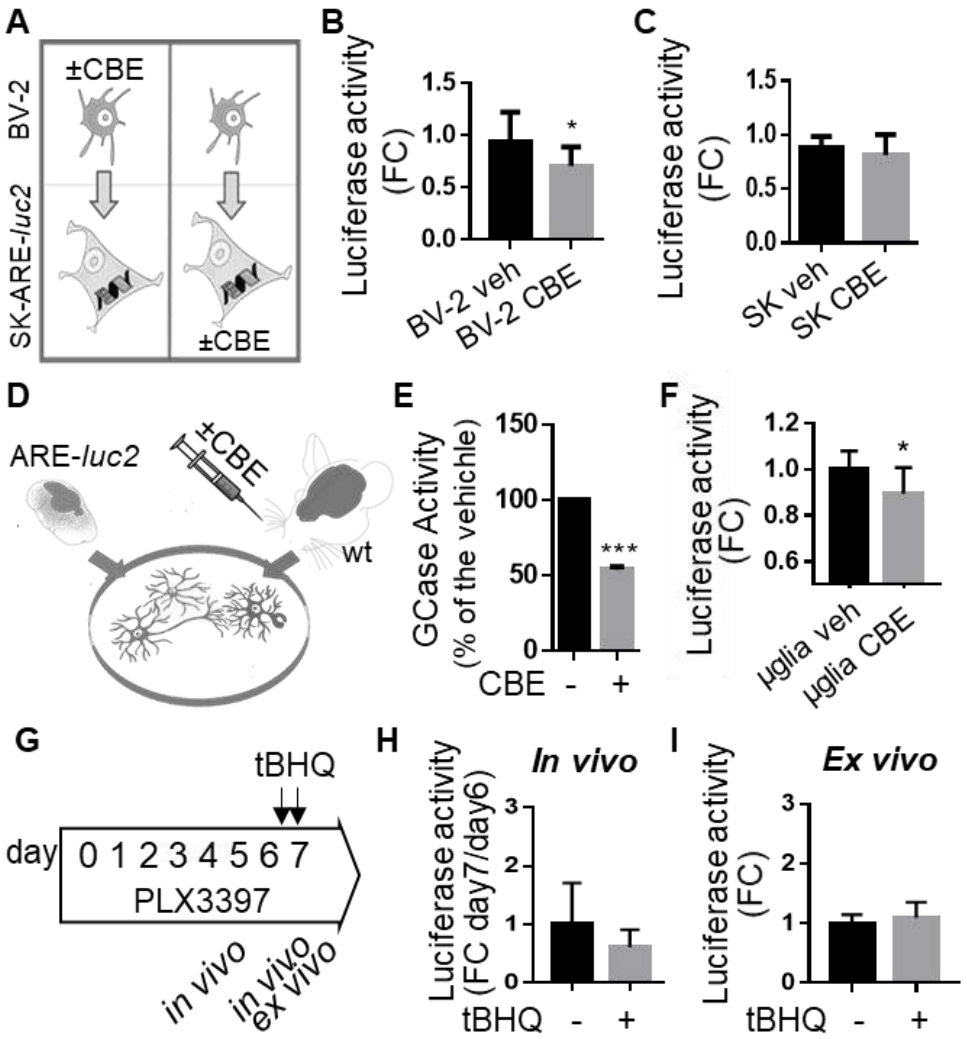

Figure 23. Inhibition of microglial GCase hamper sthe Nrf2 response of neurons. A) Schematic representation of the experiments summarized in (B, C) to assess the effect of the selective GCase inhibition in microglial or neuronal cells. BV-2 (B) or SK-ARE-*luc2* (C) were pre-treated with 200 μM CBE for 48 hours before seeding the co-cultures; graphs report the luciferase activity as FC on the vehicle. Data are represented as mean ± SD of n= 4 measures in triplicate. **P*<0.05 by unpaired *t*-test. D) Schematic representation of the experiments reported in (E, F) aimed at testing the effect of primary microglia extracted from CBE treated mice. E) GCase activity in primary microglia extracted from mice treated i.p. with vehicle or with CBE 100 mg/kg/die for 3 days; enzymatic activity is expressed as μmol of the reaction product 4-Methylumbelliferone (4-MU) generated in 1 hour normalized on μg of proteins and expressed as % of the activity detected in microglia extracted from the vehicle treated animals. Data are represented as mean ± SD of n=2 in duplicate. ****P*<0.001 calculated by unpaired *t*-test. F) Luciferase activity measured in protein extracts derived from ARE-*luc2* neurons co-cultured with microglia derived from CBE or vehicle-treated mice. Data are represented as mean ± SD of n=4 measures in duplicate. **P*<0.05 calculated by unpaired *t*-test. G) Schematic representation of the pharmacological depletion of microglia by treating mice with 100 μg PLX3397 every 12 hours for 1 week: 20 and 16 hours before the end of the experiment mice received two i.p. injection of tBHQ 75 mg/kg or vehicle (1%DMSO, 20%PEG300, PBS). BLI from the brain area (ROI Fig. 19C) or from the dissected brain acquired for each mouse by *in vivo* (H) and *ex vivo* imaging (I) is expressed as FC on the value obtained before tBHQ administration (day 6) (for the *in vivo* imaging) or on the value of the vehicle-treated mice (for *ex vivo* imaging). Data are represented as mean ± SD of n=3 measures. Differences were not significant, by unpaired *t*-test.

5.4 GCase inhibition hampers neuroprotective functions of microglia

The NRF2 pathway is of key importance in the detoxification from oxidative insults, thus, we tested whether the microglia-induced activation of the neuronal NRF2 pathway was sufficient to increase the detoxification capability of neurons. The microglia-induced neuroprotection was tested in SK-N-BE neuroblastoma cells treated with 0.5 mM MPP+, the active metabolite of MPTP that blocks the mitochondrial electron transport enzyme NADH:ubiquinone reductase (H(+)-translocating) (Nicklas et al., 1985; Vyas et al., 1986) and induces cellular death as a consequence of the formation of reactive oxygen species (Zawada et al., 2011). This treatment increased the cell death of about 50% in the monoculture population of neuroblastoma (Fig. 24A), as quantified by flow cytometry analysis of the dead cells stained with propidium iodide. The cell death was attenuated by about 20% when neuroblastoma cells were co-cultivated with BV-2 microglia cells (Fig. 24B), confirming that microglia was able to increase neuronal resistance to oxidative insults. Conversely, the microglial-dependent neuroprotection was blunted when GCase was inhibited with the 200 µM CBE for 48 hours (Fig. 24D), while the CBE treatment alone did not produce any effect on cell viability in the absence of the neurotoxic stimulation (Fig. 24C). These data demonstrated that GCase inhibition hampers the neuroprotective functions of microglia cells.

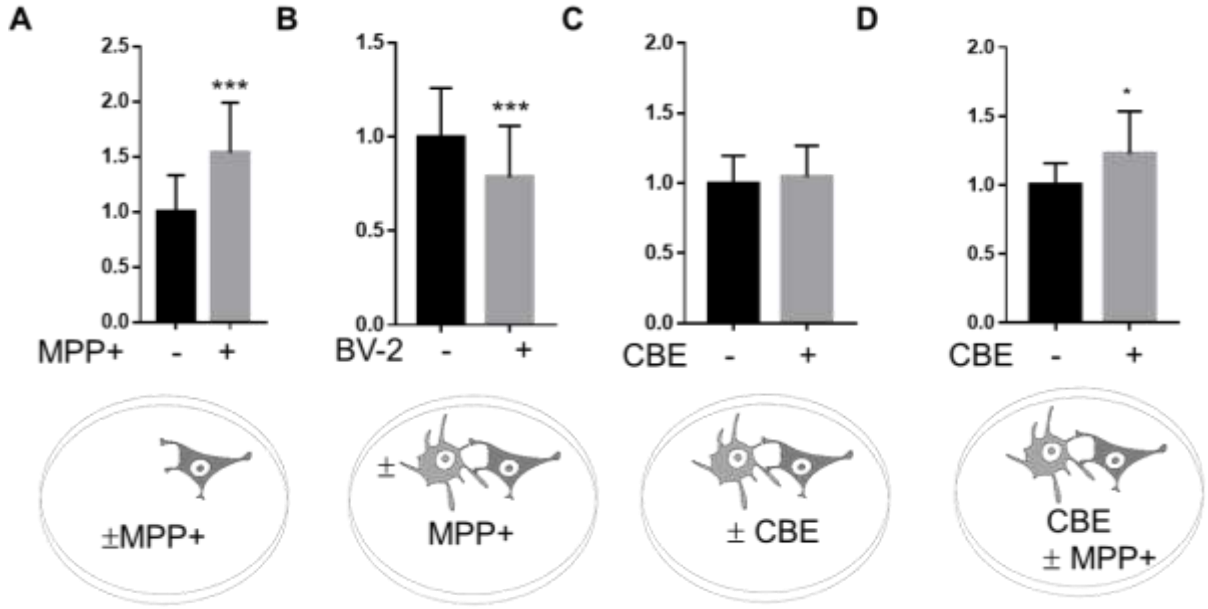

Figure 24. GCase inhibition hampers neuroprotective functions of microglia. Flow cytometry analyses of propidium iodide fluorescence in: A) SK-N-BE treated with 0.5mM MPP+ or vehicle for 24 hours; B) SK-N-BE cultured alone or in co-culture with BV-2 and treated with 0.5 mM MPP+; C) co-cultures treated with 200 µM CBE for 48 hours or (D) with 200µM CBE for 48 hours and 0.5mM MPP+ for 24 hours. Data are mean values ± SD of n=6 measures in triplicate of FC *vs* vehicle-treated (A, C, D) or monoculture sample (B). **P*<0.05, ****P*<0.001 calculated by unpaired *t*-test.

5.5 Inhibition of microglial GCase increases the expression of genes associated with neurodegeneration

To gain molecular insights into the mechanism of neuroprotection, we measured the expression of genes previously associated with specific microglial phenotypes by real-time PCR analysis on mRNAs purified from BV-2 cells treated with 200 µM CBE or vehicle for 48 hours (Fig. 25). The analysis did not show any increased expression of the proinflammatory cytokine interleukin 1 beta (*Il-1β*), neither we observed altered regulation of Nrf2 target genes (*Nqo1* and *Nrf2*) confirming that the GCase inhibitions did no trigger an inflammatory phenotype (Allan et al., 2005; Henkel et al., 2009), neither induce variations in the regulation of the antioxidant and detoxification response in microglia. Surprisingly, the expression of genes involved in the lysosomal pathway (*Lamp1* and *Tfeb*) as well as the expressions of *Cx3cr1, C3* and *P2ry12* involved in intercellular communication and selective phagocytosis (Kettenmann et al., 2011; Butovsky et al., 2014), were unaffected suggesting that microglia maintained their homeostatic functionality (Moore et al., 2014; Franco-Bocanegra et al., 2019). Interestingly, two different genes involved in the anti-inflammatory and repairing pathways, *Arg1* and *Trem2* (Benitez and Cruchaga, 2013; Liu et al., 2018; Zhao et al., 2018), were upregulated following microglial GCase inhibition. In particular, the latter involved also in microglia metabolic reprogramming, represents a disease-associated gene which mutations are linked with the onset of neurodegenerative diseases such as Alzheimer's disease (Karch et al., 2014; Konishi and Kiyama, 2018) and PD (Benitez and Cruchaga, 2013; Rayaprolu et al., 2013; Liu et al., 2016). Recent reports proposed Trem2 as the principal regulator triggering a specific microglial phenotype associated with neural diseases by regulating microglia's ability to phagocyte debris (Keren-Shaul et al., 2017). These data suggest that GCase may represent a key node in the regulation of the microglia neuroprotective activity ensuring the activation of detoxification/oxidative stress pathways in neurons and modulating a reparative/anti-inflammatory microglial response counteracting neurodegenerative insult.

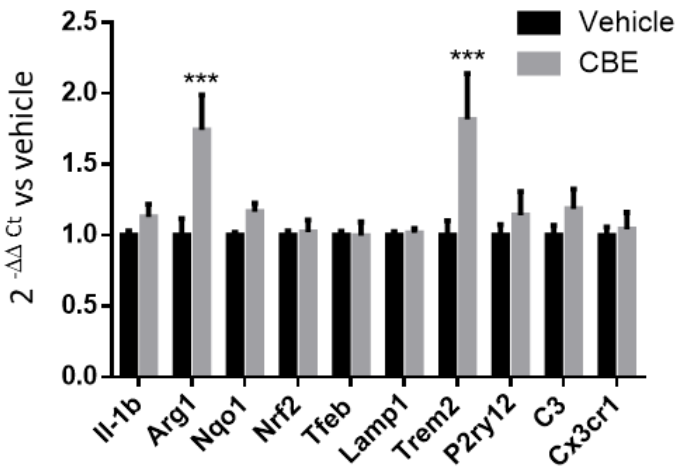

Figure 25. Modulation of gene expression by GCase inhibition in BV-2 cells. Total RNA was purified from BV-2 cells treated with 200 µM CBE for 48 hours and the expression of selected mRNA was analyzed by semiquantitative real-time PCR. Transcripts were quantified $2^{-\Delta\Delta Ct}$ method. Data are mean values ± SEM. for n=3 measures in triplicate. ***P<0.001 by two-way ANOVA followed by Sidak's multiple comparisons test.

5.6 Image-based morpho-functional analysis of living microglia reveals that GCase inhibition induces signatures of morphological changes in specific subpopulations

5.6.1 Image-based microglia analysis reveals the existence of functional clusters

A large body of evidence clearly demonstrate that microglia morphology and function are closely related (Davis et al., 1994; Heindl et al., 2018; Cserép et al., 2020). With the aim of investigating whether the microglia GCase inhibition produces specific phenotypical changes that could be correlated with the impairment of microglial neuroprotective functions observed upon CBE treatment, we set up an unbiased imaging-based method enabling us to measure variations of the microglia phenotype in the temporal dimension. To this aim, we initially seeded on petri dish a layer of primary cortical cells highly enriched in neurons to provide structural support and a correct growth environment for primary microglia cells isolated from adult *CX3CR1*$^{+/GPF}$ mice, a transgenic reporter model in which GFP is constitutively expressed in microglial cells, thus allowing easy identification and tracking (Jung et al., 2000). 24 hours after seeding, fluorescent microglia/neuron co-culture were subjected to specific treatments, and their movements and changes in their morphological shapes were recorded for 2 hours.

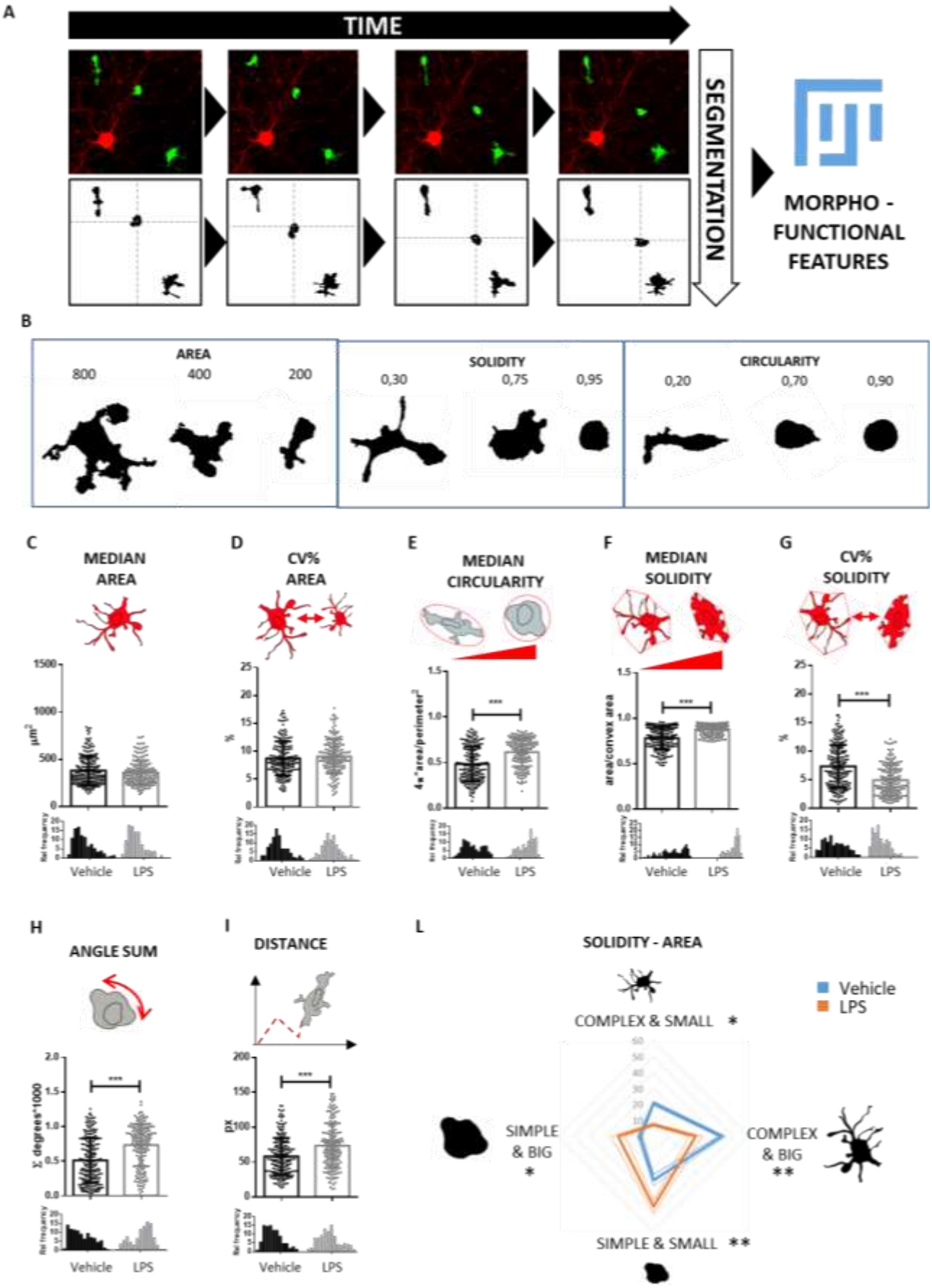

Figure 26. Unbiased morpho-metric method to detect morpho-functional changes. A) Schematic representation of the image-based method for the morpho-functional clustering, to mimic the microglia

brain environment we setup a primary co-culture consisting of pups-derived neurons with fluorescent microglia isolated from adult mice (expressing GFP). The co-culture was followed by time-lapse microscopy and the acquired images were processed with Fiji software to obtain different B) shape and dynamic descriptors for each microglia cell during the time. Single parameter were analyzed after 10 μg/ml LPS treatment from 6 to 8 hours C) median area during time, D) variation of the area, E) median circularity F) median of the solidity, reflecting the complexity of the cells and G) variation of this parameter, H) rotation and I) distance covered (three different experiments with a total of 218 vehicle cells-185 treated cells unpaired t-test **p<0,05; **p<0,01; ***p<0,001 versus vehicle*. L) To discriminate the subpopulation composition after the treatment the combinatorial analysis of solidity and area were performed creating the cluster of cells characterized by complex&small, complex&big, simple&small and simple&big microglia. Graphs represent the mean ± SEM of the sub-population percentage obtained in 3 different experiments; one-way ANOVA followed by Tukey test. *p<0,05; **p<0,001; *vs* vehicle.

The acquired movies were processed with Fiji (ImageJ) to obtain morphological and kinetic parameters descriptive for each fluorescent microglia cell present in the acquired field of view (Fig. 26A). In detail, the background was removed from the acquired images, which were in turns binarized, smoothed, and despeckled. Then, the shapes with a size greater than 130 μm^2 representing the cells, were processed to measure static descriptors such as area, circularity, and solidity (Fig. 26B), which reflects the complexity of cellular morphology (Hartig, 2013). The changes in these descriptors across time, together with the shift of relative coordinates of the center of mass and the variation of angular displacement of the ellipse in which the cells were inscribed, were elaborated to obtain numeric descriptors representing as much as possible the entire cellular dynamics observed during the recording time.

Once set up the methodology, the first step was to evaluate its efficacy in reproducing well-known morpho-functional changes of microglia occurring in pro-inflammatory conditions like those observed upon treatment with LPS (Kloss et al., 2001). Upon treatment with 10 μg/ml LPS the microglia morphology and motility were analyzed from 6 to 8 hours. For a potent stimulus like LPS, even the analysis of single descriptors was sufficient to identify changes in the microglia population. While the area of the cells did not change during the acquisition (Fig. 26C-D), other single descriptors where affected: in particular, the treatment induced an increase in the circular morphology (Fig. 26E) and most cells acquired a simpler shape (Fig. 26F), while maintaining their solidity across time (Fig. 26G). As expected, LPS also modified the cell movements, increasing the number of rotations (Fig. 26H) and the distance covered (Fig. 26I). Being microglia population characterized by a peculiar heterogeneity in the phenotype and in the response to various stimuli across the brain (Pepe et al., 2014; Masuda et al., 2019), we decided to extend the study going from single to cluster analysis of

the descriptors, with the aim of discriminating between microglial subpopulations present in the culture dish. To this aim, we performed a biparametric analysis: the median of the parameters was used as a cutoff to assign each cell to a descriptive category. The cluster analysis allowed to discriminate 4 different microglia subpopulations in the control untreated cells. As an example, the analysis of two descriptors, solidity and area (Fig. 26L), clearly distinguish the 4 microglia subpopulations: 1) cells simple&big, 2) simple&small, 3) complex&big and 4) complex& small.

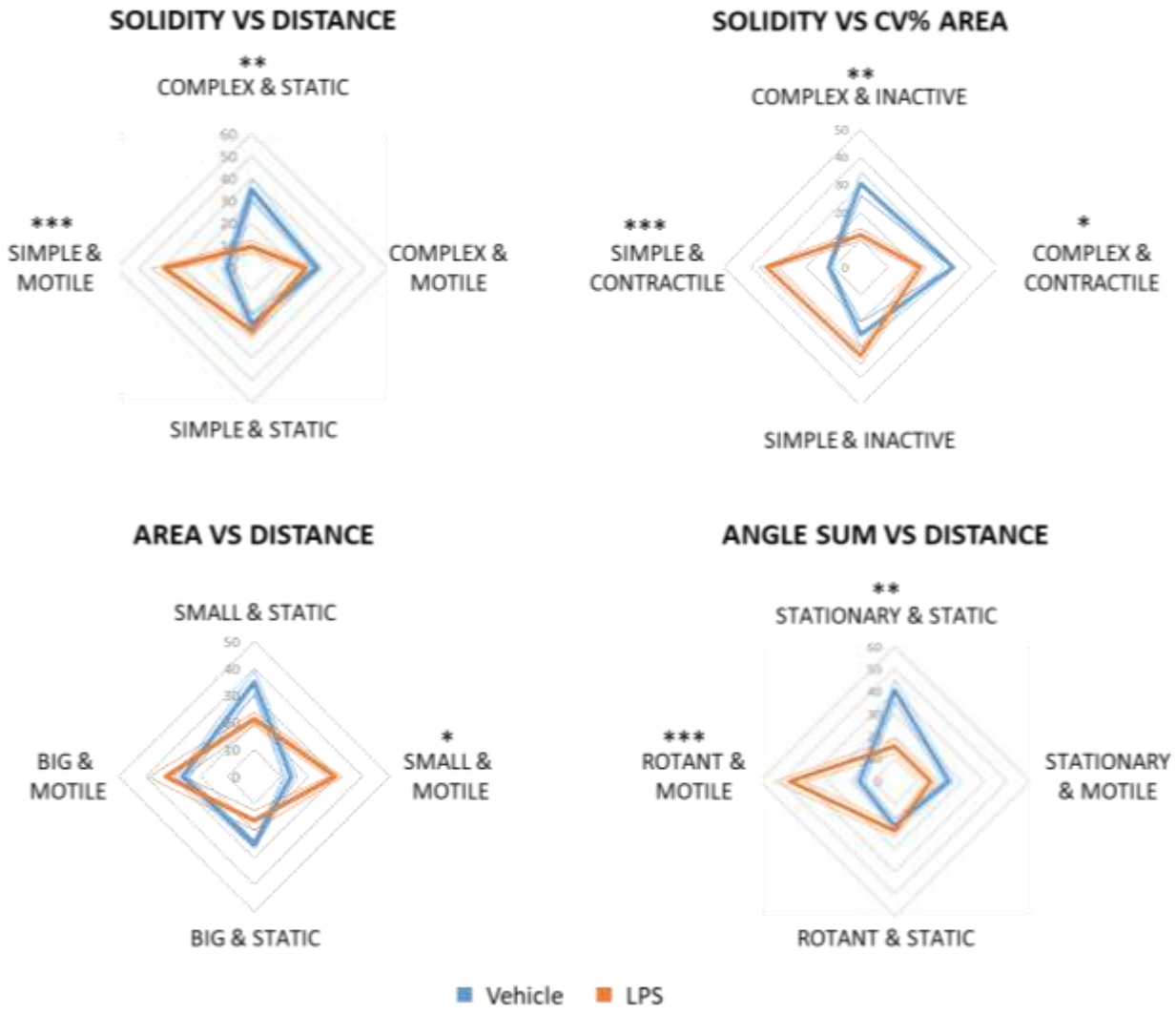

Figure 27. Biparametric analysis of 10 µg/ml LPS treated cells analysed from 6 to 8 hours. To discriminate the microglia subpopulations that respond to the pro-inflammatory stimuli was performed a combined analysis that generates 4 subpopulations for every 2 parameters. Analyzing the solidity and distance the four groups are: Complex&Static, Complex&motile, Simple&Motile, Simple&Static; the Solidity and variation of the area: Complex&Inactive, Complex&Contractile, Simple&Inactive, Simple&Contractile; Area and distance covered: Small&Static, Small&Motile, Big&Static, Big&Motile; rotation and distance covered: Stationary&Static, Stationary&Motile, Rotant&Static, Rotant&Motile. Graphs represent the mean ± SEM of the sub-population percentage obtained in 3 different experiments; one-way ANOVA followed by Tukey test. *p<0,05; **p<0,001; ***p<0,0001 *vs* vehicle.

This morpho-functional analysis was applied to the LPS treated cells revealing that a population of cells characterized by a small and complex shape disappeared, while a subpopulation of simple and small cells increased its representation (Fig. 26L). More interestingly, a subpopulation of big and simple cells, which was under-represented in the vehicle-treated samples, became prominent after LPS treatment. The approach successfully reported the morphological and kinetic features which were expected to be observed in microglia showing a pro-inflamed phenotype (Perry et al., 2010), especially an increase in the subpopulation of cells with a simple, motile and contractile morphology (Fig. 27). These results indicated that the novel analytical approach allows for accurate identification of the dynamic changes in microglial populations showing specific phenotypes, following treatments that are able to divert microglia from their physiological state.

5.6.2 GCase inhibition induces signature changes in microglia subpopulations

Next, we applied the novel morpho-functional analysis to test whether the GCase impairment was able to drive specific morpho-functional changes in microglia populations. In particular, a biparametric analysis was carried out by comparing the changes occurring during 48-50 hours of 200 µM CBE- *versus* vehicle-treatment.

These experiments highlighted selective morphological changes in some sub-populations of cells characterized by a static and less contractile phenotype (Fig. 28A). In detail, we observed an increase in the population of cells with simple&static and big&static morphologies, while a decrease in the sub-populations of cells complex&contractile and stationary&motile was detected (Fig. 28A). Overall, these data suggest a morphological shift in microglia subpopulations occurring after GCase inhibition, a specific microglial phenotype markedly different from the pro-inflamed phenotype detected after LPS treatment (Fig. 28B), thus confirming the mRNA expression profile (Fig. 25) that non-phlogistic functions of microglia could be altered by GCase deficiency and that microglia morpho-functionality is early changed by the pharmacological GCase inhibition.

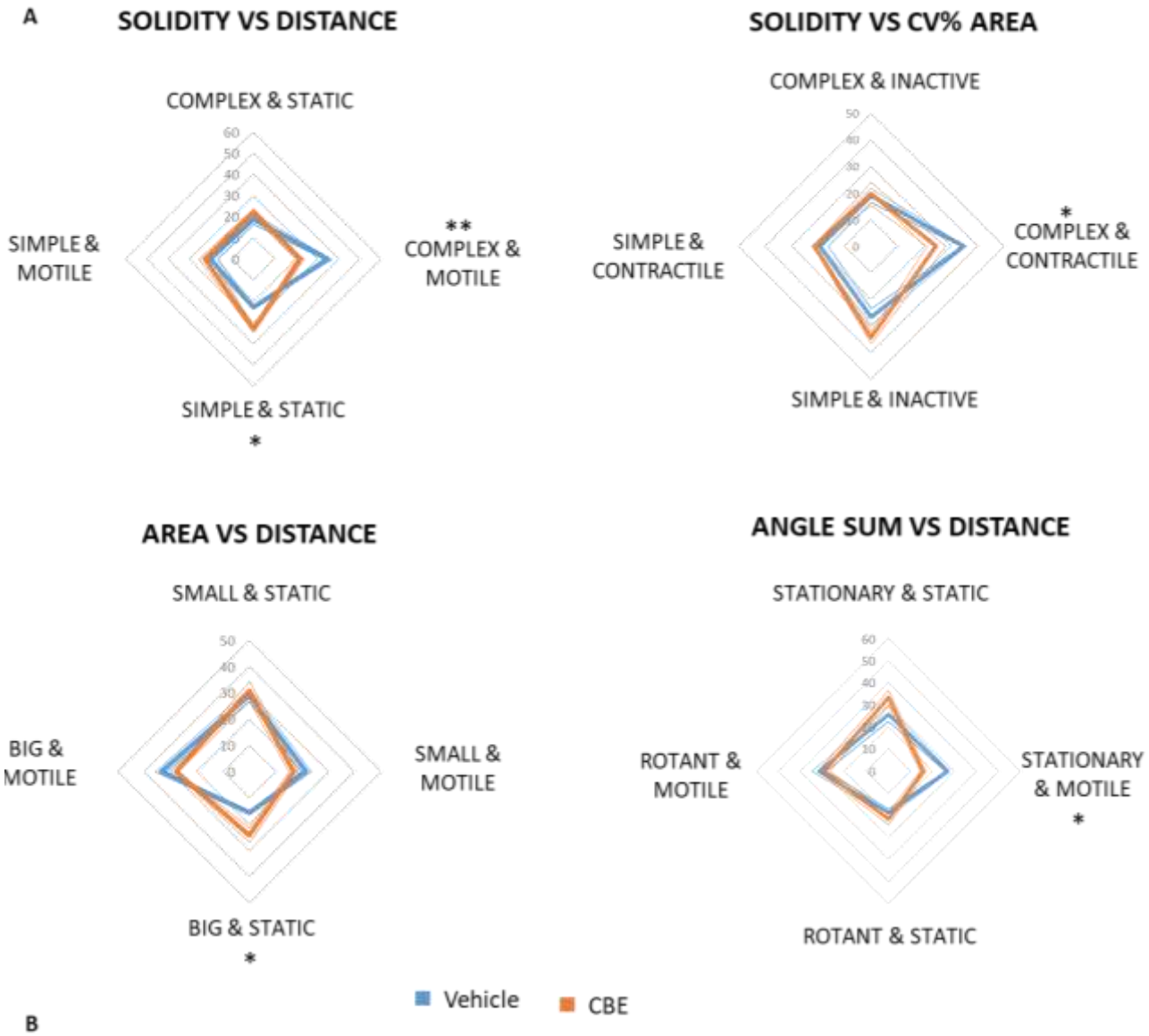

B

SUB-POPULATION	SMALL & MOTILE	BIG & MOTILE	SMALL & ROTANT	CONTRACTILE & ROTANT	CONTRACTILE & MOTILE	STEADY & ROTANT	VARIABLE & ROTANT	STEADY & CONTRACTILE	VARIABLE & SIMPLE	CONTRACTILE & SMALL	CONTRACTILE & BIG	CIRCULAR & STEADY	ROTANT & MOTILE	SMALL & STATIC	BIG & STATIC	BIG & STATIONARY	INACTIVE & STATIONARY	INACTIVE & STATIC	CONTRACTILE & STATIC	STEADY & STATIC	VARIABLE & STATIC	STEADY & STATIONARY	COMPLEX & STATIC	SIMPLE & STATIONARY	INACTIVE & SMALL	INACTIVE & BIG	INACTIVE & ELONGATED	INACTIVE & COMPLEX	ELONGATED & STEADY	ELONGATED & STATIONARY	CIRCULAR & STATIONARY	ELONGATED & STATIC	ELONGATED & SIMPLE	STATIONARY & STATIC
LPS	+	+	+	+	+	+	+	+	+	+	+	+	+	-	-	-	-	-	-	-	-	-	-	-	-	-	-	-	-	-	-	-	-	-
CBE	-	-	-	-	-	-	-	-	-	-	-	-	-	+	+	+	+	+	+	+	+	+	+	+	+	+	+	+	+	+	+	+	+	+

Figure 28. Morpho-dynamic analysis of microglia after GCase inhibition with 200 µM CBE for 48 to 50 hours. A) microglia subjected to biparametric morphodynamic analysis, see detail in figure 27; lines represent mean ± SEM of the sub-populations percentage obtained in 4 different experiments; one way ANOVA followed by Tukey test; ns: not significant,*p<0,05; **p<0,01; ***p<0,001 *vs* vehicle. B) In the table are reported the subpopulation that increases (+) or decreases (-) differently after the LPS or CBE treatment to highlight that CBE induces a morpho-functional phenotype divergent from the LPS.

5.7 Microglia require functional actin-dependent structures to induce NRF2 in neuronal dopaminergic cells

We observed a decrease in microglial complexity and motility in GCase inhibited cultures suggesting that treatment can reduce the surfaces of interaction between microglia and neurons. Thus we proposed to investigate whether the microglia-to-neuron communication inducing NRF2 activity required a paracrine mechanism based on the release of secreted factors or physical interaction between cells (Biber et al., 2007; Kerschensteiner et al., 2009; Szepesi et al., 2018; Cserép et al., 2020). To this purpose, BV-2 and SK-ARE-*luc2* cells were grown in separate compartments (using a 0.4 µm membrane) of the same well (Fig. 29A) preventing the physical interactions between the two cell types, while preserving the exchange of soluble factors. In this condition, the neuronal NRF2 induction could not be observed (Fig. 29B), suggesting that this response does not require diffusible factors. In order to exclude that the membrane pore of 400 nm could obstruct the diffusion of larger macromolecular complexes (e.g. extracellular vesicles), conditioned media derived from co-culture of BV-2 and SK-N-BE cells were added to SK-ARE-*luc2* cells (Fig. 29C); again, the induction of neuronal NRF2 activity could not be observed (Fig. 29D), thus definitely ruling out a possible role of microglia secreted factors in this phenomenon. These experiments prompted us to test the alternative hypothesis of a mechanism based on the direct contact between the two cell lineages. Microglia use two major types of branches, strictly regulated by distinct intracellular signaling cascades, to sensing the environment: the actin-dependent filopodia and the tubulin dependent large processes (Nolte et al., 1996; Nimmerjahn et al., 2005; Bernier et al., 2019; Cserép et al., 2020). To define which of the two pathways is required for the microglia-dependent induction of the NRF2 activity, BV-2 cells were pretreated with nocodazole, an agent that prevents microtubule assembly, at a concentration and time span (25 µM for 2 hours) known to inhibit large process without affecting filopodia movement (Bernier et al., 2019). After the treatment, cells were seeded on the SK-ARE-*luc2* cells and luciferase activity was measured 24 hours later: the results demonstrated that pharmacological disruption of microglial large processes did not affect the ability of microglia to induce NRF2 signaling in neurons (Fig. 29E). On the contrary, when BV-2 cells were pretreated with 1 µM cytochalasin for 1 hour, a treatment blocking actin polymerization and reducing filopodia motility (Pan et al., 2011; Bernier et al., 2019), we observed a significant decrease (>25%) in the induction

of neuronal NRF2 activity (Fig. 29F) suggesting that actin-dependent structures are necessary for the microglia-mediated stimulation of NRF2 pathway in neurons.

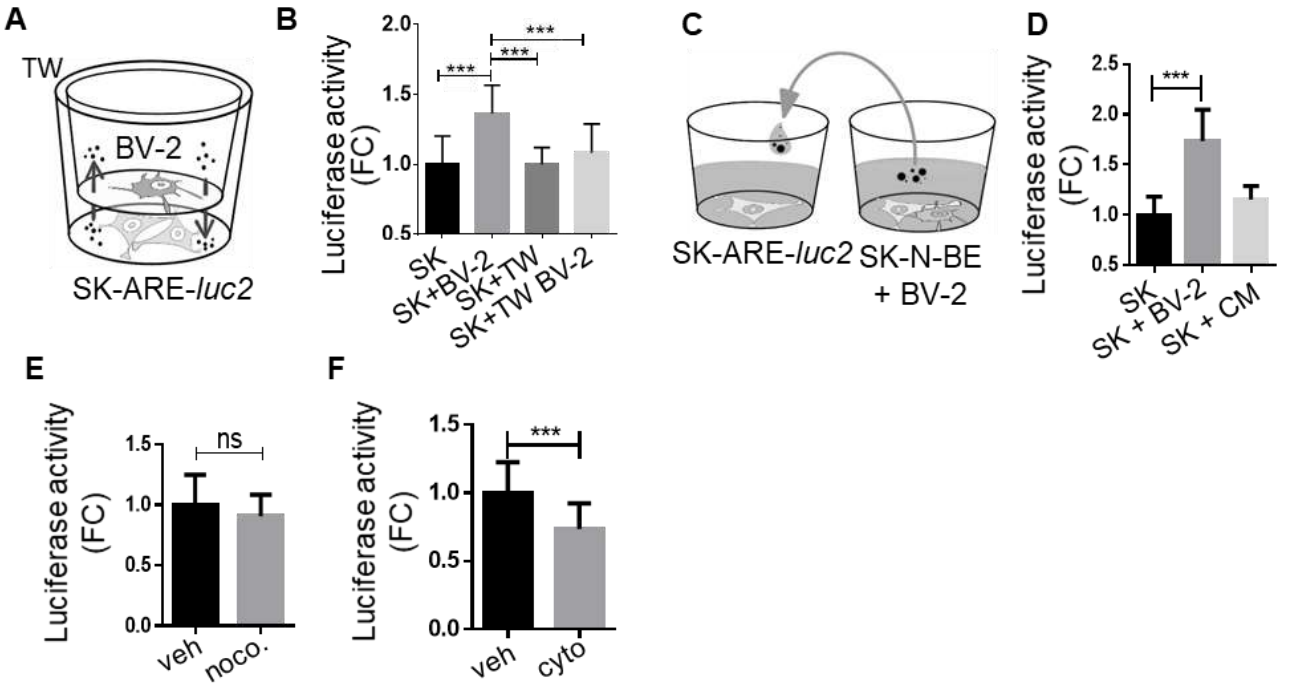

Figure 29. Mechanism of microglia-to-neuron cross-talk. A) Scheme of the transwell (TW) tool used in the experiment reported in (B): BV-2 and SK-ARE-*luc2* cells were seeded in a separate compartment of the TW. B) Luciferase enzymatic activity obtained from co-culture of SK-ARE-*luc2* and BV-2 cells (SK+BV-2), or SK-ARE-*luc2* growth alone in the transwell (SK+TW), or growth in a separated compartment with microglia (SK+TW+BV-2); values are expressed as RLU normalized *vs* monoculture of SK-ARE-*luc2* (SK). Data are mean values ± SD of n=6 measures in triplicate. ***P<0.001, by one-way ANOVA followed by Tukey's multiple comparison test. C) Schematic representation of the experiment reported in (D): SK-ARE-*luc2* cells were grown in co-culture with BV-2 (SK+BV-2) or in monoculture with the conditioned medium (SK+CM) obtained from the co-culture. D) Luciferase activity (RLU) is expressed as FC *vs* SK-ARE-*luc2* monoculture (SK). Data are mean values ±SD of n=3 measures in triplicate. ***P<0.001, by one-way ANOVA followed by Dunnet's multiple comparison test *vs* SK. E) BV-2 were pre-treated with 25µM nocodazole (noco) or vehicle for 2 hours and co-cultured SK; Luciferase activity (RLU) are FC *vs* vehicle (veh); data are mean values ±SD of n=12 measures in quadruplicate. Mean differences are not significant as calculated by unpaired *t*-test. F) BV-2 were pre-treated with 1µM cytochalasin (cyto) or vehicle (veh) for 1 hour and co-cultured with SK-ARE-*luc2*. Luciferase activity (RLU) are FC *vs* vehicle: data are represented as mean ± SD for n=8 measures in triplicate.

5.8 Microglial energetic toning might be a pharmaceutical approach to decrease the risk of neurodegeneration

GCase impairment has been demonstrated to trigger dysfunction in catabolic organelles (Grabowski and Beutler, 2001) and decline of mitochondrial functionality (Osellame et al., 2013); our data indicate that in microglia, the enzymatic inhibition induces the upregulation of the *Trem2* gene (Fig. 25), a key receptor sustaining energetic and biosynthetic metabolism through the mTOR signaling (Ulland et al., 2017a). This observation led us to analyze the energetic metabolism in our SK-ARE-*luc2/*BV-2 model. Co-cultures were treated with 200 µM CBE for 48 hours and MTT colorimetric assay was applied on living cells to eventually detect metabolic modulations. The MTT colorimetric assay is based on the conversion of 3-(4,5-dimethylthiazol-2-yl)-2,5-diphenyltetrazolium bromide into purple-colored formazan, and allows to quantify the activity of NAD(P)H-dependent oxidoreductase enzymes (Stockert et al., 2018): decreased activity of this enzyme may be due to cell death or to reduced energetic metabolism. Treatment with CBE demonstrated a significant reduction in the MTT substrate conversion (Fig. 30A); since CBE did not have any effect on cell viability (Fig. 24C), neither decreased the number of microglia cells (not reported), we hypothesized that GCase impairment was decreasing the energetic metabolism. Previous data from other labs showed that microglia functionality is tightly connected with energetic metabolism (Bernier et al., 2020), therefore we hypothesized that the reduced metabolic energy available after CBE treatment, could promote the poorly communicative microglial phenotype observed after CBE treatment. To test this hypothesis, we assayed the effect of a reduced energetic supply (starvation) on the ability of microglia to increase neuronal NRF2 activity.

Co-cultures of SK-ARE-*luc2*/BV-2 were grown in complete media for 24 hours, which was replaced for 6 hours with dilutions of the media with different percentages of HBSS. Reduction of the nutrients proportionally decreased NRF2 activity measured as luciferase level in the protein extract (Fig. 30C) suggesting that nutrients may play a direct role in the mechanism of microglia-to-neuron communication promoting the detoxification pathway. In line with this result, the replacement of exhausted medium with fresh media increased the microglial-mediated NRF2 expression (Fig. 30B) without altering basal NRF2 modulation in SK-ARE-Luc2. These preliminary data though did not completely exclude that some specific medium component could be connected with the ability of microglia to communicate with neurons, support that an appropriate supply of cellular energy might be needed to trigger microglia neuroprotective functions.

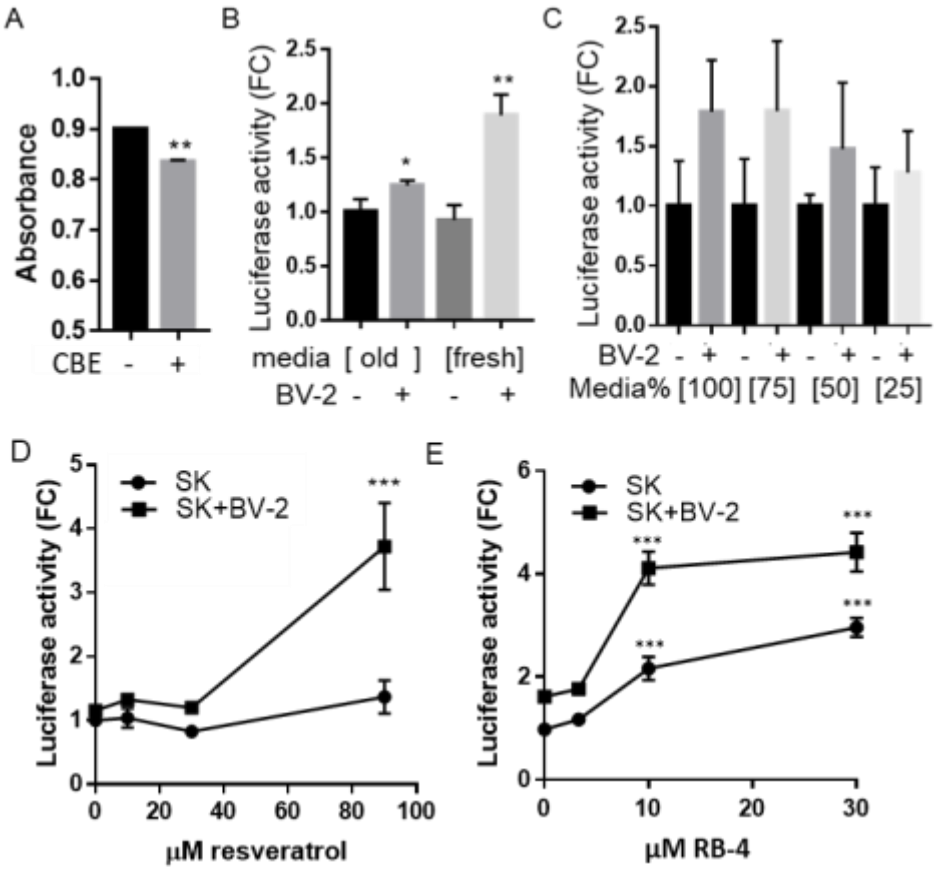

Figure 30. Energetic tuning can boost neuroprotection. A) MTT assay was performed on co-culture treated with 200 µM CBE for 48 hours. Graph reports mean absorbance at 570 nm ± SD n=4 measures. ** p<0.01, by t-test *vs* vehicle. B) The graph reports the luciferase enzymatic activity obtained from co-culture of SK-ARE-*luc2* cells grown alone or with BV-2 cells 6 hours after the substitution of the old media (old) with a fresh one (fresh). Graphs report mean ± SD of FC of RLU vs SK-ARE-*luc2* cell grown in old media. n=3 measures, *p<0.05, ** p<0.01, by t-test *vs* old. C) The graph reports the luciferase enzymatic activity obtained from co-culture of SK-ARE-*luc2* cells grown alone or with BV-2 cells 6 hours after the substitution of the media composed by 100%, 75%, 50% or 25% of complete media and 0%, 25%, 50%, 75% of HBSS. Graph reports mean ± SD of FC of RLU on SK-ARE-*luc2* grown alone n = 3 measured in triplicate, **p<0.01, *** p<0.001, by two-way ANOVA vs SK-ARE-*luc2*. D) Graph reports the luciferase enzymatic activity obtained from co-culture of SK-ARE-*luc2* cells grown alone or with BV-2 cells 6 hours after treatment with 10, 30, 90 µM resveratrol or vehicle (DMSO). Graphs are mean ± SEM of FC of RLU on SK-ARE-*luc2* vehicle n=3 measured in duplicate, *** p<0.001, by one-way ANOVA vs SK-ARE-*luc2* vehicle. E) The graph reports the luciferase enzymatic activity obtained from co-culture of SK-ARE-*luc2* cells grown alone or with BV-2 cells 6 hours after treatment with 10, 20, 30 µM RB-4 or vehicle (DMSO). Values are mean ± SEM of FC of RLU on SK-ARE-*luc2* vehicle n=6 measured in triplicate, *** p<0.001, by one-way ANOVA vs SK-ARE-*luc2* vehicle.

Since increasing energy metabolism was shown to boost microglia performance in some pathological models (Ulland et al., 2017b), we wondered whether the pharmacological modulation of nodal enzymes involved in metabolic reprogramming could be a prosecutable approach to influence neuroprotective mechanisms. In this line of thought, we tested the effect of resveratrol, a Sirtuin 1 (Sirt1) activator promoting mitochondrial biogenesis and protecting cells against metabolic decline (Price et al., 2012), for its ability to modulate the microglia-dependent induction

of neuronal NFR2 activity. SK-ARE-*luc2* were grown alone or with BV-2 and treated for 6 hours with increasing concentrations of resveratrol or vehicle (DMSO). The increased reporter activity in cellular extracts clearly confirmed that resveratrol boosted indeed the microglia-dependent NRF2 response in neurons (Fig. 30D) since up to a 4-fold increase was observed for the treatment with 90 µM resveratrol, without affecting the basal neuronal NRF2 activity. A similar increase was observed when co-cultures were treated with 10 or 30 µM RB-4 (Fig. 30E), a NAD+-mimetic molecule discovered in our lab as a direct Sirt1 activator (Dell'Omo, Della Torre, Ciana). In contrast with resveratrol, RB-4 was able to induce also the basal NRF2 activity in neuroblastoma monoculture, although to a lower extent compared to the co-culture; the basal activation might be ascribed to the physiological sensitivity of the NRF2 system to a xenobiotic molecule such as RB-4.

Taken together the starvation data and the resveratrol/RB4 effects seem to indicate that a pharmacological strategy enhancing the microglia's energetic metabolism could increase their neuroprotective functions.

5.9 Peripheral macrophages to study cerebral microglial dysfunctions

Finally, since cells of myeloid origin are able to support protective programs in neurons (Fig. 21C) we wondered to test if the effect triggered by GCase inhibitions were present also in peripheral macrophages. To this purpose, primary peritoneal murine macrophages and human peripheral blood mononuclear cells (PBMCs) differentiated towards macrophages were seeded with SK-ARE-*luc2* and treated with 200 µM CBE. The luminescence assays confirmed that both murine (Fig. 31A) and human macrophages (Fig. 31B) were able to recapitulate the NRF2 reduction observed when microglia/neuron co-culture were treated with CBE; in fact, the level of neuronal NRF2 was reduced by about 20% suggesting that the mechanism observed in the brain is conserved in the peripheral cells of the same lineage.

Taken together, these data strongly support the hypothesis that impairment of GCase in microglia could result in a decrease of the oxidative stress and detoxification response in neurons, with a mechanism that seems conserved in myeloid lineage cells of murine and human origin.

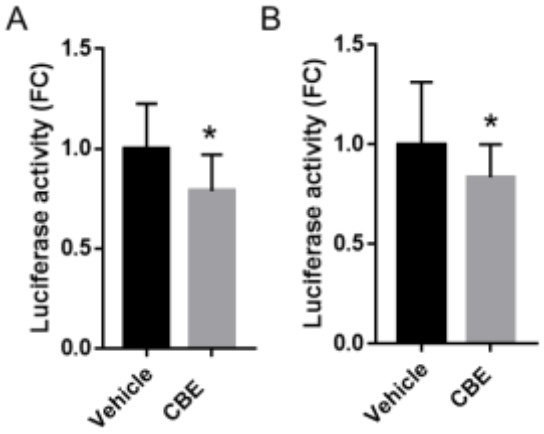

Figure 31. Macrophages are affected by GCase impairment. The effect of GCase inhibition on neuronal NRF2 activation was tested by treating co-culture of SK-ARE-*luc2* and murine A) or human B) derived macrophages with 200 µM CBE for 48 hours or vehicle (water). Luciferase activity in the graph is expressed as RLU normalised *vs* vehicle, bars represent mean values ± SD of n=4 measures in triplicate. **P*<0.05, calculated by unpaired *t*-test *vs* vehicle.

6 DISCUSSION

The inexorable dopaminergic degeneration that characterizes the brain of PD patients occurs with multiple molecular alterations leading to the accumulation of misfolded proteins, increased oxidative stress and inflammation (Toulorge et al., 2016). In idiopathic PD the longitudinal contribution of these events is not perfectly known, but to identify promising therapeutic intervention aimed at rescue neurons it became crucial to comprehend if they are the inceptive trigger cause of neuronal loss (Postuma and Berg, 2016). To investigate the molecular events occurring early in the neurodegenerative process, we studied the cellular mechanisms altered before neuronal death induced by pharmacological treatments triggering dopaminergic degeneration. We focussed on two transcription factors able to orchestrate protective pathways, which deregulation leads to oxidative stress, reduction in lysosomal-autophagic activity, accumulation of undegraded proteins or metabolic organelles, and finally cell death: the transcription factor NRF2, controlling anti-oxidant and detoxication response (Giudice et al., 2010), and TFEB, the master regulator of the lysosomal-autophagic pathway (Napolitano and Ballabio, 2016).

Reporter systems to study the dynamic of transcription factor activity in living organisms. To gain insights into the dynamic control of NRF2 and TFEB activation during early PD phases, we generated and validated reporter systems allowing to measure the activity of these transcription factors through biochemical assays and *in vivo* imaging measurements. We have taken particular care of the realization of the reporter systems to firmly establish a direct correlation between the reporter expression and the activity of the transcription factors of the study. First, we generated minimal, synthetic promoters carefully studying the response elements through bioinformatic analysis, next by transient transfections experiments we have extensively tested the selectivity and the proportional response to the transcription factor activity. In this way, we have selected ideal promoter cassettes that were superior to all previously identified reporter systems; the systems generated were able to drive the expression of the luciferase/tdTomato cassette, for accurate quantification of the promoter activity (luciferase) and the multiple imaging possibilities of fluorescent protein (tdTomato) to assess at the cellular level the transcription factor response (Fig. 9, 10, 12). With these reporter systems were created reporter cells and mice in order to study the transcription factor activity in the *spatio*-temporal dimension; generation of the reporter mice is a consolidated lab methodology based on the use of appropriate transgenic vectors designed for the prevention of positional effects and for the site-specific insertion of the reporter system into a permissive locus of the mouse genome (Rizzi et al., 2017). The reporter mice for Tfeb and Nrf2

activity were implemented with a Cre-lox conditional transgenesis strategy: tissue-specific or ubiquitous expression of reporter proteins can be obtained with appropriate breeding of the reporter mice with CRE-transgenic mice; the validation carried out confirms the functionality of reporter expression for BLI analysis.

Nrf2 activations anticipate dopaminergic degeneration. In my thesis, I have used the ARE-*luc2* reporter mouse as a tool for study the Nrf2 pathway in cell lines and in the brain of living mice, providing an important proof-of-principle of the usefulness of bioluminescence reporter imaging to study the dynamic of the Nrf2 pathway *in vivo* (Fig.17). The mechanism was firstly investigated in cell lines demonstrating that NRF2, but not TFEB, is early activated during the process of dopaminergic neuronal death induced by MPP+ (Fig 16). The data were then confirmed *in vivo* using reporter mice (Fig. 17) demonstrating that the trigger of Nrf2 signal anticipates the dopaminergic neuron death induced by MPTP that is starting *in vivo* only 2–4 days later (Tatton and Kish, 1997; Meredith and Rademacher, 2011); interestingly, the fluorescent reporter and immunohistochemical data (Fig. 18) demonstrated that also glia participates to the detoxication response, supporting the concept that the interplay among brain cells has a key role in brain detoxification. The parallelism observed among the neuronal death and the Nrf2 activation from the very initial stages of the process, may suggest that early PD biomarkers, whose expression is modulated before the occurrence of symptoms, might be identified among the Nrf2 target genes. In line with this idea, a previous study reported that increased levels of HMOX-1, a metabolizer of dopamine-derived quinones directly modulated by NRF2, were raised in the plasma of PD patients compared to healthy controls (Mateo et al., 2010).

In several PD models, it is sufficient to upregulate Nrf2 before the induction of parkinsonism to decrease neuronal degeneration (Jakel et al., 2007; Barone et al., 2011; Nouhi et al., 2011; Gan et al., 2012); moreover, genetic association studies demonstrated that haplotype in the human NRF2 gene promoter, conferring slightly increased NRF2 transcriptional activity, is associated with decreased risk of PD and with delayed age of onset of the disease in a European case-control group (von Otter et al., 2010). These data suggest that the preventive upregulation of the NRF2 pathway may protect brain cells from death. My thesis, indeed, points to the Nrf2 activation as one of the earliest detectable events when dopaminergic neurons are subjected to neurotoxic stimulation;

thus, I decided to investigate the trigger and the effects of these precocious Nrf2 modulations in the brain.

The microglial neuroprotective function identified is hinder by GCase inhibitions: a novel phenotype for GBA1 impairments. The second part of the study was carried out with the pharmacological inhibition of GCase as a physiopathological trigger of PD in cellular and animal reporter models. The results of this study enriched the armamentarium of microglia, industrious brain cells essential in maintaining brain homeostasis (Kettenmann et al., 2011), with a novel neuroprotective mechanism based on the microglia-dependent activation of the neuronal Nrf2 pathways (Fig. 21, 22, 23, 29). The mechanism identified requires a microglia-to-neuron direct contact and functional actin-dependent structures (constituent the filopodia and cytoskeleton, and required for their motility) in microglial cells (Bernier et al., 2019; Cserép et al., 2020). Interestingly we demonstrated that the GCase enzymatic inhibition, mimicking the major risk factor to develop the PD, the GBA1 impairment (Migdalska-Richards and Schapira, 2016), affects the neuronal redox pathways by interfering with the ability of microglia to induce the discovered neuroprotective response (Fig. 23). The consequence of the reduced NRF2 activity is an increased susceptibility of neuronal cells to oxidative stress or toxic molecules; in keeping with this conclusion, our co-culture experiments demonstrate that reduced GCase activity is associated with a higher sensitivity of dopaminergic neurons to MPP+ treatments (Fig. 24). The neurodegenerative phenotype promoted by GBA1 mutations has been so far attributed to the loss-of-function of the GCase enzyme in neurons, although, in the brain, the most obvious candidate target cells are microglia, commonly considered the resident macrophages, i.e. the lineage responsible for the peripheral effects of GBA1 mutations (Prinz et al., 2014).

Decreased Nrf2 activity in neurons due to microglial GCase inhibition increases the susceptibility of neurons to neurotoxic stimulations. Considering that GBA1 is highly expressed in microglia (Zhang et al., 2014) and mutations are able to significantly reduce the GCase enzymatic activity (Beutler, 1992) even a partial enzymatic inhibition could be sufficient to produce functional consequences in microglia physiology. Indeed, my thesis demonstrated that the 50% reduction of microglial GCase activity, recapitulating the enzymatic activity impairment observed in heterozygotic carriers of severe GBA1 mutations (Sanchez-Martinez et al., 2016), is enough to

destabilize the neuronal capacity of reaction against oxidative stress conditions or neurotoxic insults. The *in vivo* CBE treatment was appropriately titrated (Vardi et al., 2016) to obtain a comparable reduction; as a result, we observed a slight, 20% inhibition of neuronal Nrf2 activation (Fig. 20, 22): the extent of this impairment was proven sufficient to produce significant effects on neuron survival *in vitro* in the presence of a neurotoxic stimulus like MPP+ (Fig. 24). We believe that this vulnerability is especially relevant for dopaminergic neurons, that present high oxidative stress levels and increased susceptibility to neurotoxic stimuli, as a consequence of the dopamine metabolism (Hermida-Ameijeiras et al., 2004); indeed, high oxidative stress were observed *post mortem* in the brain of Parkinson's patients (Zhou et al., 2008). In these conditions, the slight but constant reduction of the NRF2 activity induced by GBA1 mutations in microglia may hinder the full protective response against neurotoxic stimulations. It is thus conceivable that with reduced NRF2 activity, the oxidative stress, at length, may produce negative consequences on the cellular viability selectively to dopaminergic neurons. Accumulation of damages due to the continuous impairment of NRF2 signal is fitting with the slight, but constant, neuronal death occurring in the long-lasting process of Parkinson's pathogenesis, starting years before the onset of clinical manifestations (Postuma and Berg, 2016). It is true that not all GBA1 carriers develop PD, we may hypothesize that the greater vulnerability of neurons to neurotoxic *stimuli* in GBA1 carriers depends on the individual variability of exposition to environmental factors (neurotoxic stimuli) and/or on different levels of oxidative stress due to genetic factors: both conditions may account for the different penetrance of a GBA1 mutation in the development of the neurodegenerative phenotype.

GCase inhibition modifies morphology and molecular process underlying the microglial functional state. We may hypothesize that the cell-to-cell contact needed to activate NRF2 in neurons could be hindered by the GCase inhibition, as suggested by an unbiased cell imaging analysis, showing that CBE treatment increases the sub-population of a cell characterized by a static and less motile phenotype (Fig. 28); this phenotype has reduced cell protrusions and motility, and might curtail the microglial ability to interact with neurons and then to induce the neuronal NRF2 pathway. Interestingly, the microglial response associated with GCase inhibition during early stages seems not to be related to a pro-inflammatory phenotype, since the image-based analysis support that the morpho-functional subpopulation is clearly different from the pattern obtained after a pro-inflammatory treatment (Fig. 28). Indeed, the gene expression profile analysis confirms that CBE

induces upregulation of anti-inflammatory genes involved in metabolic reprogramming and reparative responses (*Arg1* and *Trem2*) (Konishi and Kiyama, 2018; Lee et al., 2018; Liu et al., 2018). We may speculate that in early neurodegenerative stages triggered by GBA1 impairment a microglia phenotype not yet reported may prevail over the pro-inflammatory phenotype that has been observed late in the neurodegenerative process likely promoted by the extensive progression of neuronal death (Vitner et al., 2012). Future studies will clarify the relation of the anti-inflammatory program stimulated by CBE and the round-shaped, less neurosupportive phenotype of microglia highlighted in our experiments and its role in neurodegeneration.

GCase inhibition modifies microglial energetic metabolism thus suggesting novel therapeutic strategies to prevent the neurodegenerative process. Extensive evidence supports the key role of deficits in brain energy metabolism, particularly hypometabolism of glucose and mitochondrial dysfunction, in the pathophysiology of cerebral disorders (Beal, 1995; Bergsneider *et al.*, 1997; Orth and Schapira, 2002). Experiment carried out in cell and animal models demonstrated that GCase loss-of-function causes mitochondrial dysfunction since were reported a decrease in adenosine diphosphate phosphorylation, a decline in mitochondrial membrane potential, accumulation of dysfunctional and fragmented mitochondria, reduction in respiratory chain complex activities and oxygen consumption (Cleeter et al., 2013; Osellame et al., 2013). Mitochondrial activities, glucose availability, and glycolytic rate are known to influence microglia functions. In Trem2-deficient mice with amyloid pathology the administration of cyclocreatine, a creatine analogue that can supply ATP, tempered autophagy and restored microglial dysfunction (Ulland et al., 2017a). This evidence together with my observation that GCase inhibition increases Trem2 gene expression in microglial BV-2 cells, a gene that is known to empower microglial responses during AD by sustaining cellular energetic and biosynthetic metabolism (Ulland et al., 2017a), strengthen the hypothesis that microglial metabolism could play a role in neuroprotection. The preliminary evidence performed in this study seems to support this hypothesis since the data demonstrated that GCase inhibitions are able to reduce the activity of NAD(P)H-dependent oxidoreductase enzymes. Experiments showed that starvation, recapitulates the effect observed after GCase inhibition since is sufficient to hinder microglia-mediated neuroprotection (Fig. 30); on the opposite fresh media increases the ability of microglia to induce neuronal-NRF2, thus suggesting that GCase impairment might alter the energy balance of the cells, thus counteracting the microglia-to-neuron communication. The finding that SIRT1 activators, including resveratrol, were able to improve the mechanism by which microglial

induce the neuronal NRF2 activity, supports the concept that metabolic reprogramming might be a strategy to modulate the microglial-mediated neuroprotection. These data suggest SIRT1 as a possible target for therapeutic strategies aiming at providing a metabolic compensation to microglia as a preventive treatment to reduce the risk of neurodegeneration.

The translational future of my thesis findings. My experiments have demonstrated that macrophages share with microglia the ability to induce NRF2 neuronal upregulations (Fig. 21); most importantly, when human peripheral PBNC differentiated into macrophages were co-cultured with neurons, displayed a microglia-type of behaviour recapitulating the ability to increase neuronal NRF2 activity that was hindered by the GCase inhibition (Fig. 31). This finding opens to the opportunity to study the defect in macrophages obtained from GD and PD patients' blood samples, i.e. to correlate the mechanism with the risk of developing PD or to develop neuropathic pain displayed by several GD patients (Biegstraaten et al., 2010). The ability of macrophages to induce NRF2 could then be used as a test to identify persons with an increased risk to develop PD or as a simple screening test for candidate drugs able to revert the noxious microglial phenotype.

Future studies should clarify whether the macrophages ability to stimulate the NRF2 pathway in contacted, adjacent cells, is limited to neurons or is a more general mechanism present also in other tissues; since aberrant regulations of the antioxidant and detoxification pathway has been found in cardiovascular diseases (Howden, 2013), cancer (Menegon et al., 2016), fibrosis (Swamy et al., 2016) and in different pathogenetic conditions involving inflammation (Ahmed et al., 2017) and aging (Zhang et al., 2015; Kubben et al., 2016), it is tempting to speculate that recasting the macrophage communication could be a valuable therapeutic strategy also for diseases outside the CNS. For instance, it is known that tumor-associated macrophages (TAM) play an essential role in providing a suitable microenvironment for cancer development and progression (Mantovani et al., 2017) and NRF2 overexpression is often associated with poor prognosis (de la Vega et al., 2018); therefore, we might hypothesize that TAM could be involved in the modulation of NRF2 in the neoplastic tissue. If this were the case, an approach directed towards the decrease of TAM-dependent interaction with tumor cells based on the inhibition of GCase activity might decrease NRF2 expression in cancer cells and possibly counteract tumorigenesis.

Conclusive remarks. In conclusion, a large number of studies have highlighted the neuronal effects of GBA1 mutations hindering lysosomal and mitochondrial functions, leading to increased α-syn deposition and cellular vulnerability to neurotoxic insults; in my thesis, I have demonstrated that pharmacological inhibition of GCase in microglia impairs the microglial ability to induce a detoxification response through the modulation of the NRF2 signal in neurons, suggesting that GBA1 mutations affecting GCase activity may result in a similar microglial alteration. Alterations of this protective mechanism, which plays a role during early stages, could increase the risk of neurodegeneration induced by toxic molecules and oxidative stress, especially important for dopaminergic neurons characterized by an elevated oxidative metabolism. This mechanism shared by macrophages seems to be related to microglia energetic metabolism and can be modulated by Sirt1 activator. Gain further insight into the discovered mechanism might contribute to identify novel targets to restore microglial neuroprotective functions and prevent the onset of neurodegeneration in Gaucher's and Parkinson's diseases.

7 ACKNOWLEDGMENT

I am grateful and thankful to all the persons who made possible to carry out this project; your contribution was essential for the success of the project and for my personal growth.

I would to thank my Professor Paolo Ciana, and all the people whom I worked with and/or collaborated: Adriana Maggi, Elisabetta Vegeto, Alessandro Villa, Nicoletta Rizzi, Monica Rebecchi, Clara Meda, Daniela Crescenti, Federica Mornata, Giulia Dell'Omo, Sara Della Torre, Giovanna Pepe, Mara Barone, Andrea Brivio, Ilaria Colombo, Maria Chieregato, Alice Ratti, Marianna Mekhaeil, Giulia Amadeo, Stefano Nava, Francesca Stucchi, Dino Di Monte, Fabio Blandini, Silvia Cerri, Cristina Ghezzi, Patrizia Rise, Greta Cermisoni, Giovanna Levandis, Nicoletta Cesari.

This work has been supported by the EU Joint Programme Neurodegenerative, Disease Research (JPND) project: GBA-PARK and GBA-PaCTs.

8 BIBLIOGRAPHY

Abiko Y, Miura T, Phuc BH, Shinkai Y, Kumagai Y. 2011. Participation of covalent modification of Keap1 in the activation of Nrf2 by tert-butylbenzoquinone, an electrophilic metabolite of butylated hydroxyanisole. Toxicol Appl Pharmacol 255:32–39.
Abutbul S, Shapiro J, Szaingurten-Solodkin I, Levy N, Carmy Y, Baron R, Jung S, Monsonego A. 2012. TGF-β signaling through SMAD2/3 induces the quiescent microglial phenotype within the CNS environment. Glia 60:1160–1171.
Aguzzi A, Barres BA, Bennett ML. 2013. Microglia: scapegoat, saboteur, or something else? Science (80-) 339:156–161.
Aharon-Peretz J, Rosenbaum H, Gershoni-Baruch R. 2004. Mutations in the glucocerebrosidase gene and Parkinson's disease in Ashkenazi Jews. N Engl J Med 351:1972–1977.
Ahmed SMU, Luo L, Namani A, Wang XJ, Tang X. 2017. Nrf2 signaling pathway: Pivotal roles in inflammation. Biochim Biophys Acta (BBA)-Molecular Basis Dis 1863:585–597.
Alaei MR, Tabrizi A, Jafari N, Mozafari H. 2019. Gaucher disease: New expanded classification emphasizing neurological features. Iran J Child Neurol 13:7–24.
Allan SM, Tyrrell PJ, Rothwell NJ. 2005. Interleukin-1 and neuronal injury. Nat Rev Immunol 5:629–640.
Austin SA, Floden AM, Murphy EJ, Combs CK. 2006. α-synuclein expression modulates microglial activation phenotype. J Neurosci 26:10558–10563.
Austin SA, Rojanathammanee L, Golovko MY, Murphy EJ, Combs CK. 2011. Lack of alpha-synuclein modulates microglial phenotype in vitro. Neurochem Res 36:994–1004.
Awad O, Sarkar C, Panicker LM, Miller D, Zeng X, Sgambato JA, Lipinski MM, Feldman RA. 2015. Altered TFEB-mediated lysosomal biogenesis in Gaucher disease iPSC-derived neuronal cells. Hum Mol Genet 24:5775–5788.
Balogun E, Hoque M, Gong P, Killeen E, Green CJ, Foresti R, Alam J, Motterlini R. 2003. Curcumin activates the haem oxygenase-1 gene via regulation of Nrf2 and the antioxidant-responsive element. Biochem J 371:887–895.
Balstad TR, Carlsen H, Myhrstad MCW, Kolberg M, Reiersen H, Gilen L, Ebihara K, Paur I, Blomhoff R. 2011. Coffee, broccoli and spices are strong inducers of electrophile response element-dependent transcription in vitro and in vivo–Studies in electrophile response element transgenic mice. Mol Nutr Food Res 55:185–197.
Banati RB, Daniel SE, Blunt SB. 1998. Glial pathology but absence of apoptotic nigral neurons in long-standing Parkinson's disease. Mov Disord Off J Mov Disord Soc 13:221–227.
Barone MC, Sykiotis GP, Bohmann D. 2011. Genetic activation of Nrf2 signaling is sufficient to ameliorate neurodegenerative phenotypes in a Drosophila model of Parkinson's disease. Dis Model Mech 4:701–707.
Bartheld CS, Bahney J, Herculano-Houzel S. 2016. The search for true numbers of neurons and glial cells in the human brain: A review of 150 years of cell counting. J Comp Neurol 524:3865–3895.
Bas J, Calopa M, Mestre M, Mollevı DG, Cutillas B, Ambrosio S, Buendia E. 2001. Lymphocyte populations in Parkinson's disease and in rat models of parkinsonism. J Neuroimmunol 113:146–152.
Baxter PS, Hardingham GE. 2016. Adaptive regulation of the brain's antioxidant defences by neurons and astrocytes. Free Radic Biol Med [Internet] 100:147–152. Available from: http://dx.doi.org/10.1016/j.freeradbiomed.2016.06.027
Beal MF. 1995. Aging, energy, and oxidative stress in neurodegenerative diseases. Ann Neurol 38:357–366.
Bell KFS, Al-Mubarak B, Martel M-A, McKay S, Wheelan N, Hasel P, Márkus NM, Baxter P, Deighton RF, Serio A. 2015. Neuronal development is promoted by weakened intrinsic antioxidant defences due to epigenetic repression of Nrf2. Nat Commun 6:1–15.
Benakis C, Garcia-Bonilla L, Iadecola C, Anrather J. 2015. The role of microglia and myeloid immune cells in acute cerebral ischemia. Front Cell Neurosci 8:461.
Benitez BA, Cruchaga C. 2013. TREM2 and neurodegenerative disease. N Engl J Med 369:1567–1568.
Benskey MJ, Perez RG, Manfredsson FP. 2016. The contribution of alpha synuclein to neuronal survival and function - Implications for Parkinson's disease. J Neurochem 137:331–359.
Béraud D, Hathaway HA, Trecki J, Chasovskikh S, Johnson DA, Johnson JA, Federoff HJ, Shimoji M, Mhyre TR, Maguire-Zeiss KA. 2013. Microglial activation and antioxidant responses induced by the Parkinson's disease protein α-synuclein. J Neuroimmune Pharmacol 8:94–117.
Bergsneider M, Hovda DA, Shalmon E, Kelly DF, Vespa PM, Martin NA, Phelps ME, McArthur DL, Caron MJ, Kraus JF. 1997. Cerebral hyperglycolysis following severe traumatic brain injury in humans: a positron emission tomography study. J Neurosurg 86:241–251.
Bernier L-P, York EM, MacVicar BA. 2020. Immunometabolism in the Brain: How Metabolism Shapes Microglial Function. Trends Neurosci.
Bernier LP, Bohlen CJ, York EM, Choi HB, Kamyabi A, Dissing-Olesen L, Hefendehl JK, Collins HY, Stevens B, Barres BA, MacVicar BA. 2019. Nanoscale Surveillance of the Brain by Microglia via cAMP-Regulated Filopodia. Cell Rep [Internet] 27:2895-2908.e4. Available from: https://doi.org/10.1016/j.celrep.2019.05.010
Beutler E. 1992. Gaucher disease: New molecular approaches to diagnosis and treatment. Science (80-) 256:794–799.
Biber K, Neumann H, Inoue K, Boddeke HWGM. 2007. Neuronal "On" and "Off" signals control microglia. Trends Neurosci 30:596–602.
Biedler JL, Roffler-Tarlov S, Schachner M, Freedman LS. 1978. Multiple neurotransmitter synthesis by human neuroblastoma cell lines and clones. Cancer Res 38:3751–3757.
Biegstraaten M, Mengel E, Maródi L, Petakov M, Niederau C, Giraldo P, Hughes D, Mrsic M, Mehta A, Hollak CEM, Van Schaik IN. 2010. Peripheral neuropathy in adult type 1 Gaucher disease: A 2-year prospective observational study. Brain 133:2909–2919.
Bilimoria PM, Stevens B. 2015. Microglia function during brain development: new insights from animal models. Brain Res 1617:7–

17.
Blandini F, Armentero M. 2012. Animal models of Parkinson's disease. FEBS J 279:1156–1166.
Bliederhaeuser C, Zondler L, Grozdanov V, Ruf WP, Brenner D, Melrose HL, Bauer P, Ludolph AC, Gillardon F, Kassubek J. 2016. LRRK2 contributes to monocyte dysregulation in Parkinson's disease. Acta Neuropathol Commun 4:123.
Bogdanov M, Matson WR, Wang L, Matson T, Saunders-Pullman R, Bressman SS, Beal MF. 2008. Metabolomic profiling to develop blood biomarkers for Parkinson's disease. Brain 131:389–396.
Bogie JFJ, Stinissen P, Hendriks JJA. 2014. Macrophage subsets and microglia in multiple sclerosis. Acta Neuropathol 128:191–213.
Boillée S, Cleveland DW. 2008. Revisiting oxidative damage in ALS: microglia, Nox, and mutant SOD1. J Clin Invest 118:474–478.
Boka G, Anglade P, Wallach D, Javoy-Agid F, Agid Y, Hirsch EC. 1994. Immunocytochemical analysis of tumor necrosis factor and its receptors in Parkinson's disease. Neurosci Lett 172:151–154.
Bossy-Wetzel E, Schwarzenbacher R, Lipton SA. 2004. Molecular pathways to neurodegeneration. Nat Med 10:S2–S9.
Braak H, de Vos RAI, Jansen ENH, Bratzke H, Braak E. 1998. Neuropathological hallmarks of Alzheimer's and Parkinson's diseases. In: Progress in brain research. Vol. 117. Elsevier. p 267–285.
Bradford MM. 1976. A rapid and sensitive method for the quantitation of microgram quantities of protein utilizing the principle of protein-dye binding. Anal Biochem 72:248–254.
Brites D, Vaz AR. 2014. Microglia centered pathogenesis in ALS: insights in cell interconnectivity. Front Cell Neurosci 8:117.
Brockmann K. 2020. GBA-Associated Synucleinopathies: Prime Candidates for Alpha-Synuclein Targeting Compounds. Front Cell Dev Biol 8:1033.
Butovsky O, Jedrychowski MP, Moore CS, Cialic R, Lanser AJ, Gabriely G, Koeglsperger T, Dake B, Wu PM, Doykan CE. 2014. Identification of a unique TGF-β–dependent molecular and functional signature in microglia. Nat Neurosci 17:131–143.
Calkins MJ, Townsend JA, Johnson DA, Johnson JA. 2010. Cystamine protects from 3-nitropropionic acid lesioning via induction of nf-e2 related factor 2 mediated transcription. Exp Neurol 224:307–317.
Cao TT, Ma L, Kandpal G, Warren L, Hess JF, Seabrook GR. 2005. Increased nuclear factor-erythroid 2 p45-related factor 2 activity protects SH-SY5Y cells against oxidative damage. J Neurochem 95:406–417.
Caslake R, Moore JN, Gordon JC, Harris CE, Counsell C. 2008. Changes in diagnosis with follow-up in an incident cohort of patients with parkinsonism. J Neurol Neurosurg Psychiatry 79:1202–1207.
Charkhand B, Scantlebury MH, Narita A, Zimran A, Al-Hertani W. 2019. Effect of Ambroxol chaperone therapy on Glucosylsphingosine (Lyso-Gb1) levels in two Canadian patients with type 3 Gaucher disease. Mol Genet Metab reports 20:100476.
Chen C-Y, Jang J-H, Li M-H, Surh Y-J. 2005. Resveratrol upregulates heme oxygenase-1 expression via activation of NF-E2-related factor 2 in PC12 cells. Biochem Biophys Res Commun 331:993–1000.
Chen P-C, Vargas MR, Pani AK, Smeyne RJ, Johnson DA, Kan YW, Johnson JA. 2009. Nrf2-mediated neuroprotection in the MPTP mouse model of Parkinson's disease: Critical role for the astrocyte. Proc Natl Acad Sci 106:2933–2938.
Cherry JD, Olschowka JA, O'Banion MK. 2014. Neuroinflammation and M2 microglia: the good, the bad, and the inflamed. J Neuroinflammation 11:98.
Clark LN, Kartsaklis LA, Gilbert RW, Dorado B, Ross BM, Kisselev S, Verbitsky M, Mejia-Santana H, Cote LJ, Andrews H. 2009. Association of glucocerebrosidase mutations with dementia with lewy bodies. Arch Neurol 66:578–583.
Clarke DD. 1999. Circulation and energy metabolism of the brain. Basic Neurochem Mol Cell Med Asp.
Cleeter MWJ, Chau K-Y, Gluck C, Mehta A, Hughes DA, Duchen M, Wood NW, Hardy J, Cooper JM, Schapira AH. 2013. Glucocerebrosidase inhibition causes mitochondrial dysfunction and free radical damage. Neurochem Int 62:1–7.
Colton CA. 2009. Heterogeneity of microglial activation in the innate immune response in the brain. J neuroimmune Pharmacol 4:399–418.
Connolly BS, Lang AE. 2014. Pharmacological treatment of Parkinson disease: a review. Jama 311:1670–1683.
Cookson MR. 2012. Parkinsonism due to mutations in PINK1, parkin, and DJ-1 and oxidative stress and mitochondrial pathways. Cold Spring Harb Perspect Med 2:a009415.
Cortes CJ, Miranda HC, Frankowski H, Batlevi Y, Young JE, Le A, Ivanov N, Sopher BL, Carromeu C, Muotri AR. 2014. Polyglutamine-expanded androgen receptor interferes with TFEB to elicit autophagy defects in SBMA. Nat Neurosci 17:1180–1189.
Corti O, Lesage S, Brice A. 2011. What genetics tells us about the causes and mechanisms of Parkinson's disease. Physiol Rev.
Costa G, Frau L, Wardas J, Pinna A, Plumitallo A, Morelli M. 2013. MPTP-induced dopamine neuron degeneration and glia activation is potentiated in MDMA-pretreated mice. Mov Disord 28:1957–1965.
Couch Y, Alvarez-Erviti L, Sibson NR, Wood MJA, Anthony DC. 2011. The acute inflammatory response to intranigral α-synuclein differs significantly from intranigral lipopolysaccharide and is exacerbated by peripheral inflammation. J Neuroinflammation 8:166.
Coune PG, Schneider BL, Aebischer P. 2012. Parkinson's disease: gene therapies. Cold Spring Harb Perspect Med 2:a009431.
Cremades N, Chen SW, Dobson CM. 2017. Structural characteristics of α-synuclein oligomers. In: International review of cell and molecular biology. Vol. 329. Elsevier. p 79–143.
Croisier E, Moran LB, Dexter DT, Pearce RKB, Graeber MB. 2005. Microglial inflammation in the parkinsonian substantia nigra: relationship to alpha-synuclein deposition. J Neuroinflammation 2:1–8.
Cserép C, Pósfai B, Lénárt N, Fekete R, László ZI, Lele Z, Orsolits B, Molnár G, Heindl S, Schwarcz AD, Ujvári K, Környei Z, Tóth K, Szabadits E, Sperlágh B, Baranyi M, Csiba L, Hortobágyi T, Maglóczky Z, Martinecz B, Szabó G, Erdélyi F, Szipocs R, Tamkun MM, Gesierich B, Duering M, Katona I, Liesz A, Tamás G, Dénes Á. 2020. Microglia monitor and protect neuronal function through specialized somatic purinergic junctions. Science (80-) 367:528–537.
Cuadrado A, Martín-Moldes Z, Ye J, Lastres-Becker I. 2014. Transcription factors NRF2 and NF-κB are coordinated effectors of the Rho family, GTP-binding protein RAC1 during inflammation. J Biol Chem 289:15244–15258.

Cullen V, Sardi SP, Ng J, Xu Y, Sun Y, Tomlinson JJ, Kolodziej P, Kahn I, Saftig P, Woulfe J. 2011. Acid β-glucosidase mutants linked to Gaucher disease, Parkinson disease, and Lewy body dementia alter α-synuclein processing. Ann Neurol 69:940–953.

Davalos D, Grutzendler J, Yang G, Kim J V, Zuo Y, Jung S, Littman DR, Dustin ML, Gan W-B. 2005. ATP mediates rapid microglial response to local brain injury in vivo. Nat Neurosci 8:752–758.

Davis EJ, Foster TD, Thomas WE. 1994. Cellular forms and functions of brain microglia. Brain Res Bull 34:73–78.

Decressac M, Mattsson B, Weikop P, Lundblad M, Jakobsson J, Björklund A. 2013. TFEB-mediated autophagy rescues midbrain dopamine neurons from α-synuclein toxicity. Proc Natl Acad Sci 110:E1817–E1826.

Dickson DW, Braak H, Duda JE, Duyckaerts C, Gasser T, Halliday GM, Hardy J, Leverenz JB, Del Tredici K, Wszolek ZK. 2009. Neuropathological assessment of Parkinson's disease: refining the diagnostic criteria. Lancet Neurol 8:1150–1157.

ElAli A, Rivest S. 2016. Microglia in Alzheimer's disease: a multifaceted relationship. Brain Behav Immun 55:138–150.

Elmore MRP, Najafi AR, Koike MA, Dagher NN, Spangenberg EE, Rice RA, Kitazawa M, Matusow B, Nguyen H, West BL. 2014. Colony-stimulating factor 1 receptor signaling is necessary for microglia viability, unmasking a microglia progenitor cell in the adult brain. Neuron 82:380–397.

Enquist IB, Bianco C Lo, Ooka A, Nilsson E, Månsson JE, Ehinger M, Richter J, Brady RO, Kirik D, Karlsson S. 2007. Murine models of acute neuronopathic Gaucher disease. Proc Natl Acad Sci U S A 104:17483–17488.

Erikson A, Bembi B, Schiffmann R. 1997. Neuronopathic forms of Gaucher's disease. Baillieres Clin Haematol 10:711–723.

Eschbach J, Danzer KM. 2014. α-Synuclein in Parkinson's disease: pathogenic function and translation into animal models. Neurodegener Dis 14:1–17.

Fearnley JM, Lees AJ. 1991. Ageing and Parkinson's disease: substantia nigra regional selectivity. Brain 114:2283–2301.

Fernandes HJR, Hartfield EM, Christian HC, Emmanoulidou E, Zheng Y, Booth H, Bogetofte H, Lang C, Ryan BJ, Sardi SP. 2016. ER stress and autophagic perturbations lead to elevated extracellular α-synuclein in GBA-N370S Parkinson's iPSC-derived dopamine neurons. Stem cell reports 6:342–356.

Fernandez-Fernandez S, Almeida A, Bolaños JP. 2012. Antioxidant and bioenergetic coupling between neurons and astrocytes. Biochem J 443:3–11.

Ferreira SA, Romero-Ramos M. 2018. Microglia response during Parkinson's disease: alpha-synuclein intervention. Front Cell Neurosci 12:247.

Filiano AJ, Gadani SP, Kipnis J. 2015. Interactions of innate and adaptive immunity in brain development and function. Brain Res 1617:18–27.

Finkel T. 2011. Signal transduction by reactive oxygen species. J Cell Biol 194:7–15.

Fishbein I, Kuo YM, Giasson BI, Nussbaum RL. 2014. Augmentation of phenotype in a transgenic Parkinson mouse heterozygous for a Gaucher mutation. Brain 137:3235–3247.

Franco-Bocanegra, McAuley, Nicoll, Boche. 2019. Molecular Mechanisms of Microglial Motility: Changes in Ageing and Alzheimer's Disease. Cells 8:639.

Fumagalli S, Perego C, Pischiutta F, Zanier ER, De Simoni M-G. 2015. The ischemic environment drives microglia and macrophage function. Front Neurol 6:81.

Funk N, Wieghofer P, Grimm S, Schaefer R, Bühring H, Gasser T, Biskup S. 2013. Characterization of peripheral hematopoietic stem cells and monocytes in Parkinson's disease. Mov Disord 28:392–395.

Gan-Or Z, Giladi N, Rozovski U, Shifrin C, Rosner S, Gurevich T, Bar-Shira A, Orr-Urtreger A. 2008. Genotype-phenotype correlations between GBA mutations and Parkinson disease risk and onset. Neurology 70:2277–2283.

Gan L, Johnson JA. 2014. Oxidative damage and the Nrf2-ARE pathway in neurodegenerative diseases. Biochim Biophys Acta (BBA)-Molecular Basis Dis 1842:1208–1218.

Gan L, Vargas MR, Johnson DA, Johnson JA. 2012. Astrocyte-specific overexpression of Nrf2 delays motor pathology and synuclein aggregation throughout the CNS in the alpha-synuclein mutant (A53T) mouse model. J Neurosci 32:17775–17787.

Gardai SJ, Mao W, Schüle B, Babcock M, Schoebel S, Lorenzana C, Alexander J, Kim S, Glick H, Hilton K. 2013. Elevated alpha-synuclein impairs innate immune cell function and provides a potential peripheral biomarker for Parkinson's disease. PLoS One 8:e71634.

Garden GA, Möller T. 2006. Microglia biology in health and disease. J Neuroimmune Pharmacol 1:127–137.

Gegg ME, Burke D, Heales SJR, Cooper JM, Hardy J, Wood NW, Schapira AH V. 2012. Glucocerebrosidase deficiency in substantia nigra of parkinson disease brains. Ann Neurol 72:455–463.

Gelosa P, Lecca D, Fumagalli M, Wypych D, Pignieri A, Cimino M, Verderio C, Enerbäck M, Nikookhesal E, Tremoli E. 2014. Microglia is a key player in the reduction of stroke damage promoted by the new antithrombotic agent ticagrelor. J Cereb Blood Flow Metab 34:979–988.

Gerhard A, Pavese N, Hotton G, Turkheimer F, Es M, Hammers A, Eggert K, Oertel W, Banati RB, Brooks DJ. 2006. In vivo imaging of microglial activation with [11C](R)-PK11195 PET in idiopathic Parkinson's disease. Neurobiol Dis 21:404–412.

Gibrat C, Saint-Pierre M, Bousquet M, Lévesque D, Rouillard C, Cicchetti F. 2009. Differences between subacute and chronic MPTP mice models: investigation of dopaminergic neuronal degeneration and α-synuclein inclusions. J Neurochem 109:1469–1482.

Ginhoux F, Greter M, Leboeuf M, Nandi S, See P, Gokhan S, Mehler MF, Conway SJ, Ng LG, Stanley ER. 2010. Fate mapping analysis reveals that adult microglia derive from primitive macrophages. Science (80-) 330:841–845.

Ginhoux F, Guilliams M. 2016. Tissue-resident macrophage ontogeny and homeostasis. Immunity 44:439–449.

Giudice A, Arra C, Turco MC. 2010. Review of molecular mechanisms involved in the activation of the Nrf2-ARE signaling pathway by chemopreventive agents. In: Transcription Factors. Springer. p 37–74.

Giunti D, Parodi B, Cordano C, Uccelli A, Kerlero de Rosbo N. 2014. Can we switch microglia's phenotype to foster neuroprotection? Focus on multiple sclerosis. Immunology 141:328–339.

Goker-Alpan O, Schiffmann R, LaMarca ME, Nussbaum RL, McInerney-Leo A, Sidransky E. 2004. Parkinsonism among Gaucher

disease carriers. J Med Genet 41:937–940.
Goker-Alpan O, Stubblefield BK, Giasson BI, Sidransky E. 2010. Glucocerebrosidase is present in α-synuclein inclusions in Lewy body disorders. Acta Neuropathol 120:641–649.
Gold M, El Khoury J. 2015. β-amyloid, microglia, and the inflammasome in Alzheimer's disease. In: Seminars in immunopathology. Vol. 37. Springer. p 607–611.
Gomez-Nicola D, Perry VH. 2015. Microglial dynamics and role in the healthy and diseased brain: a paradigm of functional plasticity. Neurosci 21:169–184.
Gordon S, Martinez-Pomares L. 2017. Physiological roles of macrophages. Pflügers Arch J Physiol 469:365–374.
Grabowski GA. 2008. Phenotype, diagnosis, and treatment of Gaucher's disease. Lancet 372:1263–1271.
Grabowski GA, Beutler E. 2001. The Metabolic and Molecular Bases of Inherited Disease.
Grozdanov V, Bliederhaeuser C, Ruf WP, Roth V, Fundel-Clemens K, Zondler L, Brenner D, Martin-Villalba A, Hengerer B, Kassubek J. 2014. Inflammatory dysregulation of blood monocytes in Parkinson's disease patients. Acta Neuropathol 128:651–663.
Gruden MA, Sewell RDE, Yanamandra K, Davidova T V, Kucheryanu VG, Bocharov E V, Bocharova OA, Polyschuk V V, Sherstnev V V, Morozova-Roche LA. 2011. Immunoprotection against toxic biomarkers is retained during Parkinson's disease progression. J Neuroimmunol 233:221–227.
Gupta K, Patani R, Baxter P, Serio A, Story D, Tsujita T, Hayes JD, Pedersen RA, Hardingham GE, Chandran S. 2012. Human embryonic stem cell derived astrocytes mediate non-cell-autonomous neuroprotection through endogenous and drug-induced mechanisms. Cell Death Differ 19:779–787.
Haenseler W, Sansom SN, Buchrieser J, Newey SE, Moore CS, Nicholls FJ, Chintawar S, Schnell C, Antel JP, Allen ND. 2017. A highly efficient human pluripotent stem cell microglia model displays a neuronal-co-culture-specific expression profile and inflammatory response. Stem cell reports 8:1727–1742.
Hara H, Ohta M, Adachi T. 2006a. Apomorphine protects against 6-hydroxydopamine-induced neuronal cell death through activation of the Nrf2-ARE pathway. J Neurosci Res 84:860–866.
Hara T, Nakamura K, Matsui M, Yamamoto A, Nakahara Y, Suzuki-Migishima R, Yokoyama M, Mishima K, Saito I, Okano H. 2006b. Suppression of basal autophagy in neural cells causes neurodegenerative disease in mice. Nature 441:885–889.
Hartig SM. 2013. Basic image analysis and manipulation in ImageJ. Curr Protoc Mol Biol 102:14–15.
Hayes JD, Dinkova-Kostova AT. 2014. The Nrf2 regulatory network provides an interface between redox and intermediary metabolism. Trends Biochem Sci [Internet] 39:199–218. Available from: http://dx.doi.org/10.1016/j.tibs.2014.02.002
Hayes JD, McMahon M. 2009. NRF2 and KEAP1 mutations: permanent activation of an adaptive response in cancer. Trends Biochem Sci 34:176–188.
Haynes SE, Hollopeter G, Yang G, Kurpius D, Dailey ME, Gan W-B, Julius D. 2006. The P2Y 12 receptor regulates microglial activation by extracellular nucleotides. Nat Neurosci 9:1512–1519.
Heindl S, Gesierich B, Benakis C, Llovera G, Duering M, Liesz A. 2018. Automated morphological analysis of microglia after stroke. Front Cell Neurosci 12:106.
Heneka MT, Kummer MP, Latz E. 2014. Innate immune activation in neurodegenerative disease. Nat Rev Immunol 14:463–477.
Heneka MT, Kummer MP, Stutz A, Delekate A, Schwartz S, Vieira-Saecker A, Griep A, Axt D, Remus A, Tzeng T-C. 2013. NLRP3 is activated in Alzheimer's disease and contributes to pathology in APP/PS1 mice. Nature 493:674–678.
Henkel JS, Beers DR, Zhao W, Appel SH. 2009. Microglia in ALS: the good, the bad, and the resting. J Neuroimmune Pharmacol 4:389–398.
Heppner FL, Ransohoff RM, Becher B. 2015. Immune attack: the role of inflammation in Alzheimer disease. Nat Rev Neurosci 16:358–372.
Hermida-Ameijeiras Á, Méndez-Álvarez E, Sánchez-Iglesias S, Sanmartín-Suárez C, Soto-Otero R. 2004. Autoxidation and MAO-mediated metabolism of dopamine as a potential cause of oxidative stress: role of ferrous and ferric ions. Neurochem Int 45:103–116.
Hindle J V. 2010. Ageing, neurodegeneration and Parkinson's disease. Age Ageing 39:156–161.
Hoek RM, Ruuls SR, Murphy CA, Wright GJ, Goddard R, Zurawski SM, Blom B, Homola ME, Streit WJ, Brown MH. 2000. Down-regulation of the macrophage lineage through interaction with OX2 (CD200). Science (80-) 290:1768–1771.
Hong S, Dissing-Olesen L, Stevens B. 2016. New insights on the role of microglia in synaptic pruning in health and disease. Curr Opin Neurobiol 36:128–134.
Howden R. 2013. Nrf2 and cardiovascular defense. Oxid Med Cell Longev 2013.
Hristovska I, Pascual O. 2016. Deciphering resting microglial morphology and process motility from a synaptic prospect. Front Integr Neurosci 9:73.
Hruska KS, LaMarca ME, Scott CR, Sidransky E. 2008. Gaucher disease: Mutation and polymorphism spectrum in the glucocerebrosidase gene (GBA). Hum Mutat 29:567–583.
Hsieh CL, Koike M, Spusta SC, Niemi EC, Yenari M, Nakamura MC, Seaman WE. 2009. A role for TREM2 ligands in the phagocytosis of apoptotic neuronal cells by microglia. J Neurochem 109:1144–1156.
Hu R, Xu C, Shen G, Jain MR, Khor TO, Gopalkrishnan A, Lin W, Reddy B, Chan JY, Kong A-NT. 2006. Gene expression profiles induced by cancer chemopreventive isothiocyanate sulforaphane in the liver of C57BL/6J mice and C57BL/6J/Nrf2 (−/−) mice. Cancer Lett 243:170–192.
Hunot S, Boissiere F, Faucheux B, Brugg B, Mouatt-Prigent A, Agid Y, Hirsch EC. 1996. Nitric oxide synthase and neuronal vulnerability in Parkinson's disease. Neuroscience 72:355–363.
Hwang YP, Jeong HG. 2008. The coffee diterpene kahweol induces heme oxygenase-1 via the PI3K and p38/Nrf2 pathway to protect human dopaminergic neurons from 6-hydroxydopamine-derived oxidative stress. Febs Lett 582:2655–2662.
Imamura K, Hishikawa N, Sawada M, Nagatsu T, Yoshida M, Hashizume Y. 2003. Distribution of major histocompatibility complex

class II-positive microglia and cytokine profile of Parkinson's disease brains. Acta Neuropathol 106:518–526.
Innamorato NG, Jazwa A, Rojo AI, Garcıa C, Fernández-Ruiz J. 2010. Different Susceptibility to the Parkinson's Toxin MPTP in Mice Lacking the.
Innamorato NG, Rojo AI, García-Yagüe ÁJ, Yamamoto M, de Ceballos ML, Cuadrado A. 2008. The Transcription Factor Nrf2 Is a Therapeutic Target against Brain Inflammation. J Immunol 181:680–689.
Ivankovic D, Chau K, Schapira AH V, Gegg ME. 2016. Mitochondrial and lysosomal biogenesis are activated following PINK 1/parkin-mediated mitophagy. J Neurochem 136:388–402.
Jakel RJ, Townsend JA, Kraft AD, Johnson JA. 2007. Nrf2-mediated protection against 6-hydroxydopamine. Brain Res 1144:192–201.
Janda E, Boi L, Carta AR. 2018. Microglial phagocytosis and its regulation: a therapeutic target in Parkinson's disease? Front Mol Neurosci 11:144.
Jankovic J. 2008. Parkinson's disease: clinical features and diagnosis. J Neurol Neurosurg psychiatry 79:368–376.
Jing X, Shi H, Zhang C, Ren M, Han M, Wei X, Zhang X, Lou H. 2015. Dimethyl fumarate attenuates 6-OHDA-induced neurotoxicity in SH-SY5Y cells and in animal model of Parkinson's disease by enhancing Nrf2 activity. Neuroscience 286:131–140.
Joers V, Tansey MG, Mulas G, Carta AR. 2017. Microglial phenotypes in Parkinson's disease and animal models of the disease. Prog Neurobiol [Internet] 155:57–75. Available from: http://dx.doi.org/10.1016/j.pneurobio.2016.04.006
Johnson DA, Andrews GK, Xu W, Johnson JA. 2002. Activation of the antioxidant response element in primary cortical neuronal cultures derived from transgenic reporter mice. J Neurochem 81:1233–1241.
Jung S, Aliberti J, Graemmel P, Sunshine MJ, Kreutzberg GW, Sher A, Littman DR. 2000. Analysis of fractalkine receptor CX(3)CR1 function by targeted deletion and green fluorescent protein reporter gene insertion. Mol Cell Biol 20:4106–4114.
Kaidery NA, Ahuja M, Thomas B. 2019. Crosstalk between Nrf2 signaling and mitochondrial function in Parkinson's disease. Mol Cell Neurosci 101:103413.
Kaidery NA, Banerjee R, Yang L, Smirnova NA, Hushpulian DM, Liby KT, Williams CR, Yamamoto M, Kensler TW, Ratan RR. 2013. Targeting Nrf2-mediated gene transcription by extremely potent synthetic triterpenoids attenuate dopaminergic neurotoxicity in the MPTP mouse model of Parkinson's disease. Antioxid Redox Signal 18:139–157.
Kalia L V, Kalia SK, Lang AE. 2015. Disease-modifying strategies for Parkinson's disease. Mov Disord 30:1442–1450.
Kannarkat GT, Boss JM, Tansey MG. 2013. The role of innate and adaptive immunity in Parkinson's disease. J Parkinsons Dis 3:493–514.
Kapeta S, Chondrogianni N, Gonos ES. 2010. Nuclear erythroid factor 2-mediated proteasome activation delays senescence in human fibroblasts. J Biol Chem 285:8171–8184.
Karch CM, Cruchaga C, Goate AM. 2014. Alzheimer's disease genetics: from the bench to the clinic. Neuron 83:11–26.
Kensler TW, Wakabayashi N, Biswal S. 2007. Cell survival responses to environmental stresses via the Keap1-Nrf2-ARE pathway. Annu Rev Pharmacol Toxicol 47:89–116.
Keren-Shaul H, Spinrad A, Weiner A, Matcovitch-Natan O, Dvir-Szternfeld R, Ulland TK, David E, Baruch K, Lara-Astaiso D, Toth B. 2017. A unique microglia type associated with restricting development of Alzheimer's disease. Cell 169:1276–1290.
Kerschensteiner M, Meinl E, Hohlfeld R. 2009. Neuro-immune crosstalk in CNS diseases. Neuroscience [Internet] 158:1122–1132. Available from: http://dx.doi.org/10.1016/j.neuroscience.2008.09.009
Kettenmann H, Kirchhoff F, Verkhratsky A. 2013. Microglia: new roles for the synaptic stripper. Neuron 77:10–18.
Kettenmann H, Uwe Karsten H, Mami N, Alexei V. 2011. Physiology of microglia. Physiol Rev 91:461–553.
Kierdorf K, Erny D, Goldmann T, Sander V, Schulz C, Perdiguero EG, Wieghofer P, Heinrich A, Riemke P, Hölscher C. 2013. Microglia emerge from erythromyeloid precursors via Pu. 1-and Irf8-dependent pathways. Nat Neurosci 16:273–280.
Kilpatrick K, Zeng Y, Hancock T, Segatori L. 2015. Genetic and chemical activation of TFEB mediates clearance of aggregated α-synuclein. PLoS One 10:1–21.
Kim D, Hwang H, Choi S, Kwon SH, Lee S, Park JH, Kim SM, Ko HS. 2018. D409H GBA1 mutation accelerates the progression of pathology in A53T α-synuclein transgenic mouse model. Acta Neuropathol Commun 6:32.
Kim S-Y, Woo M-S, Park J-S, Kim H-S. 2010. Regulation of matrix metalloproteinase-9 gene expression in MPP+-or 6-OHDA-treated human neuroblastoma SK-N-BE (2) C cells. Neurochem Int 56:437–442.
Kim YS, Joh TH. 2006. Microglia, major player in the brain inflammation: their roles in the pathogenesis of Parkinson's disease. Exp Mol Med 38:333–347.
Klegeris A, McGeer EG, McGeer PL. 2007. Therapeutic approaches to inflammation in neurodegenerative disease. Curr Opin Neurol 20:351–357.
Klegeris A, Pelech S, Giasson BI, Maguire J, Zhang H, McGeer EG, McGeer PL. 2008. α-Synuclein activates stress signaling protein kinases in THP-1 cells and microglia. Neurobiol Aging 29:739–752.
Kloss CUA, Bohatschek M, Kreutzberg GW, Raivich G. 2001. Effect of lipopolysaccharide on the morphology and integrin immunoreactivity of ramified microglia in the mouse brain and in cell culture. Exp Neurol 168:32–46.
Knott C, Stern G, Wilkin GP. 2000. Inflammatory regulators in Parkinson's disease: iNOS, lipocortin-1, and cyclooxygenases-1 and-2. Mol Cell Neurosci 16:724–739.
Komatsu M, Ichimura Y. 2010. Physiological significance of selective degradation of p62 by autophagy. FEBS Lett 584:1374–1378.
Komatsu M, Waguri S, Chiba T, Murata S, Iwata J, Tanida I, Ueno T, Koike M, Uchiyama Y, Kominami E. 2006. Loss of autophagy in the central nervous system causes neurodegeneration in mice. Nature 441:880–884.
Konishi H, Kiyama H. 2018. Microglial TREM2/DAP12 signaling: A double-edged sword in neural diseases. Front Cell Neurosci 12:1–14.
Koros C, Simitsi A, Stefanis L. 2017. Genetics of Parkinson's disease: genotype–phenotype correlations. In: International review of neurobiology. Vol. 132. Elsevier. p 197–231.
Krabbe G, Halle A, Matyash V, Rinnenthal JL, Eom GD, Bernhardt U, Miller KR, Prokop S, Kettenmann H, Heppner FL. 2013.

Functional impairment of microglia coincides with Beta-amyloid deposition in mice with Alzheimer-like pathology. PLoS One 8:e60921.

Kraft AD, Johnson DA, Johnson JA. 2004. Nuclear factor E2-related factor 2-dependent antioxidant response element activation by tert-butylhydroquinone and sulforaphane occurring preferentially in astrocytes conditions neurons against oxidative insult. J Neurosci 24:1101–1112.

Kubben N, Zhang W, Wang L, Voss TC, Yang J, Qu J, Liu GH, Misteli T. 2016. Repression of the antioxidant NRF2 pathway in premature aging. Cell [Internet] 165:1361–1374. Available from: http://dx.doi.org/10.1016/j.cell.2016.05.017

Kumar DT, Iyer S, Christy JP, Siva R, Tayubi IA, Doss CGP, Zayed H. 2019. A comparative computational approach toward pharmacological chaperones (NN-DNJ and ambroxol) on N370S and L444P mutations causing Gaucher's disease. In: Advances in protein chemistry and structural biology. Vol. 114. Elsevier. p 315–339.

Kuo CL, Kallemeijn WW, Lelieveld LT, Mirzaian M, Zoutendijk I, Vardi A, Futerman AH, Meijer AH, Spaink HP, Overkleeft HS, Aerts JMFG, Artola M. 2019. In vivo inactivation of glycosidases by conduritol B epoxide and cyclophellitol as revealed by activity-based protein profiling. FEBS J 286:584–600.

Kwak M-K, Itoh K, Yamamoto M, Kensler TW. 2002. Enhanced expression of the transcription factor Nrf2 by cancer chemopreventive agents: role of antioxidant response element-like sequences in the nrf2 promoter. Mol Cell Biol 22:2883–2892.

de la Fuente-Fernández R, Schulzer M, Kuramoto L, Cragg J, Ramachandiran N, Au WL, Mak E, McKenzie J, McCormick S, Sossi V. 2011. Age-specific progression of nigrostriatal dysfunction in Parkinson's disease. Ann Neurol 69:803–810.

de la Vega MR, Chapman E, Zhang DD. 2018. NRF2 and the Hallmarks of Cancer. Cancer Cell 34:21–43.

Langston JW, Ballard P, Tetrud JW, Irwin I. 1983. Chronic Parkinsonism in humans due to a product of meperidine-analog synthesis. Science (80-) 219:979–980.

Lastres-Becker I, Ulusoy A, Innamorato NG, Sahin G, Rábano A, Kirik D, Cuadrado A. 2012. α-Synuclein expression and Nrf2 deficiency cooperate to aggravate protein aggregation, neuronal death and inflammation in early-stage Parkinson's disease. Hum Mol Genet 21:3173–3192.

Lau A, Villeneuve NF, Sun Z, Wong PK, Zhang DD. 2008. Dual roles of Nrf2 in cancer. Pharmacol Res 58:262–270.

De Lau LML, Breteler MMB. 2006. Epidemiology of Parkinson's disease. Lancet Neurol 5:525–535.

Lawson LJ, Perry VH, Dri P, Gordon S. 1990. Heterogeneity in the distribution and morphology of microglia in the normal adult mouse brain. Neuroscience 39:151–170.

Lee CYD, Daggett A, Gu X, Jiang LL, Langfelder P, Li X, Wang N, Zhao Y, Park CS, Cooper Y, Ferando I, Mody I, Coppola G, Xu H, Yang XW. 2018. Elevated TREM2 Gene Dosage Reprograms Microglia Responsivity and Ameliorates Pathological Phenotypes in Alzheimer's Disease Models. Neuron [Internet] 97:1032-1048.e5. Available from: https://doi.org/10.1016/j.neuron.2018.02.002

Lee J-K, Tran T, Tansey MG. 2009. Neuroinflammation in Parkinson's disease. J Neuroimmune Pharmacol 4:419–429.

Lee S-J. 2008. Origins and effects of extracellular α-synuclein: implications in Parkinson's disease. J Mol Neurosci 34:17–22.

Lee Y, Lee S-R, Choi SS, Yeo H-G, Chang K-T, Lee HJ. 2014. Therapeutically targeting neuroinflammation and microglia after acute ischemic stroke. Biomed Res Int 2014.

Lenz KM, Nelson LH. 2018. Microglia and beyond: innate immune cells as regulators of brain development and behavioral function. Front Immunol 9:698.

Lesage S, Anheim M, Condroyer C, Pollak P, Durif F, Dupuits C, Viallet F, Lohmann E, Corvol J-C, Honoré A. 2011. Large-scale screening of the Gaucher's disease-related glucocerebrosidase gene in Europeans with Parkinson's disease. Hum Mol Genet 20:202–210.

Lesage S, Brice A. 2009. Parkinson's disease: from monogenic forms to genetic susceptibility factors. Hum Mol Genet 18:R48–R59.

Lewy H, Fritz J. 1912. Paralysis agitans. I. Pathologische Anatomie. In: Lewandowski M (ed) Handbuch der Neurologie. Springer III:920–933.

Li J, Lee J-M, Johnson JA. 2002. Microarray analysis reveals an antioxidant responsive element-driven gene set involved in conferring protection from an oxidative stress-induced apoptosis in IMR-32 cells. J Biol Chem 277:388–394.

Li L, Zhang CW, Chen GYJ, Zhu B, Chai C, Xu QH, Tan EK, Zhu Q, Lim KL, Yao SQ. 2014. A sensitive two-photon probe to selectively detect monoamine oxidase B activity in Parkinson's disease models. Nat Commun [Internet] 5:3276. Available from: http://dx.doi.org/10.1038/ncomms4276

Li W, Khor TO, Xu C, Shen G, Jeong W-S, Yu S, Kong A-N. 2008. Activation of Nrf2-antioxidant signaling attenuates NFκB-inflammatory response and elicits apoptosis. Biochem Pharmacol 76:1485–1489.

Lill CM. 2016. Genetics of Parkinson's disease. Mol Cell Probes 30:386–396.

Linari S, Castaman G. 2015. Clinical manifestations and management of Gaucher disease. Clin Cases Miner Bone Metab 12:157.

Lindvall O. 2013. Developing dopaminergic cell therapy for Parkinson's disease—give up or move forward? Mov Disord 28:268–273.

Liu G, Liu Y, Jiang Q, Jiang Y, Feng R, Zhang L, Chen Z, Li K, Liu J. 2016. Convergent genetic and expression datasets highlight TREM2 in Parkinson's disease susceptibility. Mol Neurobiol 53:4931–4938.

Liu W, Taso O, Wang R, Garcia-Reitboeck P, Andrews WD, Piers TM, Pocock JM, Cummings DM, Hardy J, Edwards FA. 2018. Trem2 promotes anti-inflammatory responses in microglia and is suppressed under pro-inflammatory conditions. bioRxiv:449884.

Lively S, Schlichter LC. 2018. Microglia responses to pro-inflammatory stimuli (LPS, IFNγ+ TNFα) and reprogramming by resolving cytokines (IL-4, IL-10). Front Cell Neurosci 12:215.

Ma Q, Battelli L, Hubbs AF. 2006. Multiorgan autoimmune inflammation, enhanced lymphoproliferation, and impaired homeostasis of reactive oxygen species in mice lacking the antioxidant-activated transcription factor Nrf2. Am J Pathol 168:1960–1974.

Ma Q, He X. 2012. Molecular basis of electrophilic and oxidative defense: promises and perils of Nrf2. Pharmacol Rev 64:1055–1081.

Maegawa GHB, Tropak MB, Buttner JD, Rigat BA, Fuller M, Pandit D, Tang L, Kornhaber GJ, Hamuro Y, Clarke JTR. 2009. Identification and characterization of ambroxol as an enzyme enhancement agent for Gaucher disease. J Biol Chem 284:23502–23516.

Makin S. 2016. The prion principle. Nature 538:S13 S16.

Malik M, Parikh I, Vasquez JB, Smith C, Tai L, Bu G, LaDu MJ, Fardo DW, Rebeck GW, Estus S. 2015. Genetics ignite focus on microglial inflammation in Alzheimer's disease. Mol Neurodegener 10:1–12.

Mansueto G, Armani A, Viscomi C, D'Orsi L, De Cegli R, Polishchuk E V., Lamperti C, Di Meo I, Romanello V, Marchet S, Saha PK, Zong H, Blaauw B, Solagna F, Tezze C, Grumati P, Bonaldo P, Pessin JE, Zeviani M, Sandri M, Ballabio A. 2017. Transcription Factor EB Controls Metabolic Flexibility during Exercise. Cell Metab [Internet] 25:182–196. Available from: http://dx.doi.org/10.1016/j.cmet.2016.11.003

Mantovani A, Marchesi F, Malesci A, Laghi L, Allavena P. 2017. Tumour-associated macrophages as treatment targets in oncology. Nat Rev Clin Oncol 14:399.

Maor G, Rencus-Lazar S, Filocamo M, Steller H, Segal D, Horowitz M. 2013. Unfolded protein response in Gaucher disease: from human to Drosophila. Orphanet J Rare Dis 8:140.

Marinelli S, Basilico B, Marrone MC, Ragozzino D. 2019. Microglia-neuron crosstalk: Signaling mechanism and control of synaptic transmission. In: Seminars in cell & developmental biology. Vol. 94. Elsevier. p 138–151.

Martin I, Kim JW, Dawson VL, Dawson TM. 2014. LRRK2 pathobiology in Parkinson's disease. J Neurochem 131:554–565.

Masuda T, Sankowski R, Staszewski O, Böttcher C, Amann L, Scheiwe C, Nessler S, Kunz P, van Loo G, Coenen VA. 2019. Spatial and temporal heterogeneity of mouse and human microglia at single-cell resolution. Nature 566:388–392.

Mateo I, Infante J, Sánchez-Juan P, García-Gorostiaga I, Rodríguez-Rodríguez E, Vázquez-Higuera JL, Berciano J, Combarros O. 2010. Serum heme oxygenase-1 levels are increased in Parkinson's disease but not in Alzheimer's disease. Acta Neurol Scand 121:136–138.

Mazzulli JR, Zunke F, Tsunemi T, Toker NJ, Jeon S, Burbulla LF, Patnaik S, Sidransky E, Marugan JJ, Sue CM. 2016. Activation of β-glucocerebrosidase reduces pathological α-synuclein and restores lysosomal function in Parkinson's patient midbrain neurons. J Neurosci 36:7693–7706.

McCann H, Stevens CH, Cartwright H, Halliday GM. 2014. α-Synucleinopathy phenotypes. Parkinsonism Relat Disord 20:S62–S67.

McGeer PL, Itagaki S, Akiyama H, McGeer EG. 1988. Rate of cell death in parkinsonism indicates active neuropathological process. Ann Neurol Off J Am Neurol Assoc Child Neurol Soc 24:574–576.

McGeer PL, McGeer EG. 2007. NSAIDs and Alzheimer disease: epidemiological, animal model and clinical studies. Neurobiol Aging 28:639–647.

McNeill A, Magalhaes J, Shen C, Chau K-Y, Hughes D, Mehta A, Foltynie T, Cooper JM, Abramov AY, Gegg M. 2014. Ambroxol improves lysosomal biochemistry in glucocerebrosidase mutation-linked Parkinson disease cells. Brain 137:1481–1495.

Medina DL, Fraldi A, Bouche V, Annunziata F, Mansueto G, Spampanato C, Puri C, Pignata A, Martina JA, Sardiello M. 2011. Transcriptional activation of lysosomal exocytosis promotes cellular clearance. Dev Cell 21:421–430.

Menegon S, Columbano A, Giordano S. 2016. The dual roles of NRF2 in cancer. Trends Mol Med 22:578–593.

Meredith GE, Rademacher DJ. 2011. MPTP mouse models of Parkinson's disease: An update. J Parkinsons Dis 1:19–33.

Migdalska-Richards A, Schapira AHV. 2016. The relationship between glucocerebrosidase mutations and Parkinson disease. J Neurochem 139:77–90.

Migdalska-Richards A, Wegrzynowicz M, Rusconi R, Deangeli G, Di Monte DA, Spillantini MG, Schapira AHV. 2017. The L444P Gba1 mutation enhances alpha-synuclein induced loss of nigral dopaminergic neurons in mice. Brain 140:2706–2721.

Migdalska-Richards A, Schapira AH V. 2016. The relationship between glucocerebrosidase mutations and Parkinson disease. J Neurochem 139:77–90.

Min K-J, Yang M, Kim S-U, Jou I, Joe E. 2006. Astrocytes induce hemeoxygenase-1 expression in microglia: a feasible mechanism for preventing excessive brain inflammation. J Neurosci 26:1880–1887.

Mittelbronn M, Dietz K, Schluesener HJ, Meyermann R. 2001. Local distribution of microglia in the normal adult human central nervous system differs by up to one order of magnitude. Acta Neuropathol 101:249–255.

Moehle MS, West AB. 2015. M1 and M2 immune activation in Parkinson's disease: foe and ally? Neuroscience 302:59–73.

Moore C, Ase A, Kinsara A, Rao V, Michell-robinson M, Butovsky O, Ludwin S, Seguela P, Bar-or A, Antel J. 2014. Identification of P2Y12 as a mediator of migration and inflammation in human microglia. J Neuroimmunol 275:90.

Mornata F, Pepe G, Brunialti E, Sfogliarini C, Locati M, Maggi A, Vegeto E. 2020. Reciprocal interference between the NRF2 and LPS signaling pathways on the immune-metabolic phenotype of peritoneal macrophages. Pharmacol Res Perspect accepted.

Mott RT, Ait-Ghezala G, Town T, Mori T, Vendrame M, Zeng J, Ehrhart J, Mullan M, Tan J. 2004. Neuronal expression of CD22: novel mechanism for inhibiting microglial proinflammatory cytokine production. Glia 46:369–379.

Murphy KE, Gysbers AM, Abbott SK, Tayebi N, Kim WS, Sidransky E, Cooper A, Garner B, Halliday GM. 2014. Reduced glucocerebrosidase is associated with increased α-synuclein in sporadic Parkinson's disease. Brain 137:834–848.

Murray PJ, Wynn TA. 2011. Protective and pathogenic functions of macrophage subsets. Nat Rev Immunol 11:723–737.

Mus L, Siani F, Giuliano C, Ghezzi C, Cerri S, Blandini F. 2019. Development and biochemical characterization of a mouse model of Parkinson's disease bearing defective glucocerebrosidase activity. Neurobiol Dis [Internet] 124:289–296. Available from: https://doi.org/10.1016/j.nbd.2018.12.001

Musgrove RE, Helwig M, Bae EJ, Aboutalebi H, Lee SJ, Ulusoy A, Di Monte DA. 2019. Oxidative stress in vagal neurons promotes parkinsonian pathology and intercellular α-synuclein transfer. J Clin Invest 129:3738–3753.

Nagral A. 2014. Gaucher disease. J Clin Exp Hepatol 4:37–50.

Nalls MA, Pankratz N, Lill CM, Do CB, Hernandez DG, Saad M, DeStefano AL, Kara E, Bras J, Sharma M. 2014. Large-scale meta-analysis of genome-wide association data identifies six new risk loci for Parkinson's disease. Nat Genet 46:989–993.

Napolitano G, Ballabio A. 2016. TFEB at a glance. J Cell Sci 129:2475–2481.
Nash Y, Schmukler E, Trudler D, Pinkas-Kramarski R, Frenkel D. 2017. DJ-1 deficiency impairs autophagy and reduces alpha-synuclein phagocytosis by microglia. J Neurochem 143:584–594.
Neudorfer O, Giladi N, Elstein D, Abrahamov A, Turezkite T, Aghai E, Reches A, Bembi B, Zimran A. 1996. Occurrence of Parkinson's syndrome in type 1 Gaucher disease. QJM An Int J Med 89:691–694.
Nezich CL, Wang C, Fogel AI, Youle RJ. 2015. MiT/TFE transcription factors are activated during mitophagy downstream of Parkin and Atg5. J Cell Biol 210:435–450.
Nguyen T, Sherratt PJ, Pickett CB. 2003. Regulatory mechanisms controlling gene expression mediated by the antioxidant response element. Annu Rev Pharmacol Toxicol 43:233–260.
Nicklas WJ, Vyas I, Heikkila RE. 1985. Inhibition of NADH-linked oxidation in brain mitochondria by 1-methyl-4-phenyl-pyridine, a metabolite of the neurotoxin, 1-methyl-4-phenyl-1, 2, 5, 6-tetrahydropyridine. Life Sci 36:2503–2508.
Nimmerjahn A, Kirchhoff F, Helmchen F. 2005. Resting microglial cells are highly dynamic surveillants of brain parenchyma in vivo. Neuroforum 11:95–96.
Nishiyori A, Minami M, Ohtani Y, Takami S, Yamamoto J, Kawaguchi N, Kume T, Akaike A, Satoh M. 1998. Localization of fractalkine and CX3CR1 mRNAs in rat brain: does fractalkine play a role in signaling from neuron to microglia? FEBS Lett 429:167–172.
Niso-Santano M, González-Polo RA, Bravo-San Pedro JM, Gómez-Sánchez R, Lastres-Becker I, Ortiz-Ortiz MA, Soler G, Morán JM, Cuadrado A, Fuentes JM. 2010. Activation of apoptosis signal-regulating kinase 1 is a key factor in paraquat-induced cell death: modulation by the Nrf2/Trx axis. Free Radic Biol Med 48:1370–1381.
Noelker C, Lu L, Höllerhage M, Vulinovic F, Sturn A, Roscher R, Höglinger GU, Hirsch EC, Oertel WH, Alvarez-Fischer D, Andreas H. 2015. Glucocerebrosidase deficiency and mitochondrial impairment in experimental Parkinson disease. J Neurol Sci [Internet] 356:129–136. Available from: http://dx.doi.org/10.1016/j.jns.2015.06.030
Nolte C, Moller T, Walter T, Kettenmann H. 1996. Complement 5a controls motility of murine microglial cells in vitro via activation of an inhibitory G-protein and the rearrangement of the actin cytoskeleton. Neuroscience 73:1091–1107.
Norden DM, Godbout JP. 2013. Microglia of the aged brain: primed to be activated and resistant to regulation. Neuropathol Appl Neurobiol 39:19–34.
Nouhi F, Tusi SK, Abdi A, Khodagholi F. 2011. Dietary supplementation with tBHQ, an NRF2 stabilizer molecule, confers neuroprotection against apoptosis in amyloid β-injected rat. Neurochem Res 36:870–878.
Obeso JA, Rodriguez-Oroz MC, Goetz CG, Marin C, Kordower JH, Rodriguez M, Hirsch EC, Farrer M, Schapira AHV, Halliday G. 2010. Missing pieces in the Parkinson's disease puzzle. Nat Med [Internet] 16:653–661. Available from: http://dx.doi.org/10.1038/nm.2165
Olanow CW, Stern MB, Sethi K. 2009. The scientific and clinical basis for the treatment of Parkinson disease (2009). Neurology 72:S1–S136.
Oppenheimer. 1992. Esiri MM., Diseases of the basal ganglia, cerebellum and motor neurons. Greenfields Neuropathol 5th ed London, Melb Edward Arnold:988–997.
Orihuela R, McPherson CA, Harry GJ. 2016. Microglial M1/M2 polarization and metabolic states. Br J Pharmacol 173:649–665.
Orr CF, Rowe DB, Mizuno Y, Mori H, Halliday GM. 2005. A possible role for humoral immunity in the pathogenesis of Parkinson's disease. Brain 128:2665–2674.
Orth M, SCHAPIRA AH V. 2002. Mitochondrial involvement in Parkinson's disease. Neurochem Int 40:533–541.
Osellame LD, Rahim AA, Hargreaves IP, Gegg ME, Richard-Londt A, Brandner S, Waddington SN, Schapira AH V, Duchen MR. 2013. Mitochondria and quality control defects in a mouse model of Gaucher disease—links to Parkinson's disease. Cell Metab 17:941–953.
von Otter M, Bergström P, Quattrone A, De Marco EV, Annesi G, Söderkvist P, Wettinger SB, Drozdzik M, Bialecka M, Nissbrandt H. 2014. Genetic associations of Nrf2-encoding NFE2L2 variants with Parkinson's disease–a multicenter study. BMC Med Genet 15:131.
von Otter M, Landgren S, Nilsson S, Celojevic D, Bergström P, Håkansson A, Nissbrandt H, Drozdzik M, Bialecka M, Kurzawski M. 2010. Association of Nrf2-encoding NFE2L2 haplotypes with Parkinson's disease. BMC Med Genet 11:36.
Palmieri M, Impey S, Kang H, di Ronza A, Pelz C, Sardiello M, Ballabio A. 2011. Characterization of the CLEAR network reveals an integrated control of cellular clearance pathways. Hum Mol Genet 20:3852–3866.
Palmieri M, Pal R, Sardiello M. 2017. AKT modulates the autophagy-lysosome pathway via TFEB. Cell Cycle 16:1237.
Pan S-H, Chao Y-C, Hung P-F, Chen H-Y, Yang S-C, Chang Y-L, Wu C-T, Chang C-C, Wang W-L, Chan W-K. 2011. The ability of LCRMP-1 to promote cancer invasion by enhancing filopodia formation is antagonized by CRMP-1. J Clin Invest 121:3189–3205.
Pankratz N, Wilk JB, Latourelle JC, DeStefano AL, Halter C, Pugh EW, Doheny KF, Gusella JF, Nichols WC, Foroud T. 2009. Genomewide association study for susceptibility genes contributing to familial Parkinson disease. Hum Genet 124:593–605.
Paolicelli RC, Bergamini G, Rajendran L. 2019. Cell-to-cell communication by extracellular vesicles: focus on microglia. Neuroscience 405:148–157.
Paolicelli RC, Bisht K, Tremblay M-È. 2014. Fractalkine regulation of microglial physiology and consequences on the brain and behavior. Front Cell Neurosci 8:129.
Paolicelli RC, Bolasco G, Pagani F, Maggi L, Scianni M, Panzanelli P, Giustetto M, Ferreira TA, Guiducci E, Dumas L. 2011. Synaptic pruning by microglia is necessary for normal brain development. Science (80-) 333:1456–1458.
Parhizkar S, Arzberger T, Brendel M, Kleinberger G, Deussing M, Focke C, Nuscher B, Xiong M, Ghasemigharagoz A, Katzmarski N. 2019. Loss of TREM2 function increases amyloid seeding but reduces plaque-associated ApoE. Nat Neurosci 22:191–204.
Park J, Paik SR, Jou I, Park SM. 2008. Microglial phagocytosis is enhanced by monomeric α-synuclein, not aggregated α-synuclein: Implications for Parkinson's disease. Glia 56:1215–1223.
Parkinson J. 1817. An essay on the shaking palsy.(Republished in 2002). J Neuropsychiatry Clin Neurosci 14:223–236.

Parnetti L, Chiasserini D, Persichetti E, Eusebi P, Varghese S, Qureshi MM, Dardis A, Deganuto M, De Carlo C, Castrioto A. 2014. Cerebrospinal fluid lysosomal enzymes and alpha-synuclein in Parkinson's disease. Mov Disord 29:1019–1027.
Pb T, Patlolla AK, Centeno JA. 2003. CarcinogenY ic and systemic health effects associated with arsenic expoY sure2a critical review. Toxicol Pathol 31:575–588.
Pepe G, Calderazzi G, De Maglie M, Villa AM, Vegeto E. 2014. Heterogeneous induction of microglia M2a phenotype by central administration of interleukin-4. J Neuroinflammation 11:1–14.
Perry VH, Holmes C. 2014. Microglial priming in neurodegenerative disease. Nat Rev Neurol 10:217–224.
Perry VH, Nicoll JAR, Holmes C. 2010. Microglia in neurodegenerative disease. Nat Rev Neurol 6:193.
Perry VH, Teeling J. 2013. Microglia and macrophages of the central nervous system: the contribution of microglia priming and systemic inflammation to chronic neurodegeneration. In: Seminars in immunopathology. Vol. 35. Springer. p 601–612.
Polito VA, Li H, Martini-Stoica H, Wang B, Yang L, Xu Y, Swartzlander DB, Palmieri M, Di Ronza A, Lee VM. 2014. Selective clearance of aberrant tau proteins and rescue of neurotoxicity by transcription factor EB. EMBO Mol Med 6:1142–1160.
Polymeropoulos MH, Lavedan C, Leroy E, Ide SE, Dehejia A, Dutra A, Pike B, Root H, Rubenstein J, Boyer R. 1997. Mutation in the α-synuclein gene identified in families with Parkinson's disease. Science (80-) 276:2045–2047.
Popovich PG, Longbrake EE. 2008. Can the immune system be harnessed to repair the CNS? Nat Rev Neurosci 9:481–493.
Postuma RB, Berg D. 2016. Advances in markers of prodromal Parkinson disease. Nat Rev Neurol 12:622.
Pribiag H, Stellwagen D. 2014. Neuroimmune regulation of homeostatic synaptic plasticity. Neuropharmacology 78:13–22.
Price NL, Gomes AP, Ling AJY, Duarte F V, Martin-Montalvo A, North BJ, Agarwal B, Ye L, Ramadori G, Teodoro JS. 2012. SIRT1 is required for AMPK activation and the beneficial effects of resveratrol on mitochondrial function. Cell Metab 15:675–690.
Prinz M, Priller J. 2014. Microglia and brain macrophages in the molecular age: from origin to neuropsychiatric disease. Nat Rev Neurosci 15:300–312.
Prinz M, Tay TL, Wolf Y, Jung S. 2014. Microglia: Unique and common features with other tissue macrophages. Acta Neuropathol 128:319–331.
Prochaska HJ, Talalay P. 1988. Regulatory mechanisms of monofunctional and bifunctional anticarcinogenic enzyme inducers in murine liver. Cancer Res 48:4776–4782.
Ragland M, Hutter C, Zabetian C, Edwards K. 2009. Association between the ubiquitin carboxyl-terminal esterase L1 gene (UCHL1) S18Y variant and Parkinson's Disease: a HuGE review and meta-analysis. Am J Epidemiol 170:1344–1357.
Ramsey CP, Glass CA, Montgomery MB, Lindl KA, Ritson GP, Chia LA, Hamilton RL, Chu CT, Jordan-Sciutto KL. 2007. Expression of Nrf2 in neurodegenerative diseases. J Neuropathol Exp Neurol 66:75–85.
Rayaprolu S, Mullen B, Baker M, Lynch T, Finger E, Seeley WW, Hatanpaa KJ, Lomen-Hoerth C, Kertesz A, Bigio EH. 2013. TREM2 in neurodegeneration: evidence for association of the p. R47H variant with frontotemporal dementia and Parkinson's disease. Mol Neurodegener 8:1–5.
Rizzi N, Brunialti E, Cerri S, Cermisoni G, Levandis G, Cesari N, Maggi A, Blandini F, Ciana P. 2018. In vivo imaging of early signs of dopaminergic neuronal death in an animal model of Parkinson's disease. Neurobiol Dis [Internet] 114:74–84. Available from: https://doi.org/10.1016/j.nbd.2018.02.005
Rizzi N, Rebecchi M, Levandis G, Ciana P, Maggi A. 2017. Identification of novel loci for the generation of reporter mice. Nucleic Acids Res 45.
Rocha EM, Smith GA, Park E, Cao H, Graham A-R, Brown E, McLean JR, Hayes MA, Beagan J, Izen SC. 2015. Sustained systemic glucocerebrosidase inhibition induces brain α-synuclein aggregation, microglia and complement C1q activation in mice. Antioxid Redox Signal 23:550–564.
Roczniak-Ferguson A, Petit CS, Froehlich F, Qian S, Ky J, Angarola B, Walther TC, Ferguson SM. 2012. The transcription factor TFEB links mTORC1 signaling to transcriptional control of lysosome homeostasis. Sci Signal 5:ra42–ra42.
Rojanathammanee L, Murphy EJ, Combs CK. 2011. Expression of mutant alpha-synuclein modulates microglial phenotype in vitro. J Neuroinflammation 8:44.
Rojo AI, Innamorato NG, Martín-Moreno AM, De Ceballos ML, Yamamoto M, Cuadrado A. 2010. Nrf2 regulates microglial dynamics and neuroinflammation in experimental Parkinson's disease. Glia 58:588–598.
Rojo AI, McBean G, Cindric M, Egea J, López MG, Rada P, Zarkovic N, Cuadrado A. 2014. Redox control of microglial function: Molecular mechanisms and functional significance. Antioxidants Redox Signal 21:1766–1801.
Roodveldt C, Labrador-Garrido A, Gonzalez-Rey E, Fernandez-Montesinos R, Caro M, Lachaud CC, Waudby CA, Delgado M, Dobson CM, Pozo D. 2010. Glial innate immunity generated by non-aggregated alpha-synuclein in mouse: differences between wild-type and Parkinson's disease-linked mutants. PLoS One 5:e13481.
Sanchez-Guajardo V, Febbraro F, Kirik D, Romero-Ramos M. 2010. Microglia acquire distinct activation profiles depending on the degree of α-synuclein neuropathology in a rAAV based model of Parkinson's disease. PLoS One 5:e8784.
Sanchez-Martinez A, Beavan M, Gegg ME, Chau K-Y, Whitworth AJ, Schapira AH V. 2016. Parkinson disease-linked GBA mutation effects reversed by molecular chaperones in human cell and fly models. Sci Rep 6:31380.
Santoni G, Cardinali C, Morelli MB, Santoni M, Nabissi M, Amantini C. 2015. Danger-and pathogen-associated molecular patterns recognition by pattern-recognition receptors and ion channels of the transient receptor potential family triggers the inflammasome activation in immune cells and sensory neurons. J Neuroinflammation 12:1–10.
Sardiello M, Palmieri M, Ronza A Di, Medina DL, Valenza M, Gennarino VA, Di Malta C, Donaudy F, Embrione V, Polishchuk RS, Banfi S, Parenti G, Cattaneo E, Ballabio A. 2009. A gene network regulating lysosomal biogenesis and function. Science (80-) 325:473–477.
Sato-Hashimoto M, Nozu T, Toriba R, Horikoshi A, Akaike M, Kawamoto K, Hirose A, Hayashi Y, Nagai H, Shimizu W. 2019. Microglial SIRPα regulates the emergence of CD11c+ microglia and demyelination damage in white matter. Elife 8:e42025.
Savitt JM, Dawson VL, Dawson TM. 2006. Diagnosis and treatment of Parkinson disease: molecules to medicine. J Clin Invest

116:1744–1754.
Savitz SI, Cox Jr CS. 2016. Concise review: cell therapies for stroke and traumatic brain injury: targeting microglia. Stem Cells 34:537–542.
Schafer DP, Lehrman EK, Kautzman AG, Koyama R, Mardinly AR, Yamasaki R, Ransohoff RM, Greenberg ME, Barres BA, Stevens B. 2012. Microglia sculpt postnatal neural circuits in an activity and complement-dependent manner. Neuron 74:691–705.
Schapira AH V. 2015. Glucocerebrosidase and Parkinson disease: recent advances. Mol Cell Neurosci 66:37–42.
Schapira AH V, Chaudhuri KR, Jenner P. 2017. Non-motor features of Parkinson disease. Nat Rev Neurosci 18:435.
Schapira AH V, Cooper JM, Dexter D, Jenner P, Clark JB, Marsden CD. 1989. Mitochondrial complex I deficiency in Parkinson's disease. Lancet 333:1269.
Schapira AH V, Mann VM, Cooper JM, Dexter D, Daniel SE, Jenner P, Clark JB, Marsden CD. 1990. Anatomic and disease specificity of NADH CoQ1 reductase (complex I) deficiency in Parkinson's disease. J Neurochem 55:2142–2145.
Schapira AH V, Tolosa E. 2010. Molecular and clinical prodrome of Parkinson disease: implications for treatment. Nat Rev Neurol 6:309–317.
Schindelin J, Arganda-Carreras I, Frise E, Kaynig V, Longair M, Pietzsch T, Preibisch S, Rueden C, Saalfeld S, Schmid B. 2012. Fiji: an open-source platform for biological-image analysis. Nat Methods 9:676–682.
Schöndorf DC, Aureli M, McAllister FE, Hindley CJ, Mayer F, Schmid B, Sardi SP, Valsecchi M, Hoffmann S, Schwarz LK, Hedrich U, Berg D, Shihabuddin LS, Hu J, Pruszak J, Gygi SP, Sonnino S, Gasser T, Deleidi M. 2014. IPSC-derived neurons from GBA1-associated Parkinson's disease patients show autophagic defects and impaired calcium homeostasis. Nat Commun 5.
Schwenk F, Baron U, Rajewsky K. 1995. A cre-transgenic mouse strain for the ubiquitous deletion of loxP-flanked gene segments including deletion in germ cells. Nucleic Acids Res 23:5080.
Settembre C, De Cegli R, Mansueto G, Saha PK, Vetrini F, Visvikis O, Huynh T, Carissimo A, Palmer D, Jürgen Klisch T, Wollenberg AC, Di Bernardo D, Chan L, Irazoqui JE, Ballabio A. 2013. TFEB controls cellular lipid metabolism through a starvation-induced autoregulatory loop. Nat Cell Biol 15:647–658.
Settembre C, Di Malta C, Polito VA, Arencibia MG, Vetrini F, Erdin S, Erdin SU, Huynh T, Medina D, Colella P. 2011. TFEB links autophagy to lysosomal biogenesis. Science (80-) 332:1429–1433.
Shameli A, Xiao W, Zheng Y, Shyu S, Sumodi J, Meyerson HJ, Harding C V, Maitta RW. 2016. A critical role for alpha-synuclein in development and function of T lymphocytes. Immunobiology 221:333–340.
Shigemoto-Mogami Y, Hoshikawa K, Goldman JE, Sekino Y, Sato K. 2014. Microglia enhance neurogenesis and oligodendrogenesis in the early postnatal subventricular zone. J Neurosci 34:2231–2243.
Shih AY, Johnson DA, Wong G, Kraft AD, Jiang L, Erb H, Johnson JA, Murphy TH. 2003. Coordinate regulation of glutathione biosynthesis and release by Nrf2-expressing glia potently protects neurons from oxidative stress. J Neurosci 23:3394–3406.
Shin EC, Cho SE, Lee D-K, Hur M-W, Paik SR, Park JH, Kim J. 2000. Expression patterns of α-synuclein in human hematopoietic cells and in Drosophila at different developmental stages. Mol Cells 10:65–70.
Sica A, Erreni M, Allavena P, Porta C. 2015. Macrophage polarization in pathology. Cell Mol life Sci 72:4111–4126.
Sidransky E, Lopez G. 2012. The link between the GBA gene and parkinsonism. Lancet Neurol 11:986–998.
Sidransky E, Nalls MA, Aasly JO, Aharon-Peretz J, Annesi G, Barbosa ER, Bar-Shira A, Berg D, Bras J, Brice A. 2009. Multicenter analysis of glucocerebrosidase mutations in Parkinson's disease. N Engl J Med 361:1651–1661.
Sierra A, Paolicelli RC, Kettenmann H. 2019. Cien Años de Microglía: Milestones in a Century of Microglial Research. Trends Neurosci [Internet] 42:778–792. Available from: https://doi.org/10.1016/j.tins.2019.09.004
Silva-Palacios A, Colín-González AL, López-Cervantes SP, Zazueta C, Luna-López A, Santamaría A, Königsberg M. 2017. Tert-buthylhydroquinone pre-conditioning exerts dual effects in old female rats exposed to 3-nitropropionic acid. Redox Biol [Internet] 12:610–624. Available from: https://doi.org/10.1016/j.redox.2017.03.029
Šišková Z, Tremblay M-È. 2013. Microglia and synapse: interactions in health and neurodegeneration. Neural Plast 2013.
Skibinski G, Hwang V, Ando DM, Daub A, Lee AK, Ravisankar A, Modan S, Finucane MM, Shaby BA, Finkbeiner S. 2017. Nrf2 mitigates LRRK2-and α-synuclein–induced neurodegeneration by modulating proteostasis. Proc Natl Acad Sci 114:1165–1170.
Smith JA, Das A, Ray SK, Banik NL. 2012. Role of pro-inflammatory cytokines released from microglia in neurodegenerative diseases. Brain Res Bull 87:10–20.
Song W, Wang F, Savini M, Ake A, Di Ronza A, Sardiello M, Segatori L. 2013. TFEB regulates lysosomal proteostasis. Hum Mol Genet 22:1994–2009.
Song WM, Colonna M. 2018. The identity and function of microglia in neurodegeneration. Nat Immunol 19:1048–1058.
Soria FN, Engeln M, Martinez-Vicente M, Glangetas C, López-González MJ, Dovero S, Dehay B, Normand E, Vila M, Favereaux A, Georges F, Lo Bianco C, Bezard E, Fernagut PO. 2017. Glucocerebrosidase deficiency in dopaminergic neurons induces microglial activation without neurodegeneration. Hum Mol Genet 26:2603–2615.
Spampanato C, Feeney E, Li L, Cardone M, Lim J, Annunziata F, Zare H, Polishchuk R, Puertollano R, Parenti G. 2013. Transcription factor EB (TFEB) is a new therapeutic target for Pompe disease. EMBO Mol Med 5:691–706.
Spencer JP, Jenner P, Halliwell B. 1995. Superoxide-dependent depletion of reduced glutathione by L-DOPA and dopamine. Relevance to Parkinson's disease. Neuroreport 6:1480–1484.
Stahnke T, Richter-Landsberg C, Stadelmann C, Netzler A, Brück W. 2007. Differential upregulation of heme oxygenase-1 (HSP32) in glial cells after oxidative stress and in demyelinating disorders. J Mol Neurosci 32:25–37.
Stamenkovic I, Aruffo A, Amiot M, Seed B. 1991. The hematopoietic and epithelial forms of CD44 are distinct polypeptides with different adhesion potentials for hyaluronate-bearing cells. EMBO J 10:343–348.
Stirnemann J, Vigan M, Hamroun D, Heraoui D, Rossi-Semerano L, Berger MG, Rose C, Camou F, de Roux-Serratrice C, Grosbois B. 2012. The French Gaucher's disease registry: clinical characteristics, complications and treatment of 562 patients. Orphanet J

Rare Dis 7:77.
Stirnemann JÔ, Belmatoug N, Camou F, Serratrice C, Froissart R, Caillaud C, Levade T, Astudillo L, Serratrice J, Brassier A, Rose C, De Villemeur TB, Berger MG. 2017. A review of gaucher disease pathophysiology, clinical presentation and treatments. Int J Mol Sci 18:1–30.
Stockert JC, Horobin RW, Colombo LL, Blázquez-Castro A. 2018. Tetrazolium salts and formazan products in Cell Biology: Viability assessment, fluorescence imaging, and labeling perspectives. Acta Histochem 120:159–167.
Stokholm MG, Iranzo A, Østergaard K, Serradell M, Otto M, Svendsen KB, Garrido A, Vilas D, Borghammer P, Santamaria J. 2017. Assessment of neuroinflammation in patients with idiopathic rapid-eye-movement sleep behaviour disorder: a case-control study. Lancet Neurol 16:789–796.
Su X, Maguire-Zeiss KA, Giuliano R, Prifti L, Venkatesh K, Federoff HJ. 2008. Synuclein activates microglia in a model of Parkinson's disease. Neurobiol Aging 29:1690–1701.
Sultana S, Truong NY, Vieira DB, Wigger JGD, Forrester AM, Veinotte CJ, Berman JN, Van Der Spoel AC. 2016. Characterization of the Zebrafish Homolog of β-Glucosidase 2: A Target of the Drug Miglustat. Zebrafish 13:177–187.
Swamy SM, Rajasekaran NS, Thannickal VJ. 2016. Nuclear factor–erythroid-2–related factor 2 in aging and lung fibrosis. Am J Pathol 186:1712–1723.
Sykiotis GP, Bohmann D. 2010. Stress-activated cap'n'collar transcription factors in aging and human disease. Sci Signal 3:re3–re3.
Szepesi Z, Manouchehrian O, Bachiller S, Deierborg T. 2018. Bidirectional Microglia–Neuron Communication in Health and Disease. Front Cell Neurosci 12:1–26.
Szymanska-Chabowska A, Antonowicz-Juchniewicz J, Andrzejak R. 2002. Some aspects of arsenic toxicity and carcinogenicity in living organism with special regard to its influence on cardiovascular system, blood and bone marrow. Int J Occup Med Environ Health 15:101–116.
Tagliaferro P, Burke RE. 2016. Retrograde Axonal Degeneration in Parkinson Disease. J Parkinsons Dis 6:1–15.
Takahashi K, Prinz M, Stagi M, Chechneva O, Neumann H. 2007. TREM2-transduced myeloid precursors mediate nervous tissue debris clearance and facilitate recovery in an animal model of multiple sclerosis. PLoS med 4:e124.
Tan E-K, Tong J, Fook-Chong S, Yih Y, Wong M-C, Pavanni R, Zhao Y. 2007. Glucocerebrosidase mutations and risk of Parkinson disease in Chinese patients. Arch Neurol 64:1056–1058.
Tatton NA, Kish SJ. 1997. In situ detection of apoptotic nuclei in the substantia nigra compacta of 1-methyl-4-phenyl-1, 2, 3, 6-tetrahydropyridine-treated mice using terminal deoxynucleotidyl transferase labelling and acridine orange staining. Neuroscience 77:1037–1048.
Tay TL, Savage JC, Hui CW, Bisht K, Tremblay M. 2017. Microglia across the lifespan: from origin to function in brain development, plasticity and cognition. J Physiol 595:1929–1945.
Tian L, Ma L, Kaarela T, Li Z. 2012. Neuroimmune crosstalk in the central nervous system and its significance for neurological diseases. J Neuroinflammation 9:155.
Todorovic M, Newman JRB, Shan J, Bentley S, Wood SA, Silburn PA, Mellick GD. 2015. Comprehensive assessment of genetic sequence variants in the antioxidant 'master regulator'nrf2 in idiopathic Parkinson's disease. PLoS One 10:e0128030.
Toniolo A, Fadini GP, Tedesco S, Cappellari R, Vegeto E, Maggi A, Avogaro A, Bolego C, Cignarella A. 2015. Alternative activation of human macrophages is rescued by estrogen treatment in vitro and impaired by menopausal status. J Clin Endocrinol Metab 100:E50–E58.
Toulorge D, Schapira AH V, Hajj R. 2016. Molecular changes in the postmortem parkinsonian brain. J Neurochem 139:27–58.
Tremblay M-È, Lowery RL, Majewska AK. 2010. Microglial interactions with synapses are modulated by visual experience. PLoS Biol 8:e1000527.
Tsunemi T, Ashe TD, Morrison BE, Soriano KR, Au J, Roque RAV, Lazarowski ER, Damian VA, Masliah E, La Spada AR. 2012. PGC-1α rescues Huntington's disease proteotoxicity by preventing oxidative stress and promoting TFEB function. Sci Transl Med 4:142ra97-142ra97.
Ueno M, Fujita Y, Tanaka T, Nakamura Y, Kikuta J, Ishii M, Yamashita T. 2013. Layer V cortical neurons require microglial support for survival during postnatal development. Nat Neurosci 16:543–551.
Ulland TK, Song WM, Huang SCC, Ulrich JD, Sergushichev A, Beatty WL, Loboda AA, Zhou Y, Cairns NJ, Kambal A, Loginicheva E, Gilfillan S, Cella M, Virgin HW, Unanue ER, Wang Y, Artyomov MN, Holtzman DM, Colonna M. 2017a. TREM2 Maintains Microglial Metabolic Fitness in Alzheimer's Disease. Cell [Internet] 170:649-663.e13. Available from: http://dx.doi.org/10.1016/j.cell.2017.07.023
Ulland TK, Song WM, Huang SCC, Ulrich JD, Sergushichev A, Beatty WL, Loboda AA, Zhou Y, Cairns NJ, Kambal A, Loginicheva E, Gilfillan S, Cella M, Virgin HW, Unanue ER, Wang Y, Artyomov MN, Holtzman DM, Colonna M. 2017b. TREM2 Maintains Microglial Metabolic Fitness in Alzheimer's Disease. Cell 170:649-663.e13.
Ungerstedt U, Ljungberg T, Steg G. 1974. Behavioral, physiological, and neurochemical changes after 6-hydroxydopamine-induced degeneration of the nigro-striatal dopamine neurons. Adv Neurol 5:421.
Vaccaro AM, Motta M, Tatti M, Scarpa S, Masuelli L, Bhat M, Vanier MT, Tylki-Szymanska A, Salvioli R. 2010. Saposin C mutations in Gaucher disease patients resulting in lysosomal lipid accumulation, saposin C deficiency, but normal prosaposin processing and sorting. Hum Mol Genet 19:2987–2997.
Vardi A, Zigdon H, Meshcheriakova A, Klein AD, Yaacobi C, Eilam R, Kenwood BM, Rahim AA, Massaro G, Merrill AH, Vitner EB, Futerman AH. 2016. Delineating pathological pathways in a chemically induced mouse model of Gaucher disease. J Pathol 239:496–509.
Veerhuis R, Nielsen HM, Tenner AJ. 2011. Complement in the brain. Mol Immunol 48:1592–1603.
Villa A, Gelosa P, Castiglioni L, Cimino M, Rizzi N, Pepe G, Lolli F, Marcello E, Sironi L, Vegeto E, Maggi A. 2018. Sex-Specific Features of Microglia from Adult Mice. Cell Rep [Internet] 23:3501–3511. Available from:

https://doi.org/10.1016/j.celrep.2018.05.048
Villani A, Benjaminsen J, Moritz C, Henke K, Hartmann J, Norlin N, Richter K, Schieber NL, Franke T, Schwab Y, Peri F. 2019. Clearance by Microglia Depends on Packaging of Phagosomes into a Unique Cellular Compartment. Dev Cell [Internet] 49:77-88.e7. Available from: https://doi.org/10.1016/j.devcel.2019.02.014
Villar-Piqué A, Lopes da Fonseca T, Outeiro TF. 2016. Structure, function and toxicity of alpha-synuclein: the Bermuda triangle in synucleinopathies. J Neurochem 139:240–255.
Viola A, Munari F, Sánchez-Rodríguez R, Scolaro T, Castegna A. 2019. The metabolic signature of macrophage responses. Front Immunol 10.
Vitner EB, Farfel-Becker T, Eilam R, Biton I, Futerman AH. 2012. Contribution of brain inflammation to neuronal cell death in neuronopathic forms of Gaucher's disease. Brain 135:1724–1735.
Vyas I, Heikkila RE, Nicklas WJ. 1986. Studies on the neurotoxicity of 1-methyl-4-phenyl-1, 2, 3, 6-tetrahydropyridine: inhibition of NAD-linked substrate oxidation by its metabolite, 1-methyl-4-phenylpyridinium. J Neurochem 46:1501–1507.
Wang XJ, Hayes JD, Wolf CR. 2006. Generation of a stable antioxidant response element–driven reporter gene cell line and its use to show redox-dependent activation of Nrf2 by cancer chemotherapeutic agents. Cancer Res 66:10983–10994.
Wolf SA, Boddeke HWGM, Kettenmann H. 2017. Microglia in Physiology and Disease. Annu Rev Physiol 79:619–643.
Wong YC, Krainc D. 2017. α-synuclein toxicity in neurodegeneration: mechanism and therapeutic strategies. Nat Med 23:1–13.
Wright GJ, Puklavec MJ, Willis AC, Hoek RM, Sedgwick JD, Brown MH, Barclay AN. 2000. Lymphoid/neuronal cell surface OX2 glycoprotein recognizes a novel receptor on macrophages implicated in the control of their function. Immunity 13:233–242.
Wruck CJ, Claussen M, Fuhrmann G, Römer L, Schulz A, Pufe T, Waetzig V, Peipp M, Herdegen T, Götz ME. 2007. Luteolin protects rat PC 12 and C6 cells against MPP+ induced toxicity via an ERK dependent Keapl-Nrf2-ARE pathway. In: Neuropsychiatric disorders an integrative approach. Springer. p 57–67.
Xiao Q, Yan P, Ma X, Liu H, Perez R, Zhu A, Gonzales E, Burchett JM, Schuler DR, Cirrito JR. 2014a. Enhancing astrocytic lysosome biogenesis facilitates Aβ clearance and attenuates amyloid plaque pathogenesis. J Neurosci 34:9607–9620.
Xiao W, Shameli A, Harding C V, Meyerson HJ, Maitta RW. 2014b. Late stages of hematopoiesis and B cell lymphopoiesis are regulated by α-synuclein, a key player in Parkinson's Disease. Immunobiology 219:836–844.
Yamamoto A, Simonsen A. 2011. The elimination of accumulated and aggregated proteins: a role for aggrephagy in neurodegeneration. Neurobiol Dis 43:17–28.
Ye F, Li X, Li L, Yuan J, Chen J. 2016. T-BHQ Provides Protection against Lead Neurotoxicity via Nrf2/HO-1 Pathway. Oxid Med Cell Longev 2016.
Yun SP, Kim D, Kim S, Kim S, Karuppagounder SS, Kwon SH, Lee S, Kam TI, Lee S, Ham S, Park JH, Dawson VL, Dawson TM, Lee Y, Ko HS. 2018. α-Synuclein accumulation and GBA deficiency due to L444P GBA mutation contributes to MPTP-induced parkinsonism. Mol Neurodegener 13:1–19.
Zawada WM, Banninger GP, Thornton J, Marriott B, Cantu D, Rachubinski AL, Das M, Griffin WST, Jones SM. 2011. Generation of reactive oxygen species in 1-methyl-4-phenylpyridinium (MPP+) treated dopaminergic neurons occurs as an NADPH oxidase-dependent two-wave cascade. J Neuroinflammation 8:1–13.
Zeilhofer HU. 2008. Loss of glycinergic and GABAergic inhibition in chronic pain—contributions of inflammation and microglia. Int Immunopharmacol 8:182–187.
Zhang B, Gaiteri C, Bodea L-G, Wang Z, McElwee J, Podtelezhnikov AA, Zhang C, Xie T, Tran L, Dobrin R. 2013a. Integrated systems approach identifies genetic nodes and networks in late-onset Alzheimer's disease. Cell 153:707–720.
Zhang H, Davies KJA, Forman HJ. 2015. Oxidative stress response and Nrf2 signaling in aging. Free Radic Biol Med 88:314–336.
Zhang M, An C, Gao Y, Leak RK, Chen J, Zhang F. 2013b. Emerging roles of Nrf2 and phase II antioxidant enzymes in neuroprotection. Prog Neurobiol 100:30–47.
Zhang Y, Chen K, Sloan SA, Bennett ML, Scholze AR, O'Keeffe S, Phatnani HP, Guarnieri P, Caneda C, Ruderisch N. 2014. An RNA-sequencing transcriptome and splicing database of glia, neurons, and vascular cells of the cerebral cortex. J Neurosci 34:11929–11947.
Zhao Y, Wu X, Li X, Jiang L-L, Gui X, Liu Y, Sun Y, Zhu B, Piña-Crespo JC, Zhang M. 2018. TREM2 is a receptor for β-amyloid that mediates microglial function. Neuron 97:1023–1031.
Zhou C, Huang Y, Przedborski S. 2008. Oxidative stress in Parkinson's disease: a mechanism of pathogenic and therapeutic significance. Ann N Y Acad Sci 1147:93.
Ziegler SG, Eblan MJ, Gutti U, Hruska KS, Stubblefield BK, Goker-Alpan O, LaMarca ME, Sidransky E. 2007. Glucocerebrosidase mutations in Chinese subjects from Taiwan with sporadic Parkinson disease. Mol Genet Metab 91:195–200.

Ph.D. ACTIVITIES

Other project

During the Ph.D. I participated to others project not reported in the thesis:

- Characterizing the consequences of GCase inhibition on live microglia; his effects on lysosomal pathways, from engulfment to gastrosome, taking advantages of the zebrafish transparency.

- I am actively involved in the development of a strategy potentially able to block the infections of SARS-CoV-2.

- I provided my expertise in support of the others main projects of the laboratory, aimed at characterizing tumour extra cellular vesicles homing and identifying prodromal markers for breast cancer. In addition, I collaborated with other groups generating reporter systems useful to study specific pathways.

Teaching experiences:

Maj 2020
Position: remote lecturer “farmacologia nel trattamento del dolore”, “farmaci ansioliti, ipnotici, neurolettici e per il trattamento delle malattie neurodegenerative”, “Chemioterapia antimicrobica”.
Supervisor: Professor Paolo Ciana.
Institute: Faculty of Medicine and Surgery, University of Milan, 20133 Milan, Italy.

13 June 2019;
Position: lecturer “Farmacologia nel trattamento del dolore”.
Supervisor: Professor Paolo Ciana.
Institute: Faculty of Medicine and Surgery, University of Milan, 20133 Milan, Italy.

28-31 January 2019
Position: tutor for laboratory of “biotecnologie farmacologiche avanzate”.
Supervisor: Professor Adriana Maggi.
Institute: Faculty of Pharmacy, University of Milan, 20133 Milan, Italy.

29 January 2018 - 05 February 2018
Position: tutor for laboratory of “biotecnologie farmacologiche avanzate”.
Supervisor: Professor Adriana Maggi.
Institute: Faculty of Pharmacy, University of Milan, 20133 Milan, Italy.

Tutor for master’s degree students:

2020-onwards: Francesco Nava, Master’s Course in Pharmaceutical Biotechnology;

2020-onwards: Giulia Amadeo, Master’s Course in Pharmacy;

2019- onwards: Marianna Mekhaeil, Master’s Course in Pharmaceutical Biotechnology;

2019- onwards: Maria Chieregato, Master’s Course in Pharmaceutical Chemistry and Technology; ”Rilevanza del metabolismo energetico nella regolazione delle funzioni neuroprotettive gliali”;

2019- 2020: Ilaria Colombo, Master’s Course in Pharmacy; “Studio del ruolo dell’enzima β-glucoerebrosidasi nella comunicazione microglia-neurone: evidenze di un nuovo meccansimo di neuroprotezione”

2018-2019: Nazanin Bagherpour Hassanlouei; Master's Course in Molecular Biology of the Cell, "Characterization and validation TFEB reporter system to study TFEB modulation in Parkinson models";

2018-2019: Alice Ratti; Master's Course in Pharmacy, "Studio degli effetti dell'inibizione della β-glucoerebrosidasi sull'attivazione microgliale attraverso sistemi reporter e analisi morfodinamica dell'immagine cellulare";

2017: Andrea Brivio; Master's Course in Pharmaceutical Chemistry and Technology, "Sviluppo, creazione e validazione di un biosensore reporter per lo screening di farmaci modulatori del fattore di trascrizione EB, il principale regolatore dei segnali lisosomiali".

Congresses during PhD:

10-13 March 2021: Pharmacological impairment of Gaucher's disease gene product hinders microglia-to-neuron neuroprotective response. ***E. Brunialti***, A. Villa, M. Mekhaeil, I. Colombo, A. Ratti, F. Mornata, M. Chieregato, A. Maggi and P. Ciana. 40° Congresso Nazionale della SIF. Abstract accepted.

14-Novembrer 2020: Pharmacological impairment of Gaucher's disease gene product hinders microglia-to-neuron neuroprotective response. ***E. Brunialti***, A. Villa, M. Mekhaeil, I. Colombo, A. Ratti, F. Mornata, M. Chieregato, A. Maggi and P. Ciana. Congresso DiSS 2020. Poster.

25-28 June 2020: β-glucocerebrosidase mediate a microglial neuroprotective mechanism: a possible link between Parkinson's and Gaucher's diseases. ***E. Brunialti***, A. Villa, I. Colombo, F. Mornata, A. Maggi and P. Ciana. IV° Spring School, Chiesa in Valmalenco, Sondrio, Italy. Oral presentation.

10 December 2019: Lysosomal disorders affect morpho-functional features of microglia***. E. Brunialti***, A. Villa, I. Colombo, A. Maggi and P. Ciana. 100 Years of Microglia. International Symposium, Lausanne, Switzerland. Poster.

19 - 21 September 2019: Morpho-functional analysis of microglia in a cell culture model of Gaucher disease. ***E. Brunialti***, A. Villa, I. Colombo, A. Ratti, A. Maggi and P. Ciana. ABCD congress. Savoia Hotel Regency, Bologna, Italy. Poster and selection for the flash poster presentation.

18 September 2019: Morpho-functional analysis of microglia in a cell culture model of Gaucher disease. ***E. Brunialti***, A. Villa, I. Colombo, A. Ratti, A. Maggi and P. Ciana. NEXT STEP X. Università degli Studi di Milano, Milano, Italy. Oral presentation.

10 - 13 July 2019: Morpho-functional analysis of microglia in a cell culture model of Gaucher disease. ***E. Brunialti,*** A. Villa, I. Colombo, A. Ratti, A. Maggi and P. Ciana. XIV European Meeting on Glial Cells in Health and Disease. Porto, Portugal. Poster.

11 - 14 April 2019: Role of microglia (dys)functions in the early phases of Parkinson's disease. ***E. Brunialti***, A. Villa, A. Ratti, A. Maggi and P. Ciana. III° Spring School, Chiesa in Valmalenco, Sondrio, Italy. Oral presentation.

3 July 2018: *In vivo* imaging of early signs of dopaminergic neuronal death. ***E. Brunialti***, N. Rizzi, S. Cerri, D. Crescenti, N. Cesari, A. Maggi, F. Blandini and P. Ciana. NEXT STEP IX. Università degli Studi di Milano, Milano, Italy. Oral presentation and member of the organizing committee.

12 - 15 April 2018: Reporter systems to study early neurodegenerative events in Parkinson's models ***E. Brunialti,*** N. Rizzi, D. Crescenti, A. Maggi, and P. Ciana. New perspectives in pharmacology: from genetic to real life. Chiesa in Valmalenco, Sondrio, Italy. Oral presentation.

Third mission:

RicercaMIx Blog, www.ricercamix.org/author/electrabrunialti:

13 November 2019 “Se la microglia si “ingolfa”?”;

23 April 2019 “Cosa hai in testa?”;

18 September 2018 “Il contributo delle lucciole per comprendere la malattia di Parkinson**”.**

Publications during PhD:

Brunialti E*,* Villa A, Mekhaeil M, Mornata F, Di Monte D, Maggi A and Ciana P. Inhibition of microglial GBA hampers the microglia-mediated anti-oxidant and protective response in neurons. 2021 . bioRxiv doi: 10.1101/2021.01.20.427380.

*Villa A, **Brunialti E**, Maggi A, Paolo C. Assessing microglia phenotypes by advanced dynamic microscopy. (In preparation).*

Villa A, Garofalo M, Crescenti D, Rizzi N, ***Brunialti E***, Vingiani A, Belotti P, Sposito C, Franzé S, Cilurzo F, Pruneri G, Recordati C, Giudice C, Giordano A, Tortoreto M, Beretta G, Stefanello D, Manenti G, Zaffaroni N, Mazzaferro V, Ciana P. Transplantation of autologous extracellular vesicles for cancer-specific targeting. Theranostics. 2020; doi:10.7150/thno.51344; accepted

Garofalo M, Villa A, ***Brunialti E***, Crescenti D, Dell’Omo G, Kuryk L, Vingiani A, Mazzaferro V, Ciana P. Cancer-derived EVs show tropism for tissues at early stage of neoplastic transformation. Nanotheranostics 2021; 5(1):1-7.

Mornata F, Pepe G, Sfogliarini C, ***Brunialti E***, Rovati G, Locati M, Maggi A, Vegeto E. Reciprocal interference between the NRF2 and LPS signaling pathways on the immune-metabolic phenotype of peritoneal macrophages. Pharmacology Research & Perspectives. 2020; 8.4: e00638

Carrano N, Samaddar T, ***Brunialti E***, Franchini L, Marcello E, Ciana P, Mauceri D, Di Luca M and Gardoni F. The Synaptonuclear messenger RNF10 acts as an architect of neuronal morphology. Molecular neurobiology. 2019; 56(11);7583-7593.

Rizzi N, ***Brunialti E***, Cerri S, Cermisoni G, Levandis G, Cesari N, Maggi A, Blandini F, Ciana P. *In vivo* imaging of early signs of dopaminergic neuronal death in an animal model of Parkinson's disease. Neurobiol Dis. 2018; 114:74-84.